

The University of Manitoba

PARTIAL PURIFICATION OF SUPEROXIDE DISMUTASE
FROM HUMAN RED BLOOD CELL MEMBRANES
BY HIGH PERFORMANCE LIQUID CHROMATOGRAPHY

by
Rosemary A. Zepp Johnston

A Thesis
Submitted to the Faculty of Graduate Studies
in partial fulfillment of the requirements for the
degree of Master of Science

Department of Chemistry

Winnipeg, Manitoba
July 30, 1983

PARTIAL PURIFICATION OF SUPEROXIDE DISMUTASE
FROM HUMAN RED BLOOD CELL MEMBRANES
BY HIGH PERFORMANCE LIQUID CHROMATOGRAPHY

by

Rosemary A. Zepp Johnston

A thesis submitted to the Faculty of Graduate Studies of
the University of Manitoba in partial fulfillment of the requirements
of the degree of

MASTER OF SCIENCE

© 1983

Permission has been granted to the LIBRARY OF THE UNIVER-
SITY OF MANITOBA to lend or sell copies of this thesis, to
the NATIONAL LIBRARY OF CANADA to microfilm this
thesis and to lend or sell copies of the film, and UNIVERSITY
MICROFILMS to publish an abstract of this thesis.

The author reserves other publication rights, and neither the
thesis nor extensive extracts from it may be printed or other-
wise reproduced without the author's written permission.



Acknowledgements

I would like to acknowledge the cooperation demonstrated between the University of Manitoba and Atomic Energy of Canada Limited which allowed this work to take the form of a M.Sc. thesis project.

I am grateful for the fellowship granted by Atomic Energy of Canada Limited which financed this project and for the privilege of using their laboratory facilities at the Whiteshell Nuclear Research Establishment in Pinawa, Manitoba.

My sincere appreciation goes to Dr. A. Petkau for his supervision and guidance during the course of this research.

Also, most appreciated is the technical expertise of W.S. Chelack who performed the ultrasensitive assay for superoxide dismutase.

Abstract

Fresh human red blood cell ghosts were prepared by serial hypotonic hemolysis. Eleven preparations were used to characterize the ghosts and establish technique while six preparations were used to develop the high performance liquid chromatography (HPLC) strategy. Residual ghost hemoglobin was 0.10 ± 0.01 % of the mean corpuscular hemoglobin. The amount of membrane protein extracted was 0.7 ± 0.1 pg/ghost. The high selection factor of 1500:1 for inner membrane surface proteins over hemoglobin in the ghosts suggests a high degree of purity from cytoplasmic components. The activity of the membrane enzyme marker, acetylcholinesterase, was 1.3 ± 0.2 fmole of acetylthiocholine iodide hydrolyzed per minute per ghost. In contrast, 5'-nucleotidase specific for adenosine monophosphate was not found. Polyacrylamide gel electrophoresis of the ghost proteins, extracted with Nonidet P-40, demonstrated the presence of active superoxide dismutase (SOD) at $(3 \pm 1) \times 10^{-17}$ g/ghost or 0.4 ± 0.2 % of the total cellular active enzyme. The level of SOD activity in the RBC membranes was equal to 540 ± 240 molecules per ghost, equivalent to about 0.6 μ M for a 9 nm thick membrane. Ion exchange HPLC (Synchropak AX-300 column) followed by size exclusion HPLC (Micropak TSK G2000 column) partially purified active SOD by factors of 170 and 390 for two ghost preparations (G14 and G15, respectively). Three additional runs on the Micropak TSK G2000 column separated two fractions: the first, eluting at 11 m, did not contain active SOD while the second fraction, eluting at 12-20 m, did. For the G14 preparation, the activity of SOD in the

second fraction was increased 4.4 times raising the purification factor from 170 to 750. By HPLC on the Micropak TSK G2000 column, the second fraction was separated into two subfractions, the first of which, eluting at 12-16 m, was enriched in SOD activity and represented an overall purification of about 1500. The yield was estimated at 0.04 % of the active enzyme in the starting material. The active enzyme in the ghost membrane amounted to 0.004 ± 0.002 % of the total membrane protein.

To the author's knowledge, the work presented in this thesis includes research attempted for the first time in the following areas: (1) The presence of active and inactive membrane-associated SOD was demonstrated in human red blood cell ghosts. (2) The amount of membrane-associated SOD in human red blood cells was quantified. (3) An increase in membrane-associated SOD in human red blood cells with age was demonstrated.

Application of HPLC technology led to the following original results: (4) Human SOD, inactivated by ionizing radiation, was separated from the active form of the enzyme. This result was useful in a neutron diffraction study of SOD by other scientists. (5) Evidence for an interaction between the holo- and apo- forms of human SOD was obtained. (6) SOD, associated with human red blood cell membranes, was partially purified.

Table of Contents

	Page
Acknowledgements	ii
Abstract	iii
List of Abbreviations	vii
List of Figures	ix
List of Tables	xi
CHAPTER 1: Introduction	1
CHAPTER 2: Background	3
A) Membranes	3
B) Oxidative Hemolysis	6
C) Superoxide Dismutase	12
D) Experimental Approach	17
CHAPTER 3: Experimental	22
A) Materials	22
B) Ghost Preparation	24
C) Photography	26
D) Cell Counts	27
E) NP-40 Treatment	28
F) Protein Assay	29
G) Hemoglobin Assay	30
H) Acetylcholinesterase Assay	32
I) 5'-AMP-Nucleotidase Assay	33
J) Polyacrylamide Gel Electrophoresis	34
K) SOD Assays	37
L) High Performance Liquid Chromatography	40
M) Effect of SOD Modifications	42
N) SOD Reconstitution	44
CHAPTER 4: Results	45
A) Cell Morphology	45
B) Ghost Yield	48
C) Ghost Protein	51
D) Ghost Hemoglobin	52
E) Acetylcholinesterase Activity	52
F) 5'-AMP-Nucleotidase Activity	52
G) Polyacrylamide Gel Electrophoresis	57
H) Cytoplasmic SOD	61
I) NP-40 Treatment	61
J) High Performance Liquid Chromatography	63
K) SOD Modifications	96
L) "Burton" Ghosts	100

CHAPTER 5: Discussion	103
A) Ghost Quality and Analyses	103
B) HPLC Purification	104
C) SOD Association with the RBC Membrane	108
D) The Relevance of Membrane-Associated SOD	111
References	113

List of Abbreviations

ACHE	acetylcholinesterase
BSA	bovine serum albumin
CAT	catalase
DTNB	5',5'-dithiobis-(2-nitrobenzoic acid)
EDTA	disodium ethylenediamine tetraacetate
G-6-PD	glucose-6-phosphate dehydrogenase
G-3-PD	glyceraldehyde-3-phosphate dehydrogenase
G-Px	glutathione peroxidase
HPLC	high performance liquid chromatography
MCH	mean corpuscular hemoglobin
NADH	nicotinamide-adenine dinucleotide (reduced)
NADPH	nicotinamide-adenine dinucleotide phosphate (reduced)
Na-5'-AMP	sodium adenosine 5'-monophosphate
NaOAc	sodium acetate
NBT	nitroblue tetrazolium
NP-40	Nonidet P-40
PAGE	polyacrylamide gel electrophoresis
PBS	phosphate buffered saline
PFK	phosphofructokinase
P _i	inorganic phosphate
RBC	red blood cell
SDS	sodium dodecyl sulfate
SEM	scanning electron microscope
Serial HPLC	sequential use of Synchropak AX-300 and Micropak TSK G2000 SW in the purification of SOD from human RBC membranes
SOD	superoxide dismutase

SOD-like protein	that protein fraction of human ghost extract which behaved electrophoretically as the reference SOD of cytoplasmic origin
TCA	trichloroacetic acid
TEMED	N,N,N',N'-tetramethylethylenediamine
TRIS	Sigma 7-9 biochemical buffer
Vit.E	vitamin E
WBC	white blood cell

List of Figures

- Figure 1: Diagrammatic representation of the RBC membrane according to the Fluid Mosaic Model.
- Figure 2: The univalent path of oxygen reduction to water in biological systems.
- Figure 3: Flow diagram describing the sequence of HPLC used for two ghost preparations, G14 and G15.
- Figure 4: Human RBC ghosts as seen under a phase contrast microscope.
- Figure 5: Human RBC ghosts as seen under scanning electron microscopes.
- Figure 6: Analysis of SOD activity by PAGE.
- Figure 7: Analysis of SOD-like protein by PAGE.
- Figure 8: HPLC elution profiles of reference holo-SOD and reference apo-SOD.
- Figure 9: HPLC of EDTA.
- Figure 10: HPLC elution profiles of apo-SOD before and after dialysis against perchlorate to remove bound EDTA.
- Figure 11: Comparative HPLC elution times of radiation-inactivated SOD, the holo-form and of a 1:1 mixture of the two forms.
- Figure 12: Comparative HPLC of the holo- and apo- forms of reference SOD.
- Figure 13: HPLC elution profile of 20 ug holo-SOD in 0.01 % NP-40.
- Figure 14: HPLC elution profile of 40 ug holo-SOD after thermal denaturation.
- Figure 15: HPLC of holo-SOD and EDTA.
- Figure 16: HPLC of inactivated SOD.
- Figure 17: HPLC elution profile of ghost extract.
- Figure 18: HPLC elution profile of material previously eluted between 4 and 10 m on the Synchropak AX-300 column (fig. 17).
- Figure 19: Densitometry tracings of PAGE bands showing SOD activity in HPLC fractions.

- Figure 20: Flow diagram of the HPLC sequence used to purify SOD from two ghost preparations (G14 and G15) showing the amount of SOD activity, as determined by PAGE or the ultrasensitive assay, and the amount of protein, measured by the Lowry method at various stages.
- Figure 21: HPLC elution profile of elution buffer concentrated 4.4 times by a filtered stream of argon gas.
- Figure 22: HPLC elution profile of fraction I (Fig. 18) from serial HPLC.
- Figure 23: HPLC elution profile of pooled peak 1 material (Fig. 22) from fraction I.
- Figure 24: HPLC elution profile of a fraction (10-20 m, Fig. 23) after exhaustive dialysis against H₂O and concentration by Amicon ultrafiltration.
- Figure 25: UV absorption spectra of SOD and HPLC fractions.
- Figure 26: PAGE scans of samples of modified reference SOD stained for activity.
- Figure 27: PAGE scans of samples of modified reference SOD stained for protein.
- Figure 28: HPLC elution profiles of samples of modified reference SOD (Micropak TSK G2000 column).
- Figure 29: HPLC elution profiles of samples of modified reference SOD (Synchropak AX-300 column).

List of Tables

- Table 1: Summary of the Characteristics of Ghosts from Outdated Blood.
- Table 2: Summary of the Characteristics and Enzyme Activities in Ghosts from Fresh Human Blood.
- Table 3: Summary of 5'-AMP-Nucleotidase Assay.
- Table 4: Comparison of 5'-AMP-Nucleotidase Activity Assays in Human RBC Ghosts.
- Table 5: Effect of Ghost Solubilization by NP-40 on Ghost Assays.
- Table 6: Summary of the Purification of Active SOD from Human RBC Ghosts by Serial HPLC for Two Ghost Preparations (G14 and G15).
- Table 7: Comparison of Features of the UV Absorption Spectra of SOD from Figure 25.
- Table 8: Analysis of Peak #2 (Figure 22) of G14 and G15 after the Third HPLC on the New Micropak TSK G2000 Column.

CHAPTER 1: Introduction

The red blood cell (RBC) membrane has been the center of intensive investigation for many decades (1-5). This is partly due to its ready availability and facile, reproducible isolation, and to its similar nature to other membranes. Further, the RBC membrane has served as a model system in studies of membrane structure and function (eg.: transport, osmotic equilibrium maintenance, membrane lipid peroxidation). In addition, this membrane is studied for its role as a key element in many diseases. The oxidative hemolytic anemias, for instance, make up one group of these diseases (6).

The RBC is under much oxidative stress in its normal lifetime of 3 to 4 months. Its exposure to high oxygen concentrations and inability to resynthesize damaged components are contributing factors to this stress. Nevertheless, RBCs are equipped with defense mechanisms which protect against damage by activated oxygen such as superoxide ($O_2^{\cdot -}$), peroxides (RO_2^{\cdot} , H_2O_2), hydroxyl free radical ($\cdot OH$) and singlet oxygen (7). These defense mechanisms include the enzymes superoxide dismutase (SOD), catalase, glutathione peroxidase and other antioxidants within the cell membrane. A deficiency in these protective processes can result in the oxidation of cell components, leading to hemolysis or other pathological consequences (6, 8-10).

In processes leading to hemolysis, the membrane is exposed to various types of damage, including lipid peroxidation, protein oxidation, protein inactivation. For protection, the membrane must have defenses against oxidative stress from within as well as from the

outside. Vitamin E in the membrane and glutathione peroxidases in the cytoplasm serve these roles. However, a good defense within the RBC membrane against superoxide would be SOD since the radical is a specific substrate for the enzyme (11).

Superoxide radicals are a natural by-product of oxyhemoglobin autoxidation in the RBC cytoplasm and SOD is necessarily present to scavenge them within the cytoplasm. Unscavenged superoxide, however, might diffuse away via concentration gradients through the cytoplasm. Ultimately, it would encounter the cytoplasmic side of the RBC membrane and diffuse into it (12, 13), inflicting damage by oxidative processes. Conversely, superoxide generated outside the cell by hemolysis of other RBCs or by leucocyte action could diffuse into RBCs where damage might result at the first site of contact: the membrane. In addition, superoxide can be produced by membrane-bound enzymes such as NADPH-cytochrome c reductase (14). Clearly, an antioxidant within the membrane, specific for superoxide, could be useful. Indeed, bovine RBC membranes have been found to contain SOD (15).

The objective of this study was to determine whether SOD was present and isolable from human RBC membranes. Isolation and purification of active SOD from human RBC membranes would further support the idea that the enzyme can be associated with cell membranes.

CHAPTER 2: Background

A) Membranes

A general concept of plasma membranes, including the RBC membrane, appears to be experimentally established. The current view of membrane structure is the 'Fluid Mosaic Model' of Singer and Nicolson (16). The key feature of this model is the lipid bilayer matrix in which proteins are embedded in whole or in part. Proteins, often asymmetrically distributed, and lipids, in a mosaic arrangement, are able to diffuse laterally in the membrane bilayer, in thermodynamically favorable fashion. Flipping of proteins and lipids from the outer to the inner face of the membrane (or vice versa) is rare as it is thermodynamically unfavorable, requiring energy input. The spectrin-actin cytoskeleton underlying the membrane at its cytoplasmic face plays a part in the movement of surface proteins, in addition to having a structural role in maintaining cell shape. Fig. 1 illustrates these features of the RBC membrane.

Depending on the extent of their interactions with the lipid matrix, proteins can be either extrinsic (peripheral) or intrinsic (integral). Extrinsic proteins are functionally associated with the membrane but only by weak electrostatic interactions (eg.: spectrin). Consequently, mild treatment, such as an increase of ionic strength is needed for their lipid-free dissociation from the membrane. In the

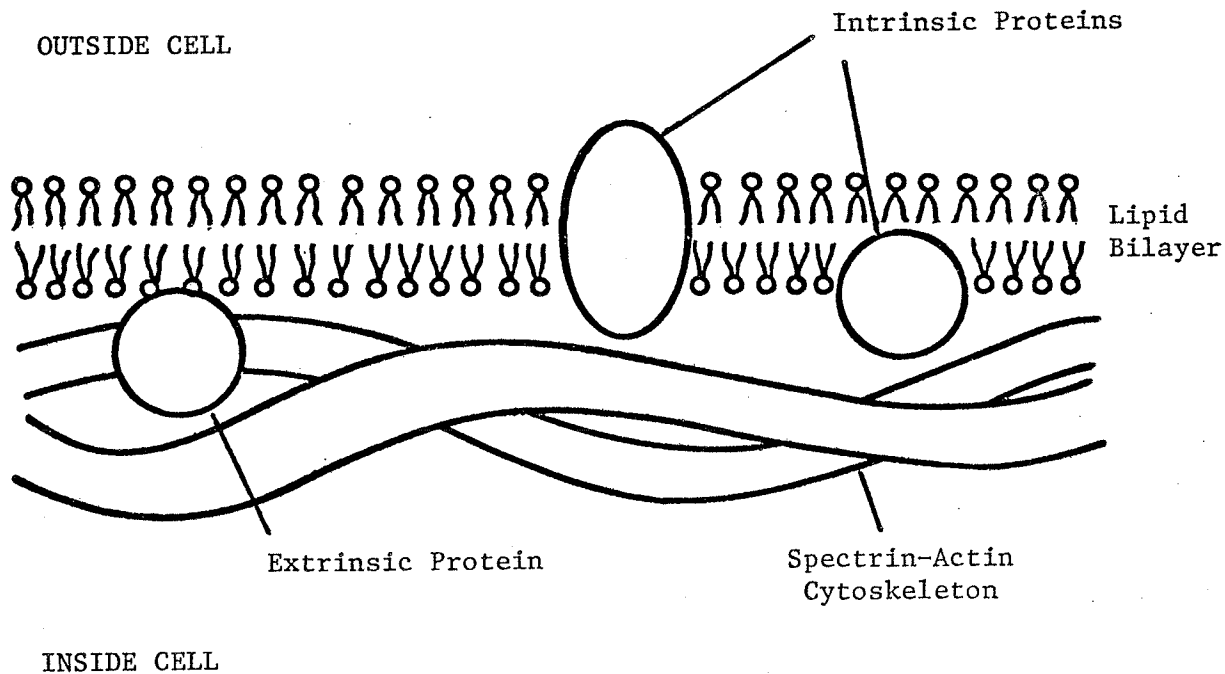


Figure 1: Diagrammatic representation of the RBC membrane according to the Fluid Mosaic Model.

dissociated state, extrinsic proteins are relatively soluble in neutral aqueous buffers. Intrinsic proteins, however, require stronger treatments (eg.: detergents, organic solvents) for their dissociation from membranes because they are bound to the lipid matrix (eg.: acetylcholinesterase). Their removal requires disruption of membrane structure. After the disruption, these proteins may remain associated with lipids. If the lipid is removed, such proteins may become insoluble and aggregate in neutral aqueous media (16). Also, selective solubilization by changes of pH, ionic strength, or solubilizing agents often is helpful in isolating one protein over another, thus indicating the diverse nature of protein association with the membrane.

Many enzymes of the RBC membrane are present as minor components. Nevertheless, they may be functionally significant. Schrier, in 1977, classified these enzymes into two groups (2). The first group includes 37 enzymes whose activities are confined strictly to the membrane (eg.: ACHE, 5'-nucleotidase, NADH-oxidoreductase). The second group includes 19 enzymes whose activities are found in both the cytosol and the membrane (eg: aldolase, glyceraldehyde-3-phosphate dehydrogenase (G-3-PD), lactate dehydrogenase). Initial reluctance to regard the latter group as being true membrane-associated enzymes was based on the fact that hemolytic conditions can produce artefactual membrane association of cytosol enzymes (3). However, membrane-associated enzymes once thought to be artefactual have been found to be inherent to the membrane as well as to the cytoplasm. They have an "ambiquitous" nature; that is, their distribution between kinetically-distinct soluble and membrane-bound forms is dependent on

the concentrations of cellular metabolites (17). This is believed to be a regulatory mechanism by which the distribution of free and bound forms of an enzyme affects its activity to suit changing metabolic needs. G-3-PDH, aldolase and phosphofructokinase (PFK) are just a few enzymes shown to possess reversible membrane association that alters their activities (18). This concept of a protein being in equilibrium between a soluble, cytosol phase and a particulate, membrane-bound phase is not new, as indicated by initial experimental methods by which ghosts were prepared (19).

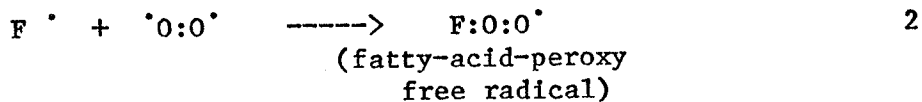
B) Oxidative Hemolysis

The oxidative stress of RBCs is exhibited in the oxidation of cellular constituents, leading to the deterioration of the cell. Lipid peroxidation of membranes and free radical damage to enzymes and other membrane components are the chemical processes involved.

In lipid peroxidation, peroxides arise from free radical intermediates produced by direct reaction of oxygen with unsaturated fatty acid groups of membrane lipids (20). The true structure of these unsaturated fatty acid groups is described by a resonance hybrid, which is a composite of all possible electronic formulas and more stable than any of the separated structures. The free radical character contributes to this resonance (equation 1), which is able to bind oxygen, creating fatty-acid-peroxy free radicals (reaction 2) (21).



(fatty acid)



After reaction 2, the process can become self-propagating via a chain reaction in which the first fatty-acid peroxy free radical seeks stability by acquiring an electron from an adjacent fatty-acid (forming another free radical with a similar destiny) or from the membrane proteins, leading to protein polymerization, polypeptide chain scission or chemical changes to individual amino acids. These events may result in a rapid deterioration of membrane structure and function by three mechanisms (21):

- a) The loss of double bonds in fatty acids causes a sharp rise in melting point, solidifying the tissue fats.
- b) Lipid peroxides and their fragmentation products can be potential metabolic poisons (eg.: malonaldehyde, which can cross-link enzymes, leading to their inactivation).
- c) Break down of the cells' anti-oxidant defenses, which normally counteract chain-initiating and chain-propagating free radicals (eg.: Vitamin E).

Free radical damage of membranes may also involve the univalent reduction of dioxygen to water (Fig. 2). This well known process has been classified into four steps, the intermediates of which are referred to as activated oxygen species (11, 22). Most dioxygen consumed by respiring cells follows the path designated as 'A' in Fig. 2, whereby O_2 is converted directly to H_2O by the mitochondrial

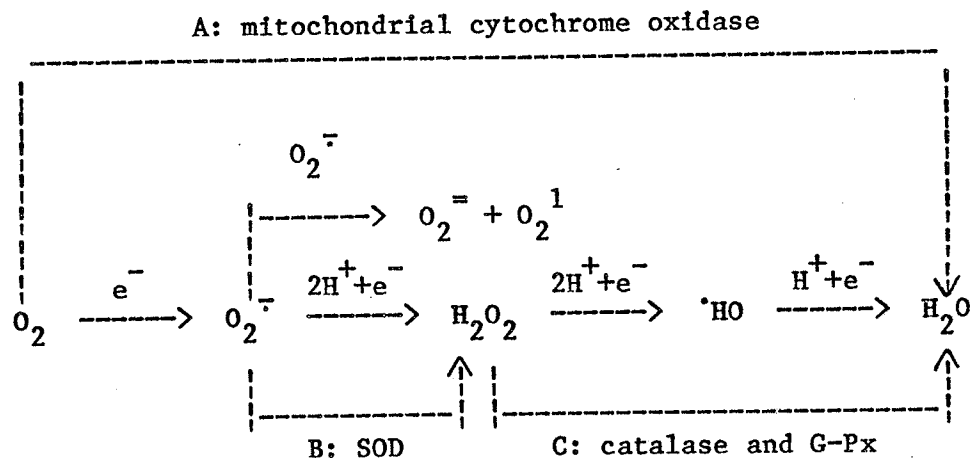


Figure 2: The univalent path of oxygen reduction to water in biological systems.

enzyme, cytochrome oxidase. The remaining dioxygen is reduced to water via the sequential reduction to superoxide anion, hydrogen peroxide and hydroxyl radical by the combined catalytic action of SOD, catalase and glutathione peroxidase (G-Px), as shown in paths B and C of Fig.2. At each step, a potentially harmful activated oxygen species is produced (23-25). In RBCs, the metabolic machinery (ie.: mitochondria) required for path A to occur is absent, thereby making these cells a natural source of activated oxygen. Thus, SOD, catalase and glutathione peroxidase are necessarily present in RBCs to scavenge these species.

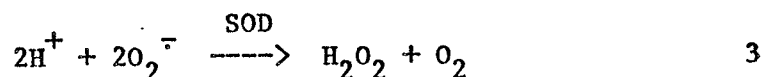
An important mechanism of superoxide formation in RBCs is via the autoxidation of oxyhemoglobin to methemoglobin (26-28). Random fluctuations of the heme pocket in the molecule allow the entry of water, forcing displacement of oxygen having an extra electron (ie.: superoxide) and loss of an electron in heme iron, forming ferric (Fe^{+3}) methemoglobin from the ferrous (Fe^{+2}) hemoglobin. In normal RBCs, approximately 3 % of the total hemoglobin is converted to methemoglobin each day, thus providing a continuous source of the superoxide radical. Interactions between heavy metal ions and oxyhemoglobin are also known to produce superoxide (29, 30), as does ionizing radiation (31, 32). In addition, within rat liver microsomal membranes, oxidoreductase enzymes such as NADPH-cytochrome c reductase have been shown to produce superoxide anion during catalysis of NADPH-dependent lipid peroxidation (14). The NADPH-acceptor oxidoreductases are also in the plasma membrane of RBCs (2).

By itself, or as a source of other activated oxygen species (33), the superoxide radical is potentially toxic. Because it is a

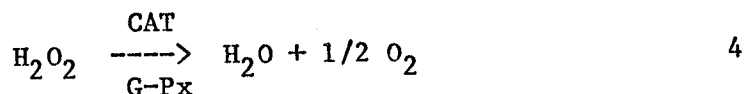
relatively stable radical (34), it can diffuse and affect targets removed from its site of production. The superoxide radical can produce direct cellular damage by iron catalyzed lipid peroxidation (35), sulfhydryl oxidation (36), and chain oxidation of dinicotinamide-adenine nucleotide, NADH (37). It participates in lipid peroxidation of membranes (38-40) via its ability to react with peroxide to form the hydroxyl free radical, which is a powerful oxidizing agent (24, 41). The hydroxyl radical initiates lipid peroxidation by abstraction of hydrogen atoms from fatty acyl groups (31). Singlet oxygen (1O_2) formed from superoxide is also capable of being a lipid peroxidizing and hemolytic agent (42). This species of activated oxygen may be more discriminating than $\cdot OH$ and hence more likely to cause peroxidative damage at critical sites (43).

Although lipid peroxidation by dioxygen or active oxygen may be a major cause of hemolysis, it is not the only mechanism of cellular damage. Exposure of RBCs to H_2O_2 or superoxide was recently shown to stimulate the degradation of cellular proteins to free amino acids without cell lysis (44). This supports the hypothesis that ATP-dependent proteolysis removes abnormally structured proteins, damaged by reactive materials in the cellular environment. Thus, in aged blood cells, this function might cease, resulting in an increase in damaged proteins that may produce altered properties and distributions.

Cytoplasmic Cu/Zn SOD is considered a first line of defense against the deleterious effects of activated oxygen (7, 36). This enzyme scavenges superoxide (reaction 3)



and thereby prevents the formation of more potent radicals and chain reactions (11). Hydrogen peroxide is eliminated by catalase (CAT) or glutathione peroxidase (G-Px), reaction 4:



SOD and catalase have also been shown to act synergistically in RBCs to prevent lipid peroxidation by activated oxygen (45, 46). Other lines of defense against superoxide are antioxidants located in the membrane. Of these, Vit.E appears to be the most important (38, 47-54). A close functional interrelationship has been proposed between Vit.E and glutathione peroxidase, a cytoplasmic enzyme loosely associated with the membrane (55). It has been stated that "Vit.E functions by neutralizing the free radicals at the site of their formation whereas G-Px appears to be involved in the intracellular decomposition of lipid hydroperoxides" (56). Not all studies, however, support the sole role of Vit.E as a membrane antioxidant. Rather, evidence exists that Vit.E may modulate the structure and permeability of the phospholipid bilayer in cellular membranes (57). Hence, stabilization of biological membranes may be the result of both antioxidant and structural interactions between Vit.E and unsaturated fatty acids.

Another membrane-based defense against activated oxygen has been postulated. It has been suggested that the cytosol-facing membrane enzyme, NADH oxidoreductase, could serve as a last line of defense (2), perhaps by accepting electrons from activated oxygen species in the oxidation of NADH. This has yet to be experimentally confirmed, however.

In certain instances these defenses can become ineffective in two ways, causing pathological conditions. Inherited rare diseases, such as thalassaemia and unstable hemoglobins, result in increased formation of activated oxygen, which overwhelms the existing defenses (58-61). This is associated with increased superoxide production and increased membrane lipid peroxidation (62). Other rare conditions, such as deficiencies in Vit.E (51), G-6-PD (8), catalase (9) and G-Px (9) result in decreased protection. In both situations, the consequence is often severe hemolytic anemia.

Radiation exposure can also lead to hemolysis. Radiolysis of aerated water forms a variety of activated oxygen species that attack the RBC membrane and cause the RBC to hemolyze. Radiation may also inactivate macromolecules directly by disruption of chemical bonds, cross-linking or membrane degradation (63). In particular, it has been shown that as sulfhydryl groups are lost, hydroxyl radical-induced lipid peroxidation ensues as the chemical precursor of structural membrane damage (31).

Prolonged exposure to oxygen (64, 65) or oxidative drugs, such as antimalarials and acetylphenylhydrazine (60), also increase formation of activated oxygen with similar consequences.

C) Superoxide Dismutase and Superoxide Anion

Although first isolated in 1939 from human RBC cytoplasm as 'haemocuprein' (66), the functional importance of SOD was unknown until 1969 when McCord and Fridovich discovered its superoxide dismutase activity (67). Since then, the 1970's have seen SOD as one

of the most intensely studied enzyme of the decade (39, 68-76). This pattern has continued into the '80's (15, 77-83) and reflects the importance of this enzyme as an intrinsic defense mechanism in aerobic organisms (11), and ultimately its potential as a therapeutic agent (84) in the control of disease and radiation exposure (85, 86).

Its physical properties have been well established in the literature (for reviews see refs. 68, 69, 72, 73, 87). Cytoplasmic SOD is a dimer of two identical subunits linked noncovalently (88). The total molecular weight is about 33,000 daltons and the isoelectric point is around 4.85 (76). Each subunit contains 153 amino acids (89) and prosthetic metals that determine the isoenzymic form of the molecule (90). Mammalian cells contain two types of SOD. One type is found in the cytoplasm and contains one atom of copper (the catalytic center) and one atom of zinc (ancillary role) per subunit. The second type is found in mitochondria and bacteria and contains one manganese atom at each active center. A third type is found in prokaryotes and contains one iron atom per subunit instead.

Association of SOD with membranes is not well documented. The first reported study appeared in 1974 and described multiple forms of Cu/Zn SOD in the blue-green alga Spirulina and in spinach. Distinct chloroplast and cytoplasmic SOD activities, in addition to a novel membrane-bound SOD in chloroplast lamellae, were detected and partially purified (91). Lamellar SOD in isolated spinach and sugarbeet chloroplasts was again observed the next year by another group (92). Theoretical considerations suggested that the membrane-bound SOD was there to protect the chloroplast lamellae and the photosynthetic apparatus within it against superoxide, generated

by photosystem I or II, by the water splitting system or by reduced ferredoxin.

A report on SOD associated with a mammalian cell membrane followed shortly (93) but the association was regarded as incidental, resulting from contamination by cytoplasmic SOD. The extent of contamination was given as < 0.3 % of the SOD originally present in the intact cell.

The distribution of SOD in bovine RBC membranes was subsequently described (75). Experiments showed that about 1 % of the SOD in bovine RBCs remained with the ghosts. Comparison of uptake of ^{125}I -labelled antibodies by intact RBCs, ghosts and inside-out vesicles suggested that the major portion of the membrane-associated SOD was located on the cytoplasmic side.

The following studies of SOD interactions with model lipid membranes and uptake of SOD by cells support the existence of SOD within membranes in a structurally and functionally significant capacity. It has been shown by electron microscopy of ghosts, reacted with ferritin-labelled antibodies, that Cu/Zn SOD is internalized in RBC ghosts (75). This implies a phospholipid association which spin label studies later demonstrated. Studies with spin-labelled egg-lecithin liposomal membranes showed that SOD associated with the surface, increasing its viscosity, and also with the hydrocarbon region, increasing its order (94). This suggests that by close contact with fatty acids, SOD could be in a preferred position to protect lipid membranes against oxidative damage by superoxide. Uptake of ^{125}I -SOD demonstrated that both holo- and apo- forms of the enzyme associated with and became embedded in lipid bilayers (95). Other

studies showed that SOD, by itself or packaged in liposomes, as well as chemically modified SOD, had variable capacity for RBC membrane penetration (82). Hence, SOD must possess the amphipathic character common to other membrane proteins.

In 1980, a new cytochemical method clearly demonstrated the presence of SOD activity in the RBC matrix, and suggested the presence of SOD in the plasma membrane (96). Xanthine and xanthine oxidase were used to generate the substrate, superoxide, while cerium chloride was used to precipitate H_2O_2 , the dismutation product of superoxide when catalyzed by SOD. After 1 % gluteraldehyde fixation, the electron dense cerium perhydroxide deposits were visualized by transmission electron microscopy and found throughout the RBC cytoplasm and in proximity to the plasma membrane. RBCs in the presence of an incomplete superoxide generating system, catalase or inhibitors of SOD, failed to show the cerium perhydroxide deposits. Together, these results implicate the presence of active SOD in the cytoplasm and at the plasma membrane.

In 1981, the association of SOD with bovine RBC membranes was described in more detail (15). It was found that solubilization of ghosts with the nonionic detergent, Nonidet P-40 (NP-40), extracted twice as much SOD as a chloroform-ethanol extraction. NP-40 extracted ghosts, when measured for active SOD by a polyacrylamide gel electrophoretic assay, were found to contain 0.4 ± 0.2 % of the cellular SOD. A double antibody solid phase radioimmunoassay measured only 0.07 ± 0.008 % of the cellular SOD, suggesting that much of the active membrane-bound SOD is antigenically distinct from the cytoplasmic SOD. Affinity chromatography, using an immunosorbent of

anti-SOD antibody coupled to Sepharose, resolved two components in NP-40 extracts of bovine RBC ghosts: an active form of the enzyme, antigenically similar to cytoplasmic SOD, and an inactive form, unreactive with antibody, of which 0.23 % was restored to active SOD by reconstitution with Cu^{2+} .

These results suggest that the membrane-associated SOD may have distinctive features, which could facilitate or reflect its role as an antioxidant within membranes. Further studies on SOD isolated from membranes are clearly needed.

Studies on the effect of superoxide on human RBC membranes also point to an association of SOD with the plasma membrane. It has been clearly demonstrated that xanthine oxidase-generated superoxide crosses RBC ghost membranes via the anion channel (12, 13). These data suggest a requirement for SOD within the membrane in defense against potential deleterious effects from the radical. Further, it has been demonstrated that RBC ghosts are protected by SOD against lipid peroxidation, induced by the xanthine oxidase-superoxide generating system (97).

Finally, the presence of copper and non-heme iron has been demonstrated in plasma membranes of various mammalian cells, including RBCs (98). Zinc was not determined. It is thought that these metals may be associated with membrane-bound redox enzymes such as NADH oxidase and glutathione oxidase. These results can similarly be discussed in support of the presence of Cu/Zn SOD within RBC membranes.

D) Experimental Approach

Investigation of proteins, in general, requires their isolation and characterization. Characterization of proteins, regardless of their origin in a biological scheme, employs classical methods like molecular weight determination, amino acid analysis, amino acid sequencing, etc. Isolation of some proteins, particularly membrane proteins, requires specialized techniques and even then, may fall short of yielding a purified protein that is identical to its *in vivo* form. Membrane proteins encounter various interactions with lipids and other proteins, the removal of which could leave the isolated protein in an altered state. Thus, the study of membrane proteins must be approached with this understanding of membrane organization.

The isolation of proteins from RBC membranes usually requires the preparation of 'hemoglobin-free' membranes (ie.: ghosts), in order to eliminate or minimize potential interferences in biochemical assays. Procedures for making ghosts are numerous but the most popular one is that of hypotonic hemolysis of which there are many variations (4). Ghosts prepared by this technique are thought to be very similar in composition to the intact cells from which they are derived (4). The technique involves five basic steps (99):

- a) Preparation of blood for lysis by removal of plasma and buffy coat of WBCs.
- b) Lysis by mechanical stress due to lowered osmotic pressure.
- c) Restoration of tonicity (optional).
- d) Resealing by incubation.
- e) Isolation by centrifugation.

Studies have proven that preparation methods and conditions can greatly influence the condition of the isolated membranes (4, 100) and consequently, enzyme activity (3). Thus, it is important to provide as many criteria as possible to identify a particular membrane preparation.

Factors influencing ghost preparation and subsequent characterization of the membranes, can be divided into three groups (3):

a) Donor (eg.: age and state of health)

It is possible to isolate three distinct groups of ghosts by hypotonic lysis. They are: fast resealers (Type I), slow resealers (Type II) and non-resealers (Type III). The age of the donor will dictate the ratio of these groups; the older the donor, the larger the proportion of Type III in a heterogeneous ghost population. Such non-resealers are less dense than the resealers and hence, may not sediment, resulting in poor yield. This factor may have caused the variations in the present study as the donated blood was obtained at random and thus, donor age was not controlled.

b) RBC Age

Within a blood sample there is an age distribution in RBCs, which results in a heterogeneous population of ghosts after isolation. Such a mixed population of RBCs also affects the yield of ghosts, as well as their hemoglobin content and enzyme activities. For example, in membranes of old cells certain enzymes have decreased activity (eg.: G-6-PD), decreased cholesterol and lipid content, decreased size, increased protein aggregates, fragility and hemoglobin (Heinz bodies) (3, 101). A decrease in cytoplasmic SOD activity has also been

demonstrated in aging RBCs (102).

c) Conditions of Preparation

Maintenance of ghost morphology and enzyme activity that remains fixed to isolated membranes will depend largely on the conditions under which they are prepared: pH and ionic strength of the hemolysing buffers, temperature, presence of proper ligands and divalent cations, centrifugal force, etc. For example, it has been shown that hemolysis at room temperature increases the number of Type I ghosts at the expense of Type II ghosts (4). This will have its disadvantage when the ghosts are to be loaded with specific substrates and salts prior to resealing. Hemolysis at 0°C will prevent this. With hemolysis at pH 6.0, Type III ghosts are virtually eliminated (4) but ghost hemoglobin is significantly increased (100). The ionic strength of the hemolysis buffer has a specific value (20 mosM) at which residual ghost hemoglobin is minimized (100). At buffer concentrations above and below this value, ghost hemoglobin is increased. In this light, ghost hemoglobin may be an indicator of the membrane-association of other cytoplasmic components.

Freshly isolated ghosts are solubilized to form a suspension from which proteins can be separated. The methods are again numerous (103) but fall into three categories (104) according to the ability of agents to solubilize membranes:

- a) totally (eg.: sodium dodecyl sulfate, SDS; non-ionic detergents; guanidine hydrochloride).
- b) selectively (eg.: change of ionic strength; acid anhydrides; detergents).
- c) glycoproteins (eg: lithium diiodosalicylate).

The solubilization method used should yield a membrane component that is inherent and biologically significant and in a state amenable to further study.

The solubilized suspension of ghost material is then subjected to separation techniques to isolate the protein of interest. These techniques include the classic methods of electrophoresis, ammonium sulfate precipitation, chromatography, alcohol extraction, etc.

To illustrate the overall procedure of the isolation of a membrane-bound protein, consider the case of the classic RBC membrane-marker enzyme, ACHE. Situated within the lipid core, its active site is exposed to the outside face of the cell. This enzyme constitutes about 0.01 % of the total membrane protein (105). A method reported in 1974 (106) was thought to yield ACHE of the highest purity and specific activity from human RBCs. This method used the hypotonic hemolysis technique of Dodge et al. (100) to prepare the hemoglobin-free ghosts, which were then totally solubilized with the ionic detergent, deoxycholate (1.3 %, w/v). Other detergents like SDS completely inactivated the product while Triton X-100 led to heterogeneous proteins and Tween 80 gave products of unpredictable properties. Precipitation of the active protein with $(\text{NH}_4)_2\text{SO}_4$ to remove the lipids followed. The protein fraction was then chromatographed on a Sephadex G-200 column and desalted by passing through a Sephadex G-75 column. Dialysis against distilled water and then TRIS buffer prepared the protein for activity determination, polyacrylamide gel electrophoresis (PAGE) and lyophilization.

Another example of membrane protein isolation is that of SOD from bovine ghosts (15). Although only a partial purification, it is more

pertinent to this study. It begins with ghost preparation from fresh bovine blood using the hypotonic hemolysis method of J.Th. Hoogeveen et al. (19). Its high selection factor of 1500:1 for inner membrane surface proteins over hemoglobin in the ghosts suggests a high degree of purity from cytoplasmic components. The non-ionic detergent, Nonidet P-40 (NP-40), was used to extract the enzyme from the membranes. It may be noted that precipitation of proteins with chloroform-ethanol extracted only half the SOD activity that the detergent did. NP-40 treated ghosts were concentrated, clarified and subjected to affinity chromatography on a column of Sepharose-rabbit anti-bovine-SOD antibody, which separated the extract into the two components: active and inactive SOD. After dialysis against phosphate buffered saline, samples were subjected to PAGE and radioimmunoassay.

The experimental approach in this study has drawn on developments like these, in addition to developing new approaches. Thus, human RBCs were made into ghosts using the Hoogeveen method (19) and compared with another method (107). The resultant ghosts were assayed for protein, hemoglobin, ACHE activity, and 5'-nucleotidase activity. Observation of the ghosts under phase contrast and electron microscopy revealed their morphology. Ghost solubilization with NP-40, dialysis against H₂O and sodium perchlorate and further concentration prepared the extract for separation of the membrane-associated SOD by high performance liquid chromatography (HPLC). Polyacrylamide gel electrophoresis (PAGE) was used to assay semi-quantitatively the amount of enzyme in the membrane.

CHAPTER 3: Experimental

A) Materials

The following materials were obtained from the Sigma Chemical Company, St. Louis, Missouri:

Acetylthiocholine iodide

Bovine serum albumin (BSA; essentially fatty acid-free; from fraction V albumin)

Coomassie Brilliant Blue R 250

5',5'-Dithiobis-(2-nitrobenzoic acid) (DTNB)

Ferricytochrome c (type VI; from horse heart)

Glycine (free base)

D,L-Methionine (grade I)

Nitroblue tetrazolium (NBT; grade III)

5'-Nucleotidase (grade IV; from *Crotalus atrox* venom)

Potassium phosphate

Quinidine sulfate

Riboflavin

Sigma 7-9 biochemical buffer (TRIS)

Sodium adenosine-5'-monophosphate (Na-5'-AMP)

Sodium chloride

Xanthine (Sigma grade)

Xanthine oxidase (grade III; from buttermilk)

The following certified A.C.S. reagents were obtained from the Fisher Scientific Company, Winnipeg, Manitoba:

Ammonium molybdate

Ammonium persulfate

Amyl acetate

Cupric sulfate

Cyanogum 41 gelling agent

Ethanol

Glycerol

Mercuric chloride

Phenol reagent solution 2N (Folin-Ciocalteu)

Potassium cyanide

Potassium hydroxide

Potassium tartrate

Sodium acetate (HPLC grade)

Sodium carbonate (anhydrous)

Sodium hydroxide

Sodium perchlorate

Sodium phosphate

Sodium sulfate

These 'Baker Analyzed' materials were obtained from the J.T. Baker Chemical Company, Phillipsburg, New Jersey:

Acetic acid (glacial)

Boric acid

Disodium ethylenediamine tetraacetate (EDTA)

Magnesium chloride

Ascorbic acid was supplied by the Aldrich Chemical Co, Milwaukee,

Wisconsin; cyanmethemoglobin reagent was obtained from Hycel, Inc., Houston, Texas through Canlab, Winnipeg, Manitoba; human RBC cytoplasmic Cu/Zn SOD from Isolab Inc., Akron, Ohio; reagent grade isopropanol, sodium bicarbonate and trichloroacetic acid (TCA) from Anachemia Ltd., Toronto, Ontario; Nonidet P-40 from Particle Data Laboratories, Elmhurst, Illinois; N,N,N',N'-tetramethylethylenediamine (TEMED) and sodium dithionite from Eastman Kodak Co., Rochester, New York; pyridine (spectroquality) from Matheson, Coleman and Bell, Norwood, Ohio; phosphatidyl choline (di-[cis-9,12-C₁₈2=]) from Avante Polar Lipids, Birmingham, Alabama; reagent grade zinc sulfate from Baker and Adamson, New York, New York. All aqueous solutions were made with double distilled water.

B) Ghost Preparation

Fresh human whole blood was collected by the local Canadian Red Cross in one unit quantities (63 ml of anticoagulant citrate phosphate dextrose solution, USP, plus 450 ml \pm 10 % blood). Ghosts were prepared by the serial hypotonic hemolysis method of J. Th. Hoogveen et al. (19) with minimal modification. For a preparation, one-half unit of blood was divided equally among fifteen to twenty 15 ml polystyrene culture tubes and centrifuged at 3,000xg (IEC clinical centrifuge) for 10 m at 5°C. The plasma and buffy coat were removed by aspiration. The packed cells were then pooled into 40 ml polyethylene centrifuge tubes and washed three times in 3 volumes of isotonic saline (0.05 M sodium phosphate with 0.15 M NaCl, pH 8.0). The supernatant was clear and colorless after the second wash if fresh

cells were used but still pink after the final wash if outdated blood was used. (Outdated blood is too old to be used for transfusion.) An aliquot of washed, packed RBCs was retained for hemoglobin determination.

The hemolysis was performed in 3 steps using in sequence 60, 30, and 20 mosM buffer pH 7.4, prepared by dilution in H₂O of a stock buffer solution containing 0.20 M NaCl, 0.075 M Na₂HPO₄, and 0.025 M KH₂PO₄ (total osmolarity: 675 mosM). The washed cells, further distributed among the appropriate number of centrifuge tubes, were exposed to 8 volumes of buffer at room temperature. EDTA was added to 1 mM (as a protease inhibitor and to aid resealing by removing divalent ions), then the tubes were balanced, mechanically shaken for 30 m at 30°C and finally centrifuged at 10,000xg in a JA-20 rotor for 20 m at 5°C in a Beckman Model J-21B ultracentrifuge. This procedure was repeated once for the 60 and 30 mosM buffer and twice for the 20 mosM buffer. At each step, the supernatant was carefully aspirated. Cream-colored pellets of aggregated WBCs (rich in proteolytic activity) were removed when present. In the last steps, buttons of resistant RBCs were also aspirated. The contents of the tubes were pooled in the final step. Initially, the process was stopped after cells were shaken in one of the 20 mosM steps and the samples stored overnight at 5°C. The process was completed the following day. Eventually, the process was completed in one day. The resultant ghost pellets were pooled, measured for volume and stored briefly at 5°C until further use.

For comparison purposes, another ghost preparation procedure was attempted. The procedure described Burton et al. (107) is reported to

be an improved method for the isolation of unsealed ghost membranes from human RBCs. In the present work, this method was modified to produce resealed ghosts. Whole blood was washed and prepared for hemolysis as described above. The hemolysis was performed at room temperature in three steps using eleven volumes of 5.0, 2.5, and 1.25mM phosphate buffer, pH 8.0 (about 10, 5, and 3 mosM, respectively), prepared by dilution of a 0.05 M sodium phosphate stock buffer (about 100 mosM). Addition of EDTA and shaking at 30°C as above were steps incorporated into this technique to reseal the ghosts. Pellets of resistant RBCs were also removed. Ghost suspensions were sedimented at 22,000 $\times g_{\max}$ for 10 m at 5°C. Since some hemolysates were faintly pink, the process was repeated once, followed by pooling of the cells for the hemolysis in 1.25 mM buffer.

C) Photography

Photographs of the RBC ghosts were taken under the scanning electron microscope (SEM) and the phase contrast microscope. The Anderson Critical Point Drying method (108) was used to prepare ghosts for SEM. Ghosts, air dried on sectioned glass coverslips, were dehydrated in an ethanol series (25%, 50%, 75%, 100% ethanol in H₂O; by volume). A similar series replaced ethanol with amyl acetate (25%, 45%, 50%, 90%, 100% amyl acetate in ethanol; by volume). Using a 'homemade' pressure chamber, amyl acetate was replaced with liquid CO₂, which converted to gaseous CO₂ at its critical pressure (1070 psi) and temperature (31.1°C). The slides were bonded to silver studs using 'silver tag' (an adhesive) and briefly stored in a desiccator

until ready for gold shadowing on a Balzers Union sputterer. SEM observations were made on a Cambridge Stereo Scan, Mark II or an ISI (International Scientific Instruments) DS (dual stage) - 130 SEM. Polaroid film was used in the photography.

Ghosts were photographed under phase contrast at the same time they were counted. The film used was Kodak Plus-X Pan for black and white prints.

D) Cell Counts

The RBC count was performed according to standard clinical technique (109). A suspension of 5.0 ul of whole blood in 995.0 ul of filtered Hayem's fluid (2.5 % $\text{Na}_2\text{SO}_4 \cdot 10\text{H}_2\text{O}$, 0.25 % HgCl_2 , 0.5 % NaCl ; weight to volume of H_2O) was vortexed, applied to a hemocytometer and counted under 250x power (Leitz Wetzlar light microscope). The sum of the number of RBCs in the 4 corner squares and the central square was multiplied by 10^4 (# cells in 80 squares $\times 50 \text{ mm}^3/\text{square} \times 200$ dilution factor) to express the count as #RBCs per mm^3 of whole blood or by 10^7 ($10^4 \times 10^3 \text{ mm}^3/\text{ml}$) to express the count as #RBCs per ml of whole blood.

Washed RBCs were counted similarly except a suspension of 5.0 ul washed cells in 1.995 ml of Hayem's fluid was used. This changed the dilution factor to 2×10^4 .

Freshly prepared ghosts were diluted 1:100 in 20 mosM hemolysis buffer and counted in a Petroff-Haussen bacteria counting chamber under phase contrast at 625x power (Carl Zeiss Ultraphot 11). The 4 corner squares (which each consisted of 16 smaller squares) were

counted and averaged. The number of ghosts per ml of suspension was calculated as follows:

$$\frac{\text{average count}}{16 \times 1 \text{ mm}^3 / 20,000 \text{ squares}} \times 10^3 \text{ mm}^3 / \text{ml} \times 10^2 \text{ dilution factor}$$

This result was checked against a Coulter count: the ghosts were diluted 1:10,000 in 20 mosM buffer and then diluted 1:20 in PBS. The count of the diluted ghost suspension was corrected for background counts of the buffer. The average number of ghosts per ml of ghost suspension = average Coulter count of diluted sample x dilution factor, 4×10^5 .

E) NP-40 Treatment

Nonidet P-40 (NP-40) is a nonionic detergent. It was chosen as the solubilizing agent of the ghosts for two reasons. Firstly, its membrane disruptive properties were necessary to extract significant amounts of SOD from the ghosts, since it was shown by trypsinization that SOD is embedded within membranes (trypsin removed only a fraction of the membrane-associated SOD) (89). Secondly, (unpublished) studies in this laboratory showed that 0.1% NP-40 had less deleterious effects on bovine RBC cytoplasmic SOD activity than other membrane disruptive agents such as sodium dodecyl sulfate and Tween 80. NP-40 was added to fresh ghosts to a concentration of 0.1 % (v/v). Incubation followed for 1 hour at 37°C in a water bath with periodic agitation. The sample was then dialyzed (12,000 MW cutoff) for 3 days at 5°C against double distilled H₂O. Volumes of sample were measured before and after dialysis to obtain the dilution factor. The samples were centrifuged

in an Eppendorf tabletop centrifuge (12,800xg) for 4 m prior to PAGE.

Ghost material to be analyzed by HPLC was further dialyzed (immediately after H₂O dialysis) against 0.10 M NaClO₄, pH 7.4 plus 0.05 M NaH₂PO₄·H₂O for 24 hours to remove bound EDTA (110). Three days of dialysis against H₂O removed the perchlorate. The sample was centrifuged at 42,000xg at 5°C (45 m) for clarification (15). Two approaches were then used to concentrate and clean-up these samples for HPLC:

- a) Concentration at 0°C by vacuum filtration (Millipore^R CX-10 ultrafiltration unit; 10,000 M.W. cutoff; Millipore, Mississauga, Ont.) followed by evaporation at 0°C under a filtered argon stream. The concentrate was then clarified by Millipore^R filtration (Millex GS 0.22 um filter) or centrifugation at 12,800xg as above.
- b) Concentration by rotary evaporation at room temperature, followed by centrifugation at 42,000xg for 45 m or at 100,000xg for 1 hour at 5°C.

F) Protein Assay

Ghost material was assayed for total protein by the method of Lowry et al. (111) using bovine serum albumin (BSA) as standard. The color production in this assay is the result of two chemical reactions:

- a) formation of a copper-protein complex in alkaline solution.
- b) reduction of the phosphomolybdic-phosphotungstic reagent (i.e.: the phenol reagent) by the copper-protein complex.

Aliquots (0, 10.0, 20.0, 40.0, 100.0, 150.0, 200.0, 250.0, 300.0 ul) of standard BSA solution (0.500 mg / ml H₂O) and aliquots of ghost material were adjusted to 1.00 ml with H₂O in liquid scintillation vials. Exactly one ml of alkaline copper reagent was then added to each vial, mixed and allowed to stand undisturbed for at least 30 m.

The alkaline copper reagent was prepared in two steps:

- a) 2.0 g NaOH dissolved in 40 ml H₂O was added to 10.0 g Na₂CO₃ and mixed until dissolved.
- b) 0.0500 g CuSO₄·5H₂O was dissolved in 40 ml H₂O after which 0.100 g K₂C₄H₄O₆·1/2H₂O was added and dissolved.
- c) The above two solutions were quantitatively combined in a 100 ml volumetric flask and diluted to the mark with H₂O.

After the standing period, 4.00 ml of a phenol working solution (12.5 ml of 2 N phenol reagent plus 200.0 ml H₂O) was added quickly with force to each vial. The vials were capped, placed in a 55°C H₂O bath for 5.0 m and then cooled to room temperature in cold H₂O. The absorbance was read at 650nm using a Beckman Model UV 5230 spectrophotometer. From the standard curve (A_{650nm} versus mg protein per vial), the protein concentration of the ghost samples was determined and expressed as mg protein per ml of ghost suspension. Knowing the ghost count, the protein was expressed as g protein per ghost.

G) Hemoglobin Assay

The hemoglobin content of the ghosts was determined by the pyridine-hemochromogen method as described by Dodge et al. (100). The

principle of the assay is based on the conversion of the pyridine-hemoglobin complex by sodium hydrosulfite to pyridine-hemochromogen, which adsorbs strongly in the Soret band at 418nm. In the assay, diluted washed RBCs (5.0 ul in 21.0 ml H₂O) and diluted fresh ghosts (1.00 or 2.00 ml ghost suspension in 8.00 ml H₂O) were divided into four ml aliquots. One ml pyridine was added with mixing by vortex. After 45 m, 25.0 mg Na₂S₂O₄ was added to each test tube in the dark (0.100 ml of Na₂S₂O₄ stock: 0.2500 g/10.00ml H₂O). The absorbance at 418nm was read after 10 m with distilled H₂O as the blank and reference.

The average weight of hemoglobin per RBC was measured by the Hycel^R method (Hycel Inc., Houston, U.S.A.) as the mean corpuscular hemoglobin (MCH). The principle of the assay is as follows: the Hycel Cyanmethemoglobin reagent contains saponin, which causes the lysis of the RBCs and the release of their hemoglobin. The potassium ferricyanide in the reagent oxidizes the ferrous iron of the hemoglobin to the ferric state, forming methemoglobin. Methemoglobin then reacts with cyanide ions (from potassium cyanide) to form cyanmethemoglobin, which has A_{max} at 540nm. In the assay, 6.0 ml of cyanmethemoglobin reagent was mixed with 0.200 ml washed RBCs. After standing for 10 m, %T was measured at 540nm on a Coleman Junior 11 Model 6/20 spectrophotometer. From the standard curve (%T_{540nm} as a function of % hemoglobin or g of hemoglobin per dl) gram % hemoglobin was determined for the RBCs from which MCH was calculated:

$$\text{MCH} = \frac{\text{g \% hemoglobin}}{\text{RBC count (millions/mm}^3\text{)}}$$

Finally, ghost hemoglobin was calculated and expressed as a percentage

of the MCH using the following equations:

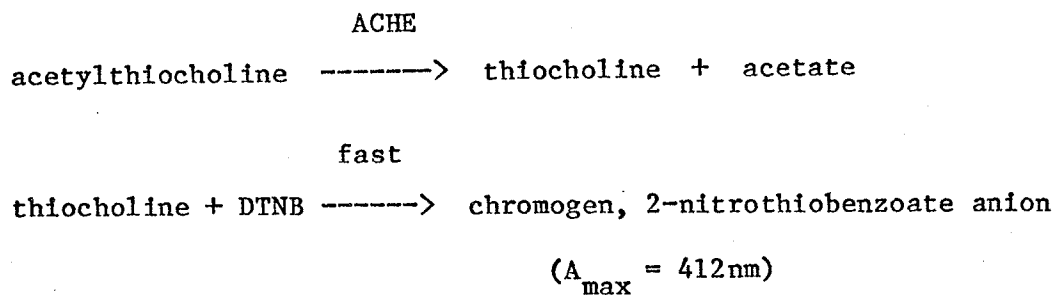
$$\text{Ghost hemoglobin} = \frac{A_G}{A_E} \times \frac{DF_G}{DF_E} \times \text{MCH}$$

$$\text{Hemoglobin \%} = \frac{\text{Ghost hemoglobin}}{\text{MCH}} \times 100$$

where A_G and A_E are the absorbance values at 540nm of the pyridine hemochromogen from the ghosts and RBCs, respectively. DF_G and DF_E are the respective dilution factors in the assay solutions.

H) Acetylcholinesterase (ACHE) Assay

ACHE activity of the RBC ghosts was determined by the method of Ellman et al. (112). This activity is measured spectrophotometrically following the increase of the yellow color formed when the hydrolysis product, thiocholine, reacts with dithiobisnitrobenzoate ion (DTNB):



The spectrophotometric cells (sample and reference) contained the same solutions except the reference cell lacked the substrate. To each 3.5 ml cell is added 3.00 ml of 0.10 M sodium phosphate buffer, pH 8.0, 10.0 ul of ghost extract and 50.0 ul of reagent. The reagent contains 39.6 mg DTNB, 10.0 ml 0.10 M sodium phosphate buffer, pH 7.0 and 15.0 mg sodium bicarbonate. After mixing, the cells are placed in

the spectrophotometer set at 412nm. Then, 20.0 ul of 0.075 M acetylthiocholine iodide was added quickly to the sample cell only, stirring the contents of the cell with the microPipetman tip. The development of the yellow anion was then followed for at least 6 m as an increase in absorption at 412nm.

Data analysis involved plotting $A_{412\text{nm}}$ as a function of time (m) to give a line with slope ΔA , which represented the rate of formation of the chromogen. Since the extinction coefficient of the 2-nitrothiobenzoate anion is known ($13,600 \text{ m}^{-1} \text{ cm}^{-1}$ at 412nm), the rates were converted to absolute units:

R = moles of substrate hydrolyzed per m per RBC or ghost.

$$= \frac{\Delta A}{C} \times \frac{DF}{13,600} \times \frac{1}{10^6 \text{ RBC mm}^3/1}$$

where: ΔA = change in absorbance per m (slope)

C = RBC (or ghost) count (millions/ mm^3)

DF = dilution factor

I) 5'-AMP-Nucleotidase Assay

5'-Nucleotidase is a widely distributed and an externally orientated, membrane-bound enzyme with broad substrate specificity for ribonucleotides. In this study, 5'-nucleotidase, specific for 5'-AMP, was assayed by the method of Touster and Aronson (113) where the activity of the enzyme is determined by measuring the rate of release of P_i from 5'-AMP in human RBC ghosts. P_i was measured by the sensitive colorimetric method of Chen et al. (114).

Samples of freshly prepared ghosts and extracts (50.0 ul), a H_2O

blank, 20, 30, and 60 mosM hemolysis buffer (50.0 ul), RBC wash buffer (50.0 ul), standard phosphate solution (3.0 to 30.0 ul of 0.025 M $\text{NaH}_2\text{PO}_4 \cdot \text{H}_2\text{O}$), and 8 ug standard 5'-nucleotidase (with and without 1 mM EDTA) were made up to 0.050 ml with distilled H_2O and combined with 0.450 ml of the assay mixture (50 mM Na-5'-AMP, 0.50 M glycine-NaOH buffer, pH 9.1, 0.10 M MgCl_2 , and distilled H_2O in a ratio of 1:2:1:5) to start the reaction. Tubes were incubated at 37°C in a shaking incubator bath for 30 m (accurately measured). The reaction was stopped by adding 2.5 ml of 8 % trichloroacetic acid (TCA). Samples were centrifuged at 3000xg at 5°C to sediment protein precipitates. One ml aliquots were removed for P_i determinations by the method of Chen et al. (114). Samples were diluted to 1.20 ml by adding 200 ul of distilled H_2O . Then 2.8 ml of 'mix' (1 volume of 10 % ascorbic acid, w/v, plus 6 volumes of 0.42 % ammonium molybdate, w/v, in 1.0 N H_2SO_4) was added to each sample. Incubation at 37°C for one hour followed to permit color development. After returning the samples to room temperature, their absorbances at 820nm were read. Using a standard curve of $A_{820\text{nm}}$ as a function of umole P_i , the activity of 5'-nucleotidase, specific for 5'-AMP, was found and expressed as umole P_i released per m per mg protein.

J) Polyacrylamide Gel Electrophoresis (PAGE)

PAGE was performed by the method of Beauchamp and Fridovich (115), as described by Petkau et al. (15). This technique had the advantage of resolving SOD activity and protein from other proteins while allowing a direct comparison with Cu/Zn cytoplasmic SOD. Twelve

10 % disc gels were prepared just before use as follows: 3.00 g Cyanogum 41 was dissolved in 30.0 ml PAGE buffer (see below) to which 30.0 ul TEMED was added and mixed. Just before pouring, 0.0150 g $(\text{NH}_4)_2\text{S}_2\text{O}_8$ was added and dissolved. After pouring, the gels were carefully layered with PAGE buffer to prevent meniscus formation.

PAGE buffer was prepared by a 1:10 dilution of stock PAGE buffer with distilled H_2O , the pH being adjusted to 8.40 with 4 M NaOH. The stock buffer was prepared by dissolving 2.531 g EDTA, 12.368 g boric acid and 25.431 g TRIS in distilled H_2O and then diluted to one liter.

Following polymerization under fluorescent light, the gel tubes were placed into the grommets of a Gelman cylindrical electrophoresis chamber. The buffer was added to the chambers and the gels were pre-run for one hour at 2 mA per tube (24 mA total) to remove impurities and $(\text{NH}_4)_2\text{S}_2\text{O}_8$ which may interfere in the separation.

Six gels were layered with variable amounts (2 to 64 ul) of the standard reference enzyme solution (1.5 uM aqueous solution of cytoplasmic Cu/Zn SOD from human RBCs for the activity assay or 3.1 uM aqueous solution of the same enzyme for the protein assay). The remaining 6 gels were layered with variable amounts (50 to 300 ul) of ghost extract. All samples, prior to gel application, were mixed in 20 % glycerol to increase density.

For the first 15 m of the electrophoresis, the current was held constant at 0.5 mA per tube and then increased to 2 mA per tube for the duration of the run. The total run time for SOD activity was 80 m and for SOD protein was 90 m.

Using a long needle for rimming, the gels were removed immediately from the tubes after the run and placed in test tubes for

staining. The nitroblue tetrazolium (NBT) reduction method of Beauchamp and Fridovich (115) was used to stain for SOD activity. Gels were soaked at 30°C in the following three solutions for 20, 15, and 30 m, respectively:

- a) 0.321 g NBT in 200 ml distilled H₂O.
- b) 3.0 mg riboflavin in 0.97 ml TEMED, 8.5 ml 0.10 M KH₂PO₄, 91.5 ml 0.10 M K₂HPO₄ and 200 ml distilled H₂O.
- c) 7.4 mg EDTA in 8.5 ml 0.10 M KH₂PO₄, 91.5 ml 0.10 M K₂HPO₄ and 100 ml distilled H₂O.

Soaking in the first two solutions took place in the dark. During the soaking in the third solution, the gels were brightly illuminated under a 20 watt fluorescent light. The developed gels were stored in the dark (0 to 24 h) until scanned by optical transmittance at 580nm, using an ISCO Model UA 5 Absorbance/Fluorescence Monitor and Gel Scanner Model 1310.

Gels were stained with Coomassie Brilliant Blue for protein. The stain consisted of 0.05 % (w/v) Coomassie Brilliant Blue R-250, 10 % acetic acid, 25 % isopropanol in distilled H₂O. The staining period (2 hours) was followed by a destaining period of several days using 7 % acetic acid (one change per day). The gels were scanned for optical absorbance at 580nm as above.

The areas corresponding to the peaks of the two reference enzyme activity bands were integrated by planimetry. These areas increased with log(SOD) and the slope of this line was used to calculate the amount of active enzyme in each extracted sample. Similarly, SOD-like protein in the extracts was determined, but peak areas increased linearly with the amount of SOD standard applied.

Identification of enzyme activity bands in the ghost extracts was based on their migration rates and their absence in boiled samples of extract. Boiling ghost extracts should denature proteins in the sample and render enzymes inactive. Thus, on PAGE gels, boiled ghost extracts failed to show any SOD activity band, in contrast to unboiled extracts. Similarly, the addition of a known aliquot of reference SOD to the ghost extract prior to PAGE and protein staining, identified the position of the SOD-like protein band with respect to other protein bands.

K) SOD Assays

The measurement of cytoplasmic SOD activity in the RBCs from which the ghosts were derived required the removal of hemoglobin. Briefly, the method used is as follows: 0.500 ml of whole blood was centrifuged in an Eppendorf centrifuge for 2 m. Plasma was removed. The pellet of RBCs was suspended in 0.500 ml isotonic saline and centrifuged as above. After repeating this step once, the pellet was suspended in 0.400 ml distilled H₂O; 150 ul ethanol and 90 ul chloroform were then added and mixed. This solution was stored in the fridge for 15 m with periodic shaking. After adding 100 ul distilled H₂O, the sample was again centrifuged. The supernatant was saved and its volume measured.

This lysate was then assayed for SOD activity by the NBT photoreduction method of Beauchamp and Fridovich (115). In this assay, superoxide is generated photochemically by the photoreduction of riboflavin. In the presence of methionine (an electron donor) and

reduced riboflavin, oxygen is converted to superoxide. The detector, NBT, is reduced to blue formazan by superoxide. If SOD is present, it will compete with this reaction resulting in an inhibition of formazan formation. Peroxidases present in the lysate are able to oxidize formazan back to NBT. Thus, cyanide is added to the system to inhibit them.

In this assay, aliquots of the standard solution of cytoplasmic SOD from human RBCs (8.0 to 50.0 μ l of 0.92 μ M SOD stock solution) and of the RBC lysate (2.0 to 30.0 μ l) were measured into liquid scintillation vials and placed in a dark room at 30°C. The reaction mixture was then prepared from stock solutions as follows:

55.6 ml 0.050 M potassium phosphate buffer, pH 7.8

2.00 ml NBT solution (0.1656 g/40 ml H₂O)

2.00 ml riboflavin solution (2.6 mg/100 ml H₂O)

0.200 ml KCN solution (3.9 mg/10 ml H₂O)

0.200 ml EDTA solution (0.112 g/10 ml H₂O)

This solution was warmed under hot tap water to 30°C and, in the dark, 0.0896 g methionine was dissolved in it. Three ml of this reaction mixture was then added to each vial. After mixing, the vials were arranged in a rotating circular illumination chamber and illuminated for 5.0 m under a 20 watt fluorescent light. The samples were measured immediately afterwards for absorbance at 560nm. Results were expressed in the form of the standard curve: % inhibition as a function of log(SOD).

This assay was not applicable for the assay of SOD in ghost membranes since variable biphasic inhibitory-stimulatory curves were obtained (15).

When HPLC fractions could no longer be analyzed for SOD activity by PAGE, the more sensitive assay developed by Kirby and Fridovich (116) was used. This ultrasensitive spectrophotometric assay is based on the fact that when cytochrome c is added to the xanthine:xanthine oxidase superoxide-generating system, its reduction by superoxide is biphasic, with the initial rapid phase dependent on the pre-existing steady state level of superoxide. This level is, in turn, dependent on the SOD activity present. The assay as described utilizes Sigma grade III xanthine oxidase and, for optimal sensitivity and reproducibility, requires that the addition of cytochrome c to the cuvettes (control and test) be equally precise and rapid, resulting ideally in homogeneous solutions at the same time.

In performing the assay, 30.0 μ l of ferricytochrome c (2.0 μ M in H_2O) and 20.0 μ l of xanthine oxidase (1:100 dilution of xanthine oxidase grade III solution) were added at time zero to a spectrophotometric cuvette containing 3.0 ml of buffer and substrate (15 mM Na_2CO_3 , 0.1 mM EDTA, 0.1 mM xanthine, pH 10.2 at ambient temperature). Cytochrome c reduction by superoxide radicals, generated over 10 m, was recorded as the rate in increase of absorbance at 550nm at a full scale span of 0.1 absorbance units. The reference cuvette contained 3.0 ml of buffered substrate and cytochrome c. The amount of xanthine oxidase used was designed to give a change in absorbance at 550nm of 0.020/m. The change in absorbance at 550nm was extrapolated back to zero time to obtain the A_{550nm} value at zero time. In running a test sample, the above manipulations were repeated with the xanthine oxidase and sample added to the buffered substrate prior to the start of a 10 m incubation period, at the end of which cytochrome c was

added and the change in $A_{550\text{nm}}$ recorded for 1 m. Extrapolation of the $A_{550\text{nm}}$ versus time to the point where cytochrome c was added gave $A_{550\text{nm}}$ after 10 m of incubation. The burst height of cytochrome c reduction was obtained by subtracting $A_{550\text{nm}}$ (zero time) from $A_{550\text{nm}}$ (10 m). By running aliquots of 16 to 100 μl of reference SOD (60 ng/ml), a standard curve was obtained, showing the decrease in burst height as a function of the amount of SOD in the sample.

L) High Performance Liquid Chromatography (HPLC)

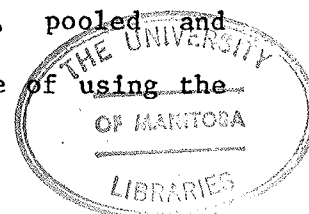
The minute amount of SOD available for extraction from ghosts necessitated the use of HPLC for purification. The method has the additional advantages of being fast, efficient and non-destructive. Its use in the study of macromolecules has only evolved recently and its adaptation to membrane proteins is novel.

HPLC was performed at room temperature on a Beckman Model 334 Gradient Liquid Chromatograph System using two columns with different separation mechanisms. A Synchronpak AX-300 4 mm x 15 cm column (Varian Associates, Georgetown, Ont.) operated on the principle of ion exchange, while a Micropak TSK G2000 SW 7.5 mm x 30 cm column (Varian) separated proteins by size exclusion. The columns were stored in degassed double distilled H_2O . Prior to running a sample, the columns were washed with degassed double distilled H_2O and equilibrated with degassed 0.10 M NaOAc, pH 7.0 (Synchronpak) or 0.010 M NaOAc, pH 6.0 (Micropak) at a flow rate of 1.0 ml/m. The flow was reduced to 0.5 ml/m before sample injection from a 20 or 380 μl injection loop. Eluted proteins were monitored for absorbance at 254nm. Fractions were

collected manually.

Reference SOD included holo-, apo-, irradiated or thermally denatured forms of the enzyme. The holo-SOD was prepared in double distilled H₂O to a concentration of 31 uM and diluted in the appropriate HPLC buffer or H₂O. The apo-SOD was prepared according to Fee (110) whereby the holo-enzyme (31 uM in H₂O) was dialyzed against 0.050 M NaOAc, 1.0 mM EDTA, pH 3.8, for 3 days at 5°C with one change of dialyzing medium. Some samples of the apo-SOD were dialyzed against 0.1 M NaClO₄, pH 7.4 to remove bound EDTA as described earlier. Solutions of holo-enzyme (31 uM in H₂O) were irradiated at 21°C with ⁶⁰Co gamma rays (Gammacell 220, Radiochemical Co., Atomic Energy of Canada Ltd., Ottawa) at a dose rate of 36 Gy/m for a period of 30 m (total dose: 1.08 kGy). The sample was gassed by bubbling N₂O at a controlled flow rate before (3 m) and during irradiation in order to increase the yield of radiation-induced hydroxyl radicals. This resulted in 92 % inactivation of the enzyme as measured by the SOD assay (NBT photoreduction method). Thermally denatured SOD was prepared by boiling holo-SOD (62 uM in H₂O) for 30 m. All samples were stored at 5°C and, prior to column injection from the 20 ul loop, passed through a Millex GS 0.22 um filter to remove particles larger than 22 um.

Prepared ghost material was first chromatographed on the Synchronpak AX-300 column. Various fractions were collected, pooled and concentrated at 0°C under a filtered argon stream. These fractions were then centrifuged (Eppendorf) prior to injection onto the Micropak TSK G2000 column. Fractions were again collected, pooled and concentrated on ice with an argon stream. This sequence of using the



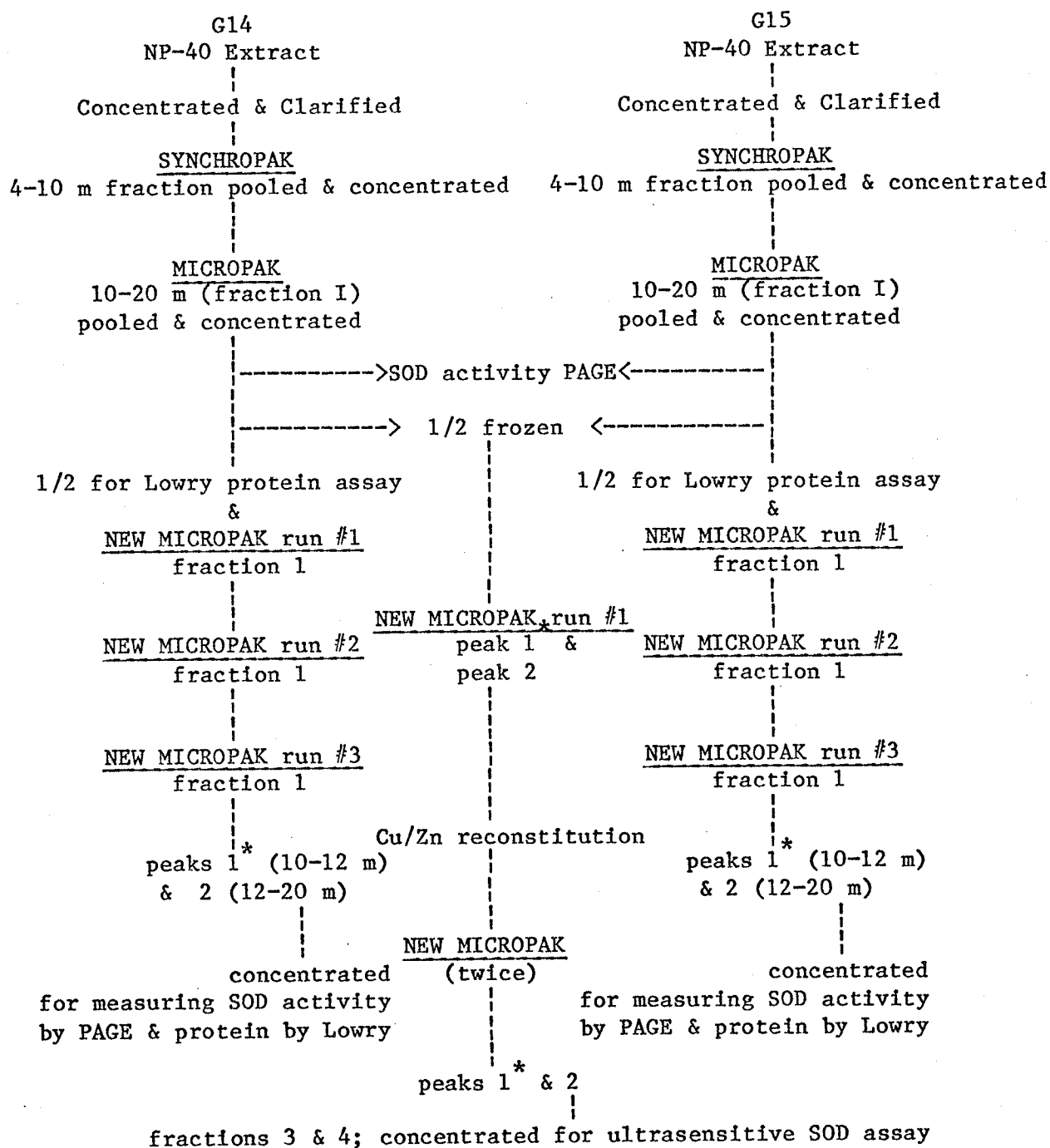
two HPLC columns will be referred to as 'serial HPLC'. HPLC of samples on the Micropak TSK G2000 column was repeated several times in an attempt to enrich the fraction containing the membrane-associated SOD. A new Micropak TSK G2000 column was used in the final stages. In order to determine where and how much of the membrane-associated SOD eluted, fractions were retained for PAGE and SOD activity staining. The protein was measured by the Lowry method to obtain purification factors. Fig. 3 summarizes the HPLC process used for two ghost preparations, G14 and G15.

In addition to using an argon stream to concentrate collected HPLC fractions, an ultrafiltration system, operated at room temperature, was tried in the latter stages of the study. It consisted of the Multi-Micro Ultrafiltration System, model MMC with Diaflo^R Ultrafiltration membranes, UM 05 type (5,000 MW cutoff) (Amicon Corporation, Lexington, Mass.).

UV absorption spectra of final HPLC fractions of ghost extracts and reference SOD (holo-, apo-, irradiated, thermally denatured) were made on a Beckman Model UV 5230 spectrophotometer.

M) Effect of SOD Modification

To determine whether SOD was modified by NP-40, dialysis or lipid interactions, so as to affect its behavior during HPLC, the following experiment was performed. An aqueous solution of reference SOD (15 μ M) was treated in three different ways. One 2 ml aliquot was reserved as



* All peak 1's were pooled, concentrated and run again on the new Micropak.

Figure 3: Flow diagram describing the sequence of HPLC used for two ghost preparations, G14 and G15.

a control and stored at 5°C. A second sample was treated with NP-40 as described before, then dialyzed against H₂O for 4 days at 5°C (one change per day). The third sample (9.0 ml) was exposed to 50 mg (0.62 umole) of the phospholipid, L-alpha-dilinoleoyl phosphatidyl choline (di-[cis-9,12-C₁₈2=]) and homogenated for 5 m at 0°C with a Teflon^R piston, motor driven tissue homogenizer. This suspension was then purged with argon for 20 m at 0°C. Sonication of this sample followed in a bath type sonicator for 1 hour. This sample was then treated with NP-40 and dialyzed as described for the second sample. All three samples were electrophoresed, stained for protein and SOD activity, and chromatographed on both HPLC columns.

N) SOD Reconstitution

Some ghost material was subjected to Cu/Zn reconstitution after serial HPLC. It was hoped this would increase the activity of SOD. Using the method of Jewett et al. (117) and assuming all protein in the sample to be SOD, Cu (CuSO₄·5H₂O) and Zn (ZnSO₄·7H₂O) were added directly to the samples in the proportions of 1 molecule Cu and 1.1 molecule Zn per active site. Incubation at 5°C for 24 hours was followed by exhaustive dialysis against H₂O at 5°C to remove free Cu and Zn. The samples were concentrated by Amicon ultrafiltration at room temperature and centrifuged (Eppendorf) prior to injection onto the new Micropak TSK G2000 column.

CHAPTER 4: Results

Tables 1 and 2 summarize the biochemical characterization of ghosts prepared from outdated and fresh blood, respectively. Outdated blood was used initially to establish technique. The variable results in Table 1 reflect the combined effects of using aged blood and technical inexperience in preparing ghosts. The results of Table 2 are an improvement from those in Table 1 in that the standard deviations are reduced and there is better agreement with literature values. Before a detailed discussion of these results is given, the physical appearance of RBCs and ghosts will be considered. Analysis of ghosts prepared by the Burton method (107) will be discussed separately.

A) Cell Morphology

The RBCs and ghosts were observed for general morphology during cell counts. Fresh RBCs showed their typical biconcave, smooth, round shape under the light microscope. Aged cells showed a high incidence of crenation and reduced concavity. The state of the starting material and the method of ghost preparation was reflected in the appearance of the ghosts. By the Hoogeveen technique, outdated blood yielded ghosts which appeared irregular in shape and size and were also darker under phase contrast (due perhaps to more hemoglobin being retained). Ghosts prepared similarly from freshly drawn blood were in much better shape.

Table 1: Summary of the Characteristics of Ghosts from Outdated Blood

<u>ANALYSIS</u>	<u>AVERAGE VALUE + s.d.</u>	<u>n</u>
1) Ghost Yield (%)	16 ± 3	3
2) Ghost Protein (g/ghost)	(1.0 ± 0.3) × 10 ⁻¹²	3
3) Ghost Hemoglobin (% of MCH)	0.38 ± 0.38	2
4) SOD Activity:		
(ng SOD/ghost)	(9 ± 6) × 10 ⁻⁸	3
(molecules/ghost)	1600 ± 1200	

Table 2: Summary of the Ghost Characteristics and Enzyme Activities in Ghosts from Fresh Human Blood

<u>ANALYSIS</u>	<u>AVERAGE VALUE + s.d. (n)</u>	<u>LITERATURE VALUE (REF.)</u>
1-Ghost Yield (%)	11 ± 2 (14)	---
2-Ghost Protein (g/ghost)	(0.7 ± 0.1) × 10 ⁻¹² (13)	0.91 × 10 ⁻¹² (19)
3-Ghost Hemoglobin (% of MCH)	0.10 ± 0.01 (7)	0.15 (100)
4-Membrane Associated Enzymes		
a) ACHE (mole/m/ghost) (umole/m/mg protein)	(1.3 ± 0.2) × 10 ⁻¹⁵ (7) 1.7 ± 0.3 (7)	--- 1.59 (119)
b) 5'-AMP-Nucleotidase	0 (6)	See Table 4
c) SOD		
- % of total cellular active SOD	0.4 ± 0.2 (3)	0.4 ± 0.2 (15) (bovine RBC ghosts; NP-40 extracted)
- Active SOD: (ng/ghost) (molecules/ghost)	(3 ± 1) × 10 ⁻⁸ (14) 540 ± 240	--- 320 ± 105 (15) (bovine RBC ghosts; chloroform/ethanol extracted)
(% of ghost protein)	0.004 ± 0.002 (14)	
- SOD-like protein: (ng/ghost)	(2.3 ± 0.9) × 10 ⁻⁶ (12)	---

They were smooth, round, of uniform size and concave. Shrunken and crenated cells were rare (Fig. 4).

Attempts to observe the ghosts under SEM were less successful. Fig. 5 illustrates that the ghosts prepared from fresh blood were typically poised for inside-out vesicle formation as the membranes appeared to bud into the cytoplasmic space (118). Only the odd ghost appeared to possess any degree of concavity. The SEM preparative procedure may have been responsible for this budding effect.

B) Ghost Yield

Data in Tables 1 and 2, respectively, show that the ghost yield was consistently low for both outdated and fresh blood. It was expected that the more fragile RBCs from outdated blood would result in a lower yield of ghosts. That this did not occur suggests a technical error, possibly in ghost preparation or cell counting at this early stage in the study.

In general, ghost yield was low due to cell loss at each stage of the Hoogeveen technique. Removal of the plasma and buffy coat of leucocytes inadvertently removed minor quantities of RBCs. Major amounts of ghost materials were unavoidably aspirated with each hemolysate. Observation of hemolysates under phase contrast microscopy revealed that many ghosts (and perhaps membrane fragments) did not sediment after centrifugation, suggesting they had a reduced density. Some RBCs were inherently resistant to hemolysis and during centrifugation formed a hard red pellet beneath the more viscous ghost pellet. The removal of this resistant pellet meant that the ghost

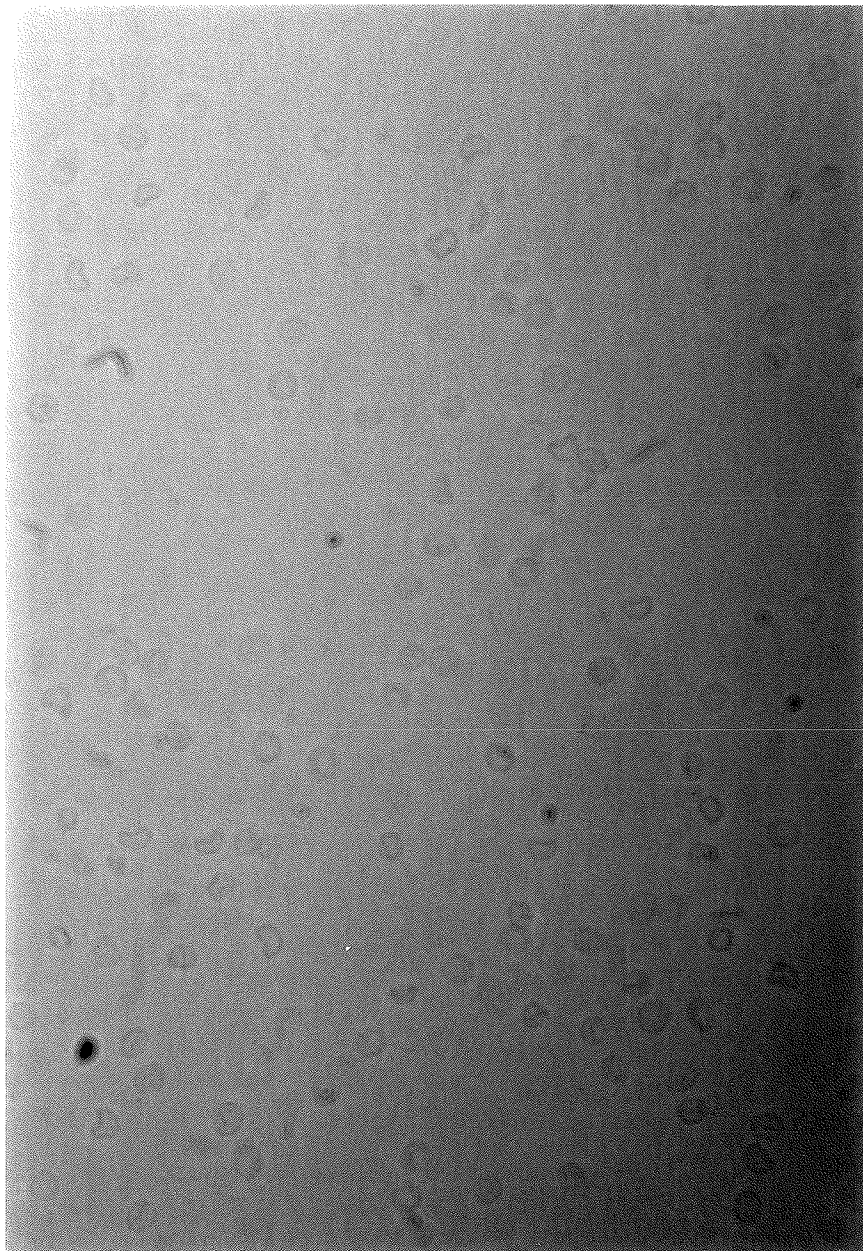


Figure 4: Human RBC ghosts as seen under a phase contrast microscope (Carl Zeiss Ultraphot II, 625 x power). Ghosts were prepared from fresh blood by the method of Hoogeveen (19) and diluted 1:100 in 20 mosM hemolysis buffer.

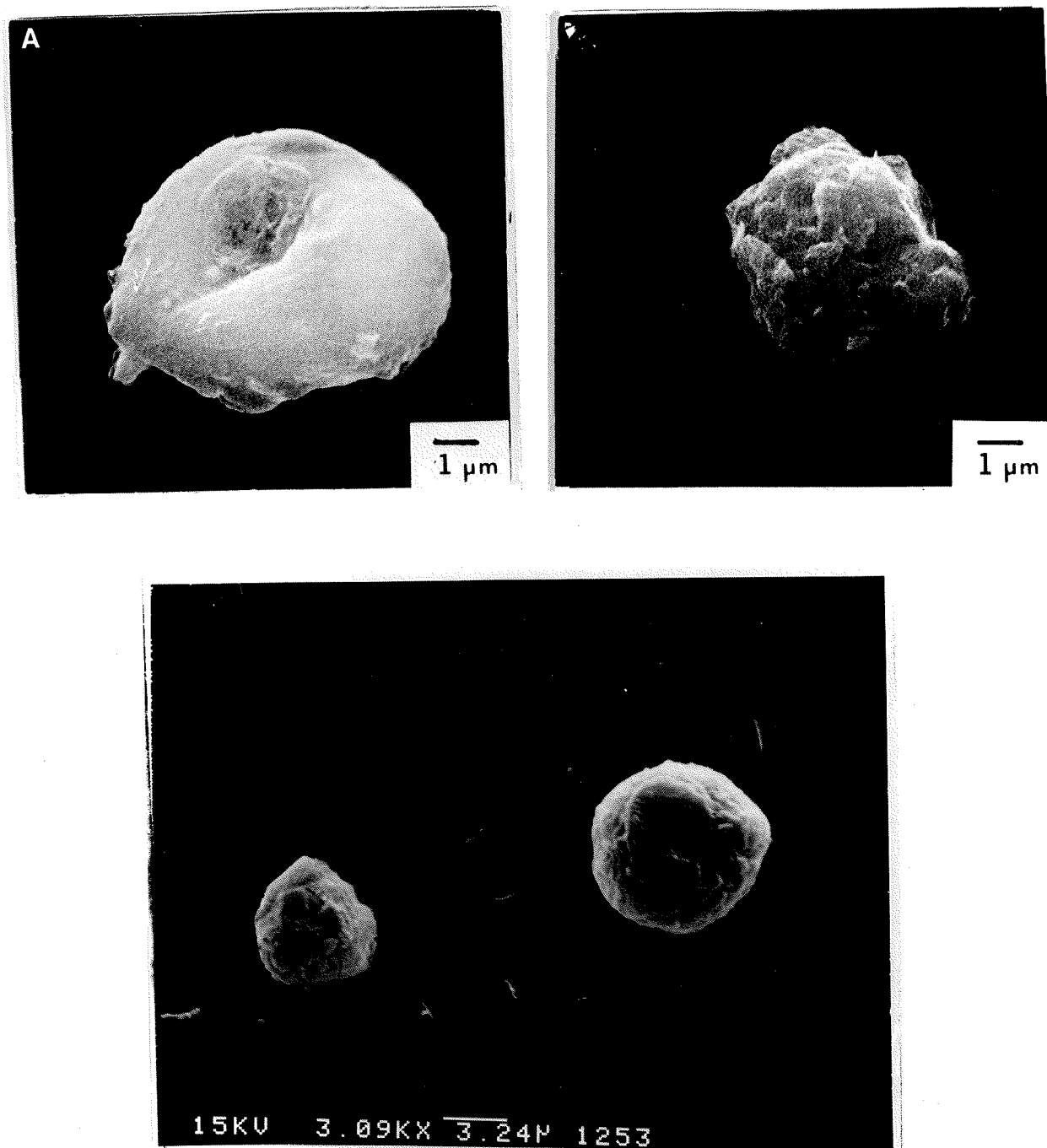


Figure 5: Human RBC ghosts as seen under Scanning Electron Microscopes. The microscopes used were the Cambridge Stereo Scan, top, and the ISI Dual Stage 130, bottom. Ghosts were prepared from fresh blood by the method of Hoogveen (19) and fixed by the Anderson critical point drying method (108).

pellet above it had to be separated by gently rotating the centrifuge tube in a slant position. Some ghosts adhered to the harder pellet and were subsequently removed with it. Hence, only a small portion of RBCs became ghosts that were harvested and although losses were large, they were tolerated in the interest of obtaining high quality ghosts.

C) Ghost Protein

The total ghost protein was measured at $(0.7 \pm 0.1) \times 10^{-12}$ g for ghosts prepared from fresh blood. This mean value from thirteen determinations is significantly lower than $(1.0 \pm 0.3) \times 10^{-12}$ g/ghost from outdated blood ($P > 0.05$) and from 0.91×10^{-12} g/ghost ($P > 0.05$) as reported by Hoogeveen et al. (19) (Tables 1 and 2). Hoogeveen, however, noted no significant difference between ghost protein from fresh and recently outdated blood (19). The age of the outdated blood used in this study may have contributed to the difference obtained in the present study. Based on the fact that the hemolysis procedure desorbs, rather than adsorbs protein, the lower amount of ghost protein in the preparations is probably due to the extra third hemolysis in 20 mosM buffer. The comparatively low amount of protein in the ghost preparations was considered desirable for isolating membrane-bound enzymes. No significant difference in protein was found between the ghosts from outdated blood and the literature values ($P < 0.01$).

D) Ghost Hemoglobin

Residual hemoglobin in ghosts from fresh blood was measured at 0.10 ± 0.01 % of MCH, which is significantly less than that measured for ghosts from outdated blood (0.38 ± 0.38 ; $P > 0.05$) and significantly less than the 0.15 % reported by Dodge et al. (100) ($P > 0.05$). The larger amount of hemoglobin in ghosts from old blood could indicate that cytoplasmic components had adsorbed to the membranes. Perhaps this is why active SOD was more than doubled in ghosts prepared from outdated blood, in parallel with the higher amounts of hemoglobin and total protein (Table 1).

E) Acetylcholinesterase (ACHE) Activity

The activity of the membrane marker enzyme, ACHE, was determined only for ghosts derived from fresh blood and amounted to $(1.3 \pm 0.2) \times 10^{-15}$ mole/m/ghost or 1.7 ± 0.3 umole/m/mg ghost protein (Table 2). This is not significantly different from the 1.59 umole/m/mg protein reported by Steck and Kant, 1974 (119) ($P < 0.05$).

The results thus far suggest that the fresh RBC ghost material from which SOD was determined was of a quality suitable for the purpose.

F) 5'-AMP-Nucleotidase Activity

Table 3 summarizes the data on ghost samples and controls

Table 3: Summary of 5'-AMP-Nucleotidase Assay

<u>SAMPLE</u>	<u>umole P_i measured in 50 ul sample + s.d.</u>	<u>n</u>
Whole ghosts in 20 mosM buffer	0.042 \pm 0.002	4
NP-40 treated ghosts in buffer	0.039 \pm 0.005	3
NP-40 treated & dialyzed ghosts	n.d.	4
Exhaustively dialyzed whole ghosts	n.d.	1
Whole RBC's	0.044 \pm 0.008	2
Washed RBC's	0.251 \pm 0.041	3
-wash #1	0.384 \pm 0.012	2
-wash #2	0.411 \pm 0.036	2
-wash #3	0.415 \pm 0.036	2
RBC wash buffer	0.415 \pm 0.004	2
Hemolysates #1-60 mosM	0.142 \pm 0.004	3
#2-60 mosM	0.138 \pm 0.008	3
#1-30 mosM	0.805 \pm 0.005	3
#2-30 mosM	0.069 \pm 0.002	3
#1-20 mosM	0.044 \pm 0.002	3
#2-20 mosM	0.047 \pm 0.006	3
#3-20 mosM	0.046 \pm 0.003	3
Hemolysis buffers: 60 mosM	0.151 \pm 0.009	3
30 mosM	0.070 \pm 0.005	3
20 mosM	0.046 \pm 0.001	3
5'-Nucleotidase reference (8 ug)	0.48	1
-after 6 hours	0.26	1
5'-Nucleotidase reference (8 ug plus 1 mM EDTA)	0.21	1
-after 6 hours	0.10	1
Water blank	n.d.	4

(n.d. = not detected)

analyzed for 5'-AMP-nucleotidase. No evidence was obtained to suggest that P_i was released as a result of 5'-AMP-nucleotidase activity in RBC membranes. Any P_i detected in the ghost material is apparently due to phosphate in the RBC wash and hemolysis buffers.

The data from other analyses of 5'-AMP-nucleotidase activity in human RBC ghosts are summarized in Table 4 and compared with the data from the present study. The results of this study agree with the earlier results of Delaunay et al. (120) in that no 5'-nucleotidase activity was found. Using a very sensitive radioassay, Parker measured a small amount of 5'-AMP-nucleotidase activity in RBC ghosts contaminated with leucocytes (< 100 WBCs / mm^3 or 10^5 WBCs / ml of packed RBCs) (121). The amount of 5'-nucleotidase activity detected by this sensitive assay was 50 pmole P_i /m/mg protein (121). This activity could be due to the contaminating leucocytes which are known to possess significant amounts of 5'-AMP-nucleotidase activity, releasing 1200 nmole P_i /m/mg protein (122).

Using an assay 3000 times less sensitive, Van den Hoek et al. colorimetrically detected about 10^3 times more activity than Parker (123). This amount of enzyme activity could be due to contaminating amounts of P_i in the buffer. Their ghosts were washed only once in a TRIS/HCl buffer prior to analysis, a treatment insufficient to remove P_i from buffers and cytoplasmic sources because P_i diffuses through lipid membranes with a significant time lag (124). Consequently, in the present study, the ghost material was exhaustively dialyzed against water before the assay was undertaken. If Van den Hoek's determination of 5'-AMP-nucleotidase activity were correct, about 0.6 umole P_i would have been released under the assay conditions. No

Table 4: Comparison of 5'-AMP-Nucleotidase Activity Assays of Human RBC Ghosts

Experimental Conditions	Study (Reference)			
	J.C.Parker (121)	Van den Hoek (123)	Delaunay (120)	Present Work
Ghost Preparation:				
Plasma & buffy coat removed?	no	yes	yes	yes
# RBC washes in iso- tonic buffer	1	3	3	3
Final buffer of ghost suspension	TRIS/0.1 mM EDTA	Na-phosphate	Na-phosphate	Na/K phosphate + 1 mM EDTA
5'-AMP-Nucleotidase Assay:				
Assay type	Radioassay	Colorimetric	Colorimetric	Colorimetric
Relative Sensitivity	3000	1	7	7
Activity found ($\mu\text{mole P}_i/\text{m/mg protein}$)	50	48000	0	n.d.

n.d. = not detected at a sensitivity of 1 nmole/m/mg protein.

release of P_i was detected at a sensitivity of 1 nmole/m/mg protein.

The effect of EDTA on 5'-nucleotidase activity has been studied but appears to be variable and the results inconclusive. For example, in hemolysates of human RBCs, which failed to show any activity specific for 5'-AMP, 5'-nucleotidase was inhibited by the chelator (125). EDTA was also found to be a potent inhibitor of the 5'-AMP specific enzyme isolated from plasma membranes of rat liver (126). Other studies showed that, while 5'-AMP-nucleotidase was sensitive to EDTA in plasma membrane fractions of some lymphoma strains, the enzyme was unaffected or only 50 % inhibited by 0.1 M EDTA in other strains (127). In other assays, EDTA was not even listed as an inhibitor of this mammalian membrane-marker enzyme (128). In the present study, 1 mM EDTA appeared to reduce the activity of the reference enzyme (from snake venom) by about 50 % or more after 6 hours, suggesting instability of the enzyme. Parker found 5'-AMP-nucleotidase activity in "ghosts" suspended in a buffer containing 0.1 mM EDTA (121), suggesting that the enzyme in WBC membranes was not totally inactivated by EDTA. Delaunay et al. did not detect activity in the absence of EDTA (120) while the present study also found no activity, but in the presence of EDTA.

In summary:

1) 5'-AMP-nucleotidase activity was not detected in the membranes of human RBCs and, hence, could not be used as a membrane marker. Other mammalian RBCs lack this membrane-bound enzyme as well (120).

2) If the enzyme is present in human RBC membranes, then the amount is so small that the colorimetric assay cannot detect it at a sensitivity of 1 nmole P_i released/m/mg protein.

3) If the enzyme is present in RBC membranes, then it may have been inactivated and/or inhibited by EDTA during the preparation of the ghosts.

G) Polyacrylamide Gel Electrophoresis (PAGE)

The amount of SOD activity determined by PAGE in the extracts of fresh ghosts (prior to any concentration and purification by HPLC) was determined to be $(3 \pm 1) \times 10^{-8}$ ng/ghost or 540 ± 240 molecules / ghost (Table 2). This represents 0.4 ± 0.2 % of the total active SOD in fresh human RBCs, a value in agreement with that determined for bovine RBC ghosts (Table 2) (15). However, the value of 540 ± 240 molecules of active SOD per human ghost is significantly greater ($P > 0.05$) than the 320 ± 105 molecules of active SOD per ghost found previously in bovine ghosts (15). This difference may perhaps be due to the fact that the bovine SOD was extracted with chloroform/ethanol, rather than with NP-40 as in the present study. However, the difference may also be species dependent.

Controls of glycerol, 20 mosM hemolysis buffer, 0.1 % NP-40, 1 mM EDTA and combinations of them showed no SOD activity bands after PAGE. Fig. 6 illustrates the standard curve used to calculate the amount of SOD activity in the PAGE bands of ghost extracts after comparative planimetry of densitometry scans of gels containing either reference SOD or material from test samples. In this figure, the active SOD in the ghost extracts migrated a distance slightly less than that of the reference enzyme. This may be the result of additional material in the ghost extract applied to the gel.

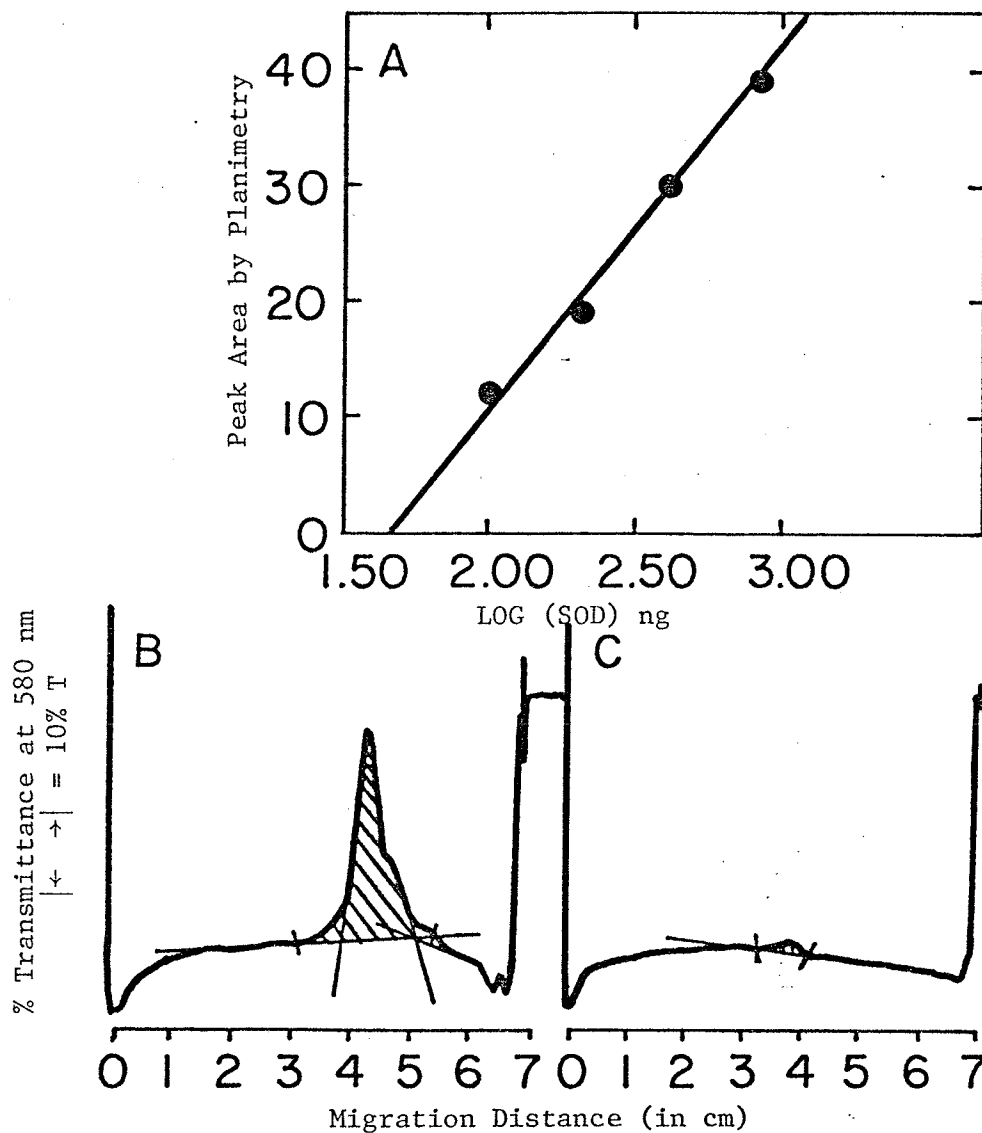


Figure 6: Analysis of SOD activity by PAGE. A- Standard curve showing peak area of reference SOD bands (shaded area in B) as a function of the amount of SOD applied to gel. B- Densitometry scan of a gel loaded with 100 ng reference SOD (4.00 ul of stock solution, 50 ng SOD/ul H_2O). C- Scan of a gel loaded with 300 ul (560 ug protein) of ghost extract (dialyzed against H_2O , perchlorate, H_2O and centrifuged in Eppendorf or at 42,000 x g).

Prior to concentration for HPLC, gels of ghost extracts stained for protein showed that the band migrating like reference SOD protein was equivalent to $(2.3 \pm 0.9) \times 10^{-6}$ ng protein / ghost. This SOD-like protein was 77 times greater than the amount of active SOD. Although this SOD-like protein was expected to contain both active and inactive SOD, it could also have contained other proteins with similar electrophoretic mobility. Fig. 7 illustrates the standard curve used to calculate the amount of SOD-like protein in the ghost extracts after comparative planimetry or densitometry scans of gels containing either reference SOD or material from test samples. As before, the slightly smaller migration distance of the SOD-like protein band may be the result of additional material in the ghost extract applied to the gel.

The relatively large errors in the results obtained by this assay reflect its semi-quantitative nature, to which several factors contributed. Firstly, membrane solubilization may not have removed all associated SOD in its native configuration. The released SOD may also have associated with other membrane components such as lipids and other proteins. The comparative assay used a reference SOD, extracted from the cytoplasm of human RBCs, to quantify the amount of SOD associated with the ghost membrane. Also, the SOD activity bands derived from unconcentrated ghost extracts were at the lower limit of detection for the assay. Finally, the inability to obtain baseline resolution of the peaks, corresponding to the SOD-like protein, in the densitometry measurements contributed to the errors.

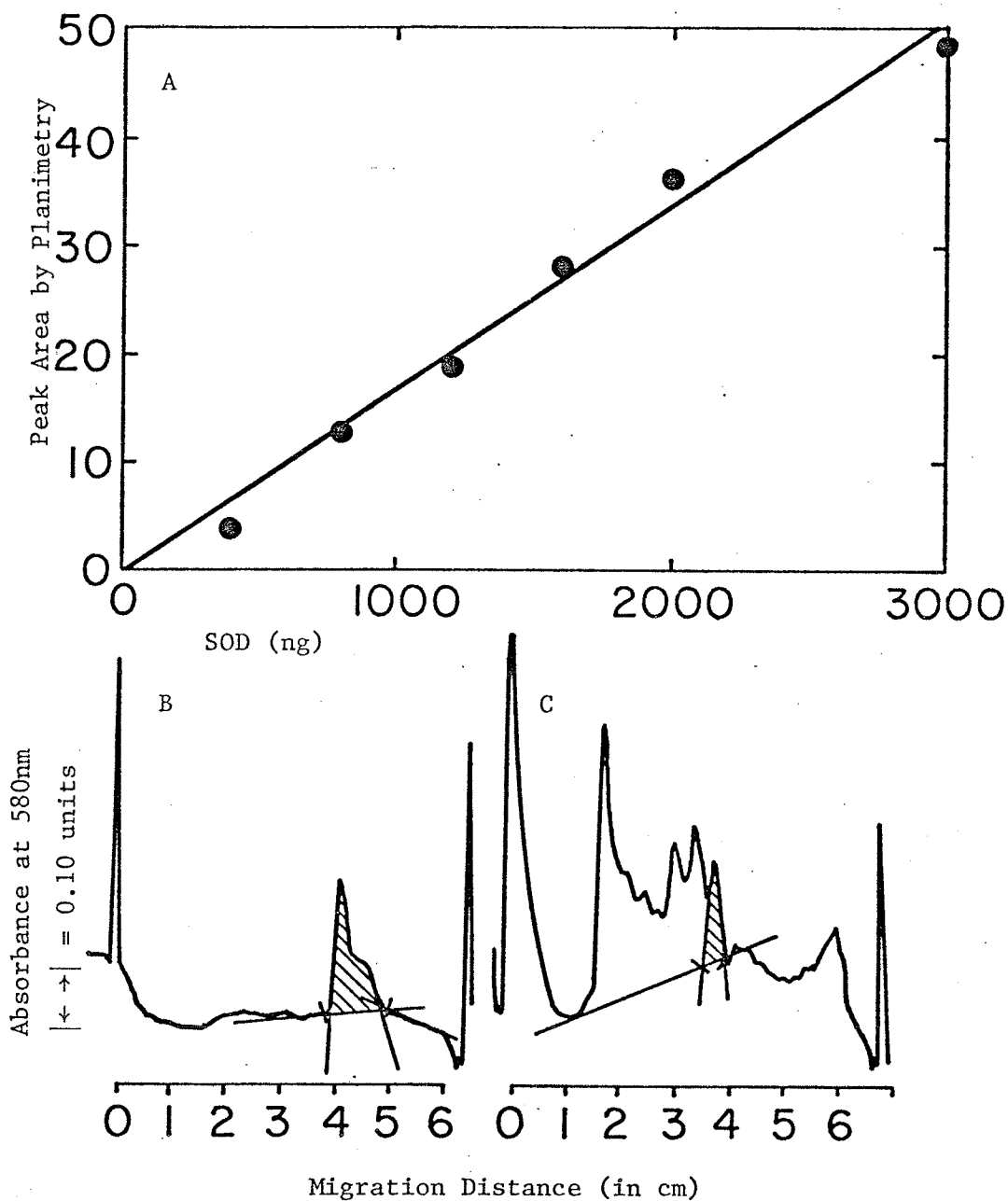


Figure 7: Analysis of SOD-like protein by PAGE. A- Standard curve showing peak area of reference SOD bands (shaded area in B) as a function of the amount of SOD applied to the gel. B- Densitometry scan of gel loaded with 1600 ng reference SOD (16.0 ul of stock solution, 100 ng/ul H_2O). C- Scan of gel loaded with 50.0 ul (160 ug protein) ghost extract (dialyzed against H_2O).

H) Cytoplasmic SOD

The cytoplasmic SOD activity in fresh RBCs was determined three times in order to define the membrane-associated SOD as a percentage of the total. The amount of active SOD in human RBC cytoplasm was measured at $(1.1 \pm 0.2) \times 10^{-14}$ g / RBC, a value not significantly different from the literature ($P < 0.05$) (93). Therefore, the human RBC membrane-associated SOD represented 0.4 ± 0.2 % of the total activity (Table 2).

I) NP-40 Treatment

Table 5 shows the effect of ghost solubilization by NP-40 on protein content and enzyme activities. The alkaline solution of the Lowry procedure disintegrated the membrane material and resulted in the measurement of the same amount of ghost protein as in NP-40 solubilized ghosts ($P < 0.05$). The ACHE activity also was not significantly different ($P < 0.05$). The active center of this enzyme is externally orientated (2) and NP-40 did not appear to inactivate it. 5'-AMP-nucleotidase activity was not detected in ghosts before or after solubilization with NP-40. PAGE did not detect any SOD bands in intact ghosts because they failed to penetrate the gel matrix. Only NP-40 solubilized ghosts penetrated the gel bed and resulted in the separation of SOD from other membrane proteins.

Table 5: Effect of Ghost^{*} Solubilization by NP-40 on Ghost Assays

<u>ASSAY</u>	<u>WHOLE GHOSTS</u> (n)	<u>NP-40 SOLUBILIZED GHOSTS</u> (n)
Ghost Protein in g/ghost	$(0.7 \pm 0.1) \times 10^{-12}$ (10)	$(0.7 \pm 0.1) \times 10^{-12}$ (13)
ACHE in mole/m/ghost	$(1.3 \pm 0.2) \times 10^{-15}$ (7)	$(1.2 \pm 0.1) \times 10^{-15}$ (3)
umole/m/mg protein	1.7 ± 0.3 (7)	1.5 ± 0.2 (3)
5'-AMP-Nucleotidase in umole P _i /m/mg protein	n.d.	n.d.
PAGE - active SOD (ng/ghost)	n.d.	$(3 \pm 1) \times 10^{-8}$ (14)
- SOD-like protein (ng/ghost)	n.d.	$(2.3 \pm 0.9) \times 10^{-6}$ (12)

* Prepared from fresh blood.
n.d. = not detectable.

J) High Performance Liquid Chromatography (HPLC)

(i) Preliminary Studies

In the expectation that HPLC could be used to separate small amounts of active and inactive forms of the membrane-associated SOD, the elution behavior of active and inactive reference SOD from the cytoplasm of human RBCs was studied on the Micropak TSK G2000 SW and Synchronpak AX-300 columns. Since the nature of inactive membrane-associated SOD is unknown, various types of inactivation methods were used. These included inactivation through loss of the coordinated metal ions (apo-SOD), irradiation and thermal denaturation. Hence, differences in HPLC elution patterns might not only distinguish between active and inactive SOD but perhaps suggest even the nature of the inactivation. With such knowledge, HPLC analysis of ghost extracts might be more readily interpreted.

Fig. 8 illustrates the profiles of holo-SOD and apo-SOD after elution from the Micropak TSK G2000 HPLC column. Although the elution times for the two enzymes are the same, 12.5 m, the apo-SOD has a reduced peak which separated from the EDTA peaks at 16 and 18 m (Fig. 9). Fig. 10 shows how the removal of bound EDTA from apo-SOD by dialysis against perchlorate virtually eliminated the EDTA peaks.

The HPLC elution profile of radiation-inactivated SOD on the Micropak TSK G2000 column is shown in Fig. 11. The inactivated enzyme eluted 2 m earlier than the holo-enzyme but showed considerable tailing. This tailing may be due to amino acid damage, which might result in ionic or hydrophobic interactions with the bonded support (83). The earlier elution time is consistent with the irradiated SOD

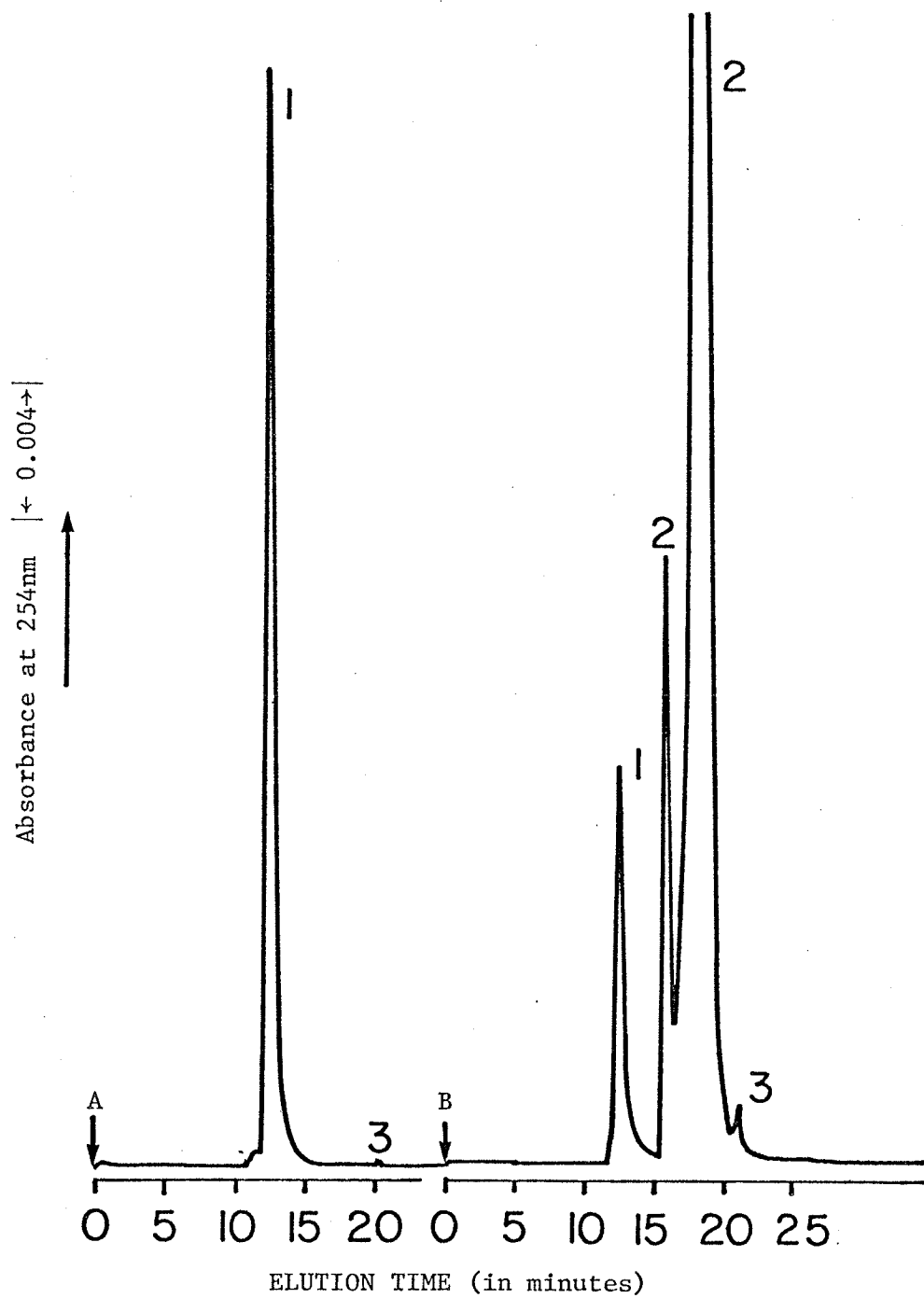


Figure 8: HPLC elution profiles of reference holo-SOD (A) and reference apo-SOD (B). Column: Micropak TSK G2000; Loop: 20 μ l; Absorbance range: 0.04; Peaks: 20 μ g SOD (1); EDTA (2); sample solvent, H_2O (3).

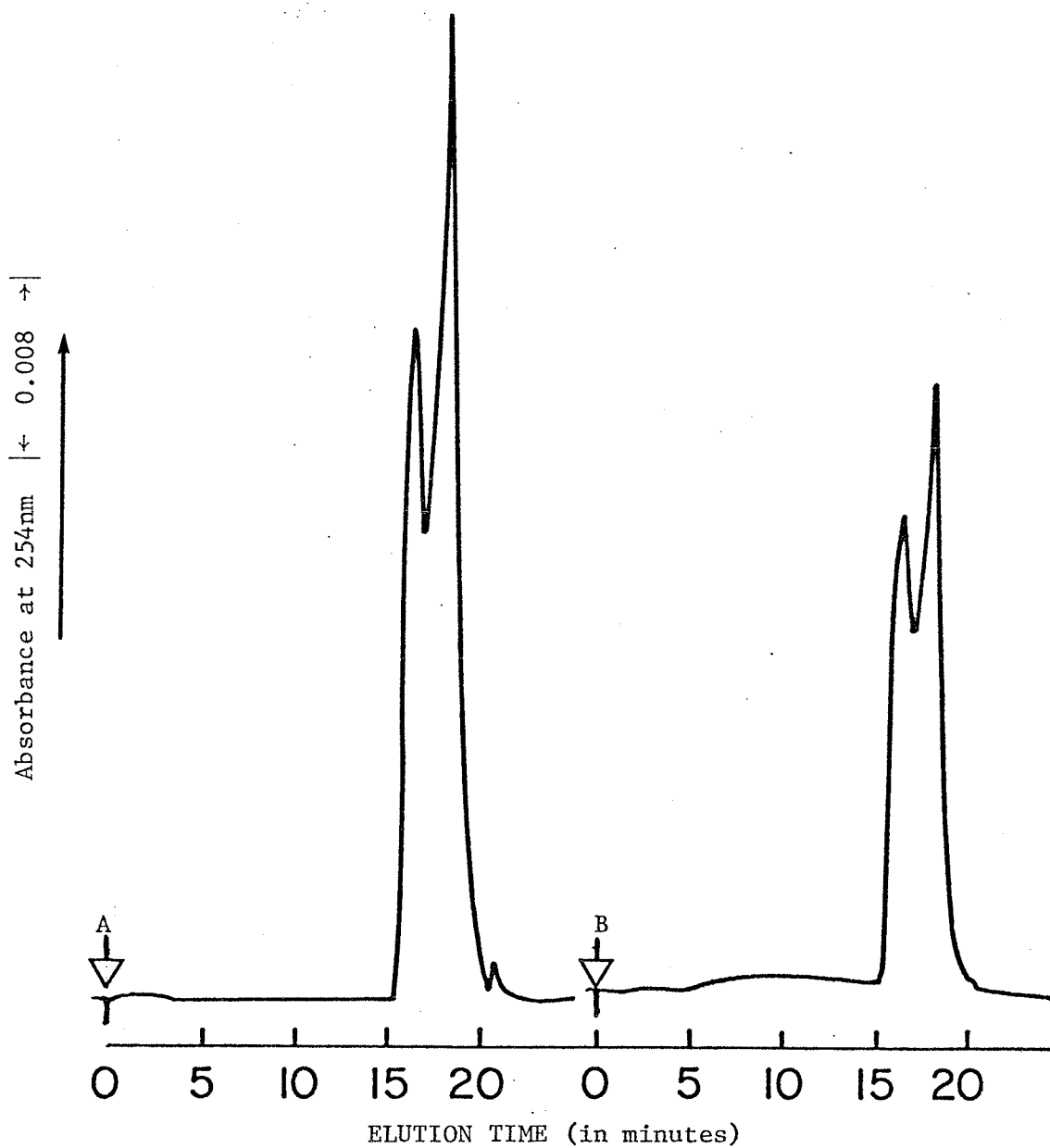


Figure 9: HPLC of EDTA. HPLC elution profiles of: A, dialyzing medium for preparing apo-SOD (0.050 M NaOAc, 1.0 mM EDTA, pH 3.8); B, 1.0 mM EDTA in H₂O. Column: Micropak TSK G2000; Loop: 20 ul; Absorbance range: 0.08.

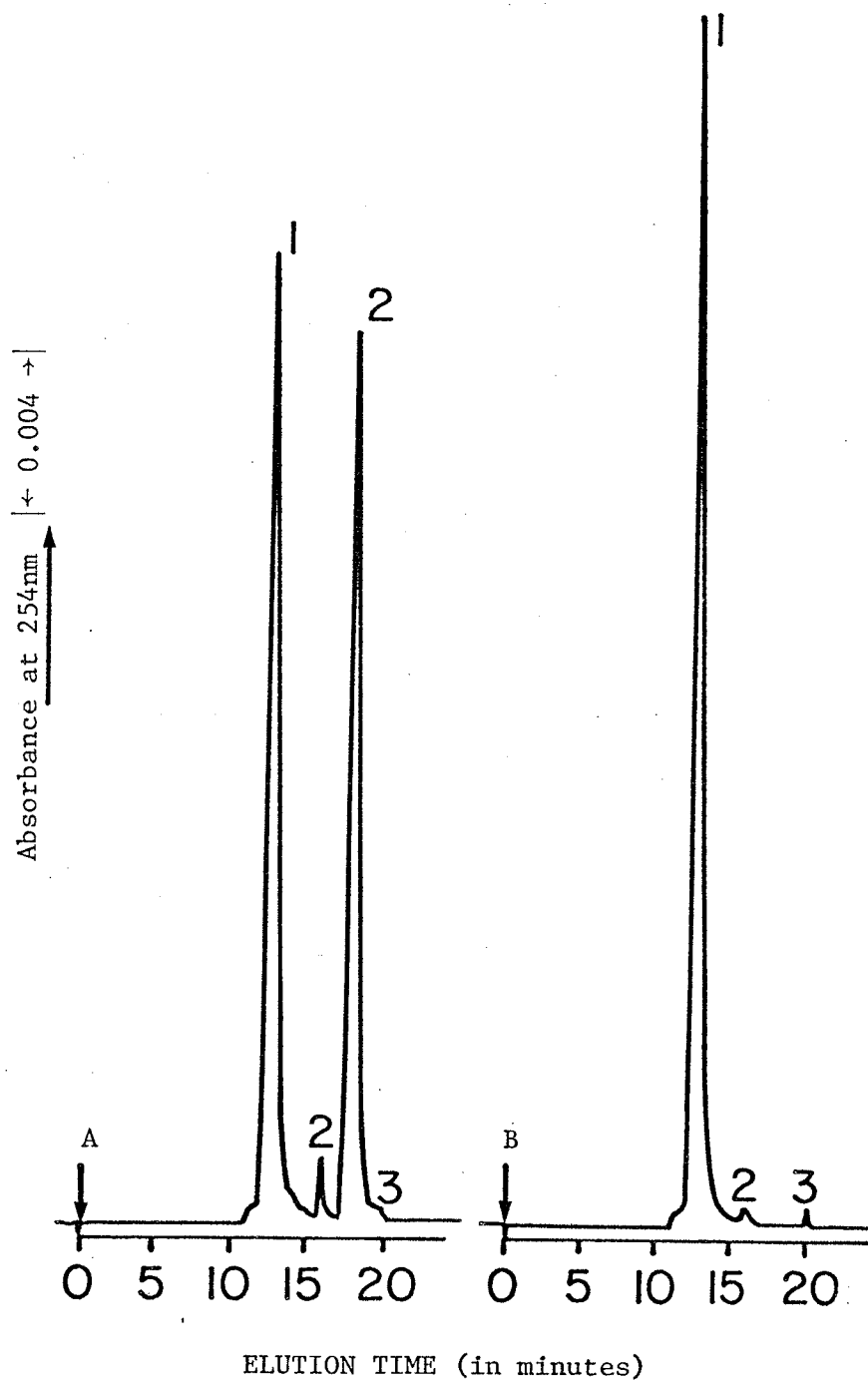


Figure 10: HPLC elution profiles of apo-SOD before (A) and after (B) dialysis against perchlorate to remove bound EDTA. Column: Micropak TSK G2000; Loop: 20 ul; Absorbance range: 0.04; Peaks: 20 ug SOD (1), EDTA (2), sample solvent (3).

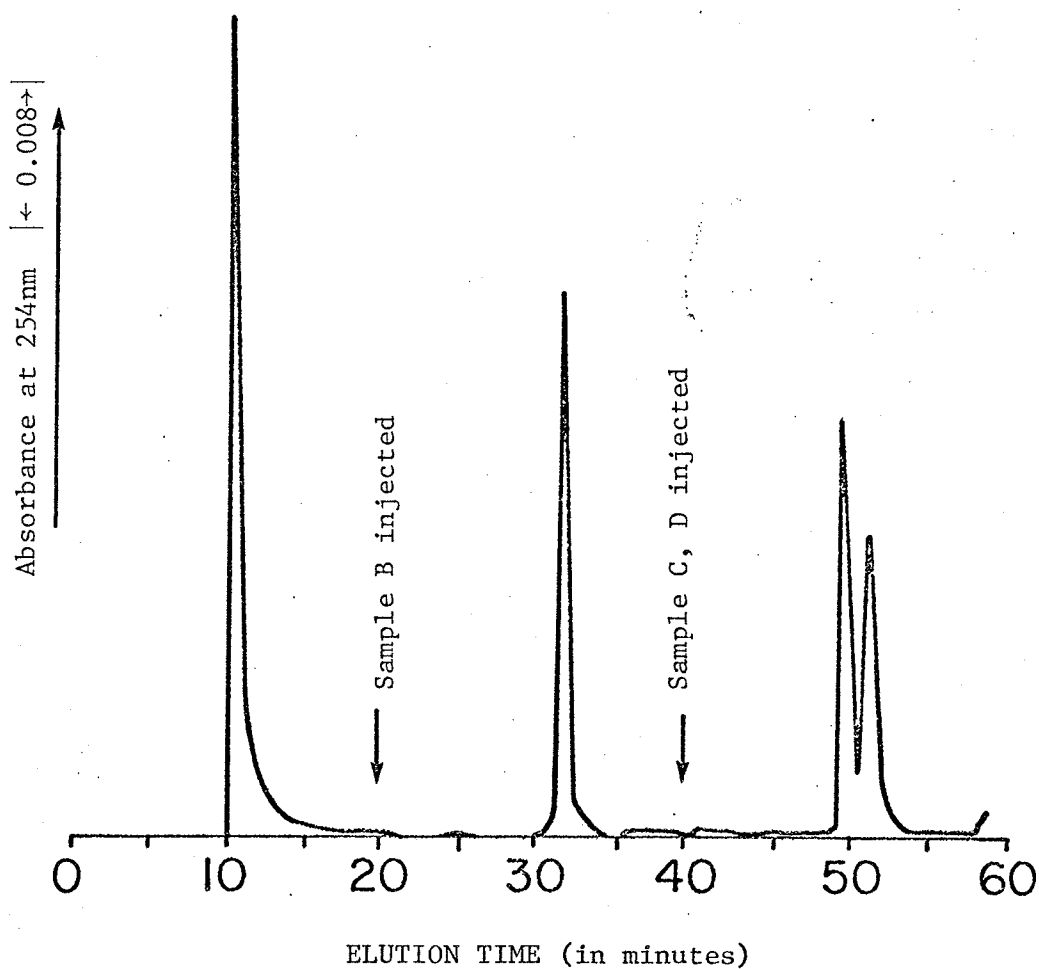
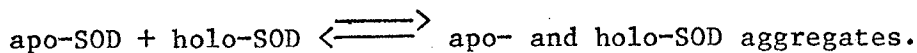


Figure 11: Comparative HPLC elution times of radiation-inactivated SOD (20 ug, peak A), the holo-form (20 ug, peak B) and of a 1:1 mixture of the two forms (total: 20 ug, peaks C, D). Column: Micropak TSK G2000; Loop: 20 ul; Absorbance range: 0.08.

molecule having a larger radius of gyration, $R_g = 24 \text{ \AA}$, than the holo-enzyme, $R_g = 18 \text{ \AA}$ (83).

When the HPLC elution peak heights and areas for various amounts of apo- and holo-SOD were compared, linear relationships were found (Fig. 12). Slopes differed because of differences in extinction coefficients at 254nm. Mixtures of holo- and apo-SOD in various proportions gave absorption peak areas that increased exponentially with the relative amount of holo-SOD (Fig. 12, inset). This empirically suggests a first order interaction between the two forms:



This interaction may be shifted to the right by irradiation (83).

The effect of the NP-40 detergent on the SOD standard was studied by HPLC, using the Micropak TSK G2000 column. The result, is shown in Fig. 13, indicates that NP-40, at the concentration used for ghost solubilization, did not alter the elution time or the height of the peak. The detergent appears to show up as a small peak at 10.5 m.

HPLC on the Micropak TSK G2000 column of thermally denatured SOD gave two peaks of reduced height. The first and larger peak eluted at the same time as holo-SOD, whereas the second, smaller peak eluted at 14 m. Although the composition of the protein, eluting as the second peak is unknown, its longer elution time suggests a molecular size smaller than that of holo-SOD and/or its structure interacts more strongly with the column matrix. On HPLC by gel filtration, thermally-denatured SOD is clearly separable from Cu/Zn SOD, inactivated by ionizing radiation.

On the Synchropak AX-300 column, reference holo-SOD eluted at 5 m and typically showed a small broad peak at 10 m (Fig. 15 A). This

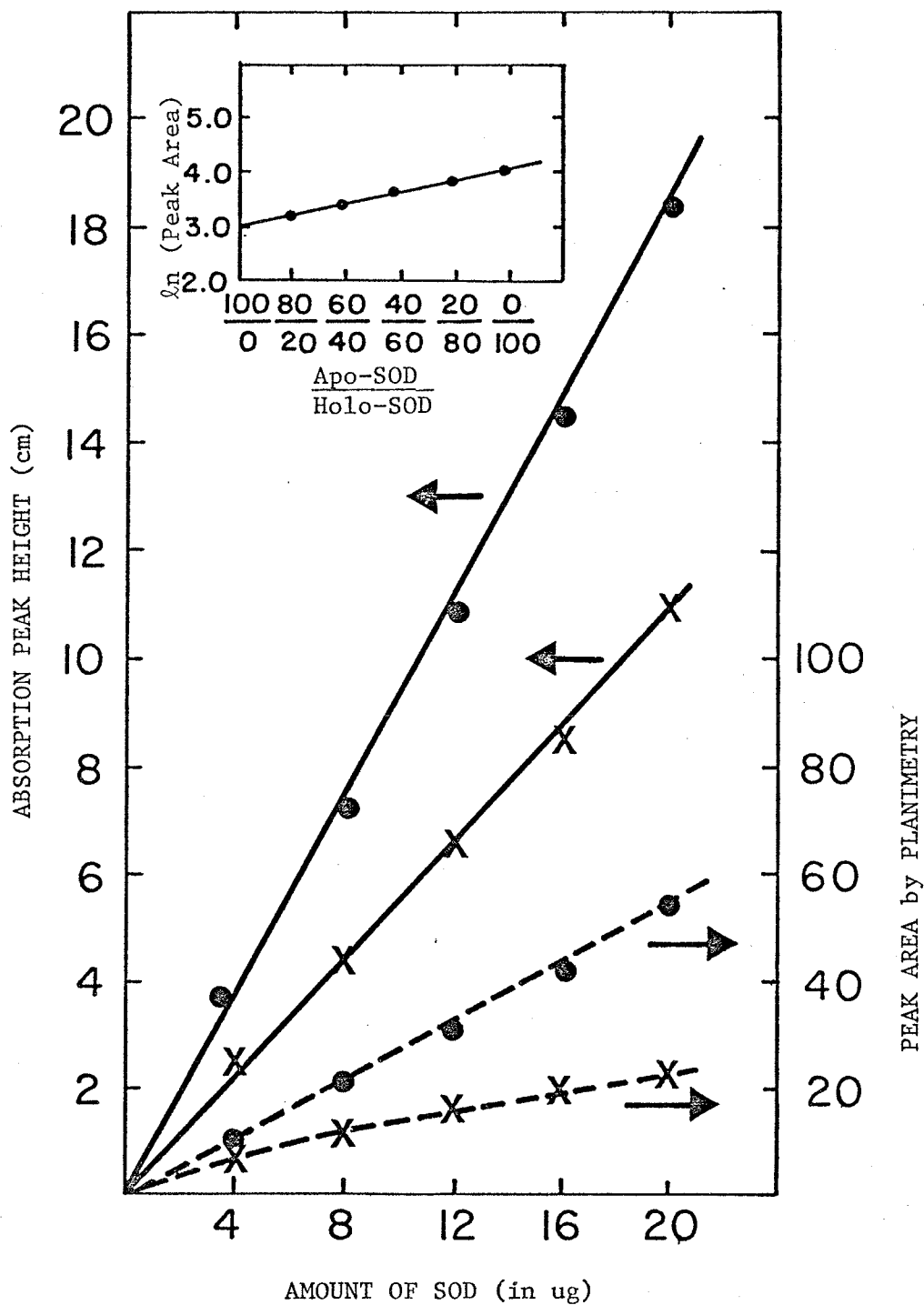


Figure 12: Comparative HPLC of the holo- (●) and apo- (x) forms of reference SOD. Height (—) and area (----) of absorption peaks at 254nm increase linearly with the amount of enzyme applied. Inset: HPLC of 20 ug samples of apo- and holo-enzyme mixtures, showing that by varying the mixture from 100 % apo- to 100 % holo-SOD, the area of the absorption peak increased exponentially. Column: Micropak TSK G2000; Loop: 20 ul; Absorbance range: 0.04.

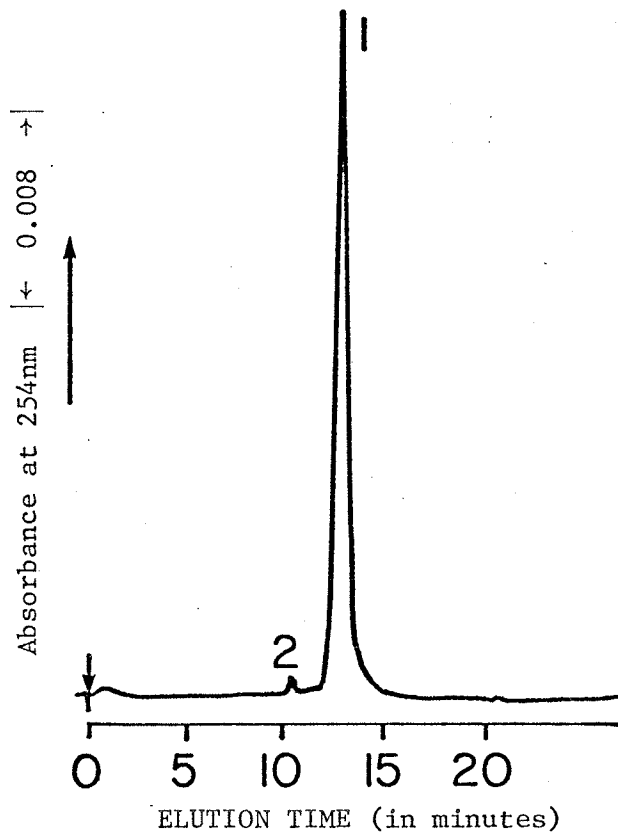


Figure 13: HPLC elution profile of 20 ug holo-SOD in 0.01 % NP-40. Column: Micropak TSK G2000; Loop: 20 ul; Absorbance range: 0.08; Peaks: holo-SOD (1), NP-40 (2).

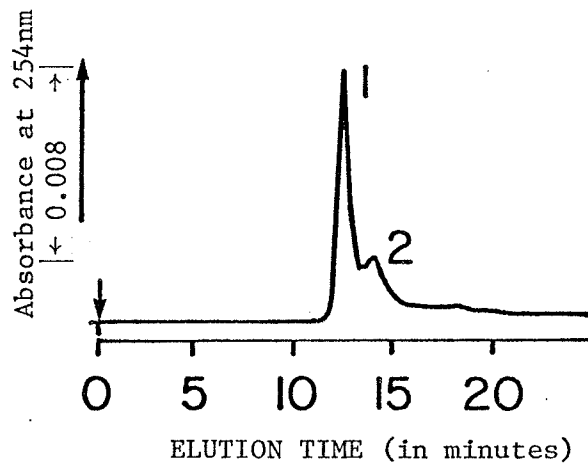


Figure 14: HPLC elution profile of 40 ug holo-SOD after thermal denaturation. Column: Micropak TSK G2000; Loop: 20 ul; Absorbance range: 0.08; Peaks: holo-SOD (1), denaturation product (2).

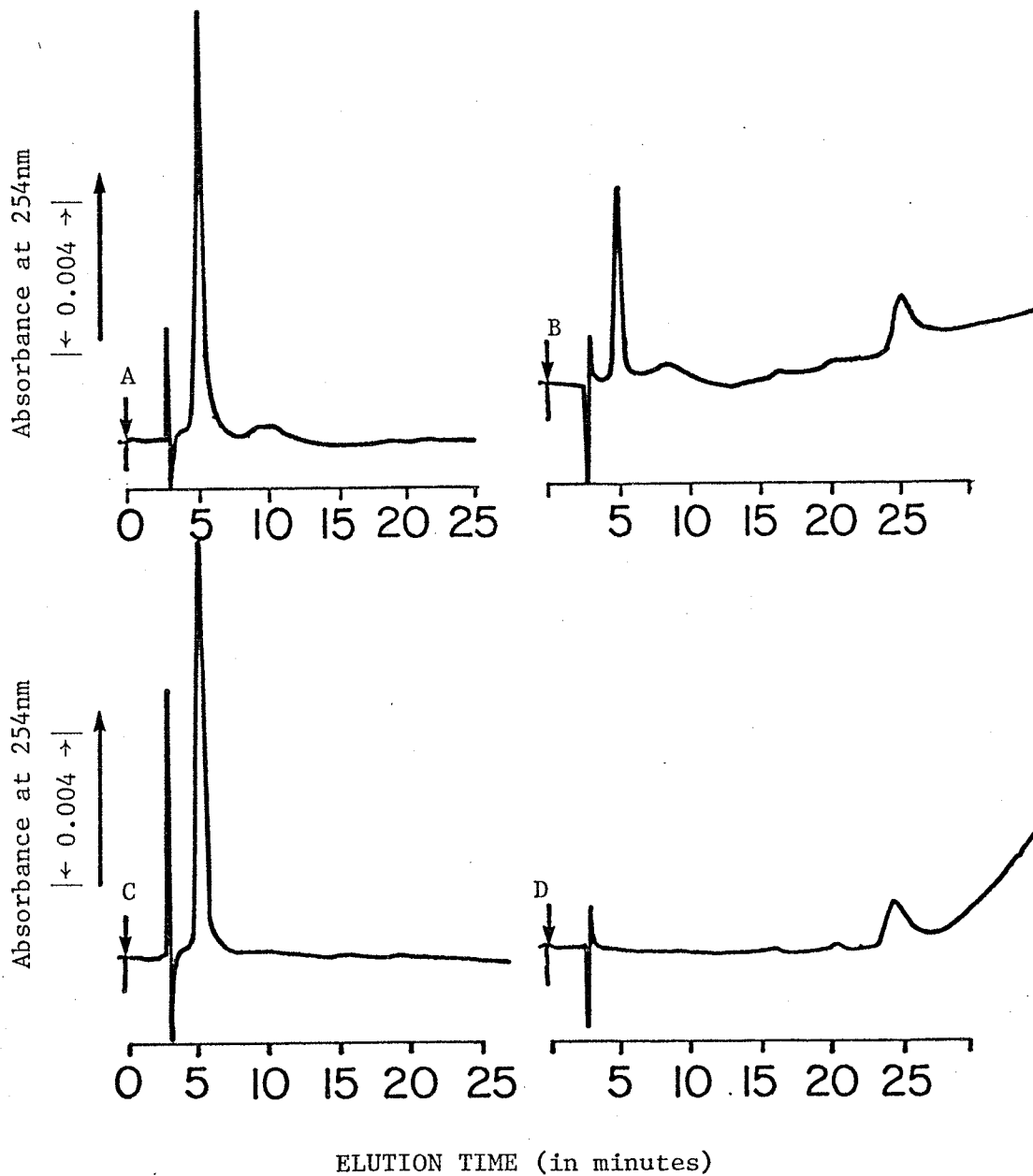


Figure 15: HPLC of holo-SOD and EDTA. HPLC elution profiles of: A, 10 ug reference holo-SOD; B, 10 ug SOD plus 20 mM EDTA; C, 10 ug SOD after dialysis to remove EDTA; D, 20 mM EDTA. Column: Synchropak AX-300; Loop: 20 ul; Absorbance range: 0.04; Peaks: solvent, H₂O (3 m); SOD (5 m); EDTA (25 m).

small peak increased with the age of the sample and is presumably a decomposition product of the preparation. The solvent peak appeared at 3 m.

In the presence of EDTA at concentration similar to that in concentrated ghost extracts (about 20 mM), the elution peak of the reference holo-SOD on the Synchropak AX-300 column was reduced in height (Fig. 15 B). However, after dialysis against perchlorate to remove bound EDTA, this peak was restored to the normal height (Fig. 15 C). EDTA was found to have a deleterious effect on the column whereby repeated injections decreased column performance by raising the baseline and reducing retrievable protein (Fig. 15 B). This chelator eluted from the Synchropak AX-300 column at about 25 m as a short broad peak of low amplitude (Fig. 15 D).

Fig. 16 A illustrates that on a Synchropak AX-300 column, irradiated holo-SOD did not appear to elute from the column, perhaps due to increased interaction with the matrix as a result of amino acid damage or due to lack of detection at 254nm. The minor peak at 15 m may be the result of a decomposition product from the enzyme, 8 % of which was not inactivated by the irradiation (vide supra). This peak was also observed on HPLC of a 60 % apo-, 40 % holo-enzyme mixture (Fig. 16 B). The single peak eluting at 5 m (Fig. 16 B), indicates that, as with the Micropak TSK G2000 column, the Synchropak AX-300 cannot distinguish between the holo- and apo- forms of SOD.

(ii) Ghost extracts

The chosen approach for the HPLC of ghost material involved

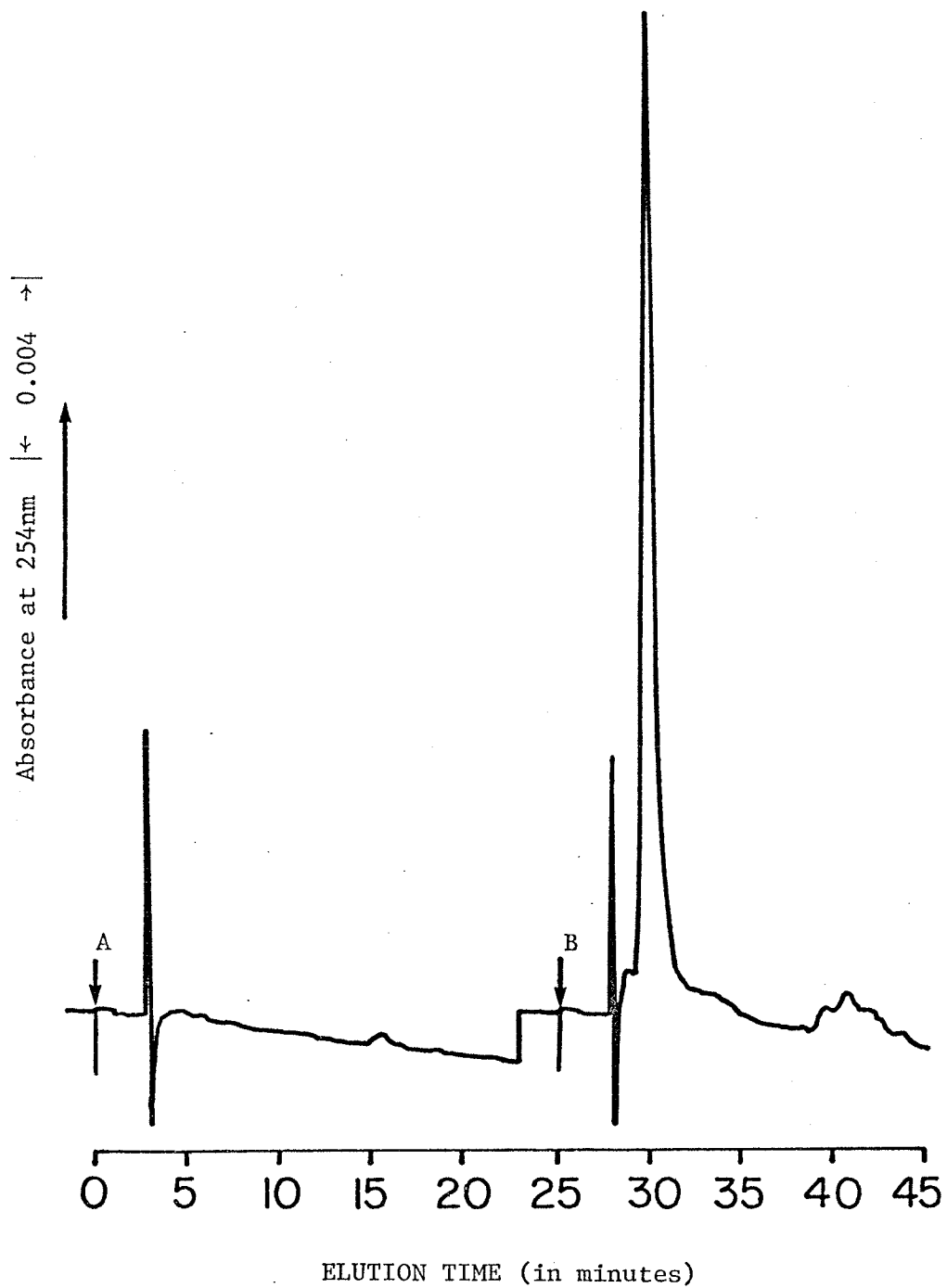


Figure 16: HPLC of inactivated SOD. HPLC elution profiles of: A, 12 ug irradiated SOD and B, a mixture of 60 % apo- and 40 % holo- SOD; total of 20 ug SOD (injected successively). Column: Synchropak AX-300; Loop: 20 ul; Absorbance range: 0.04.

concentrating the dialyzed, clarified extracts by rotary evaporation to a few ml. Concentrating by vacuum filtration resulted in significant loss of material as seen by its adsorption to the filtration membranes. Each concentrate was clarified at $42,000xg_{\max}$ for 45 m (extract of ghost preparation G14) or at $100,000xg_{\max}$ for 60 m (extract of ghost preparation G15) at 5°C , prior to injection onto the Synchronpak AX-300 column. A typical elution profile is shown in Fig. 17. To reduce the amounts of extraneous proteins, material which eluted between 4 and 10 m was collected and concentrated under argon at 0°C for quantitative injection on the Micropak TSK G2000 column. Fig. 18 illustrates an HPLC elution profile from the second column. A major portion of the material applied to the Micropak column eluted after the column permeation volume (about 20 ml), indicating that it was delayed by hydrophobic and/or ionic interactions with the column support, in addition to the size exclusion mechanism.

To determine where the membrane-associated SOD eluted, three fractions were concentrated at 0°C under an argon stream, applied to PAGE gels which were then analyzed by staining for SOD activity.

Fraction I: proteins eluting between 10 to 21 m from the Micropak

TSK G2000 column (ie.: before the permeation volume, Fig. 18).

Fraction II: proteins eluting between 21 to 40 m from the

Micropak TSK G2000 column (ie.: after the permeation volume, Fig. 18).

Fraction III: proteins eluting between 10 to 25 m from the

Synchronpak AX-300 column (ie.: the material that was not applied to the Micropak TSK G2000 column, Fig. 17).

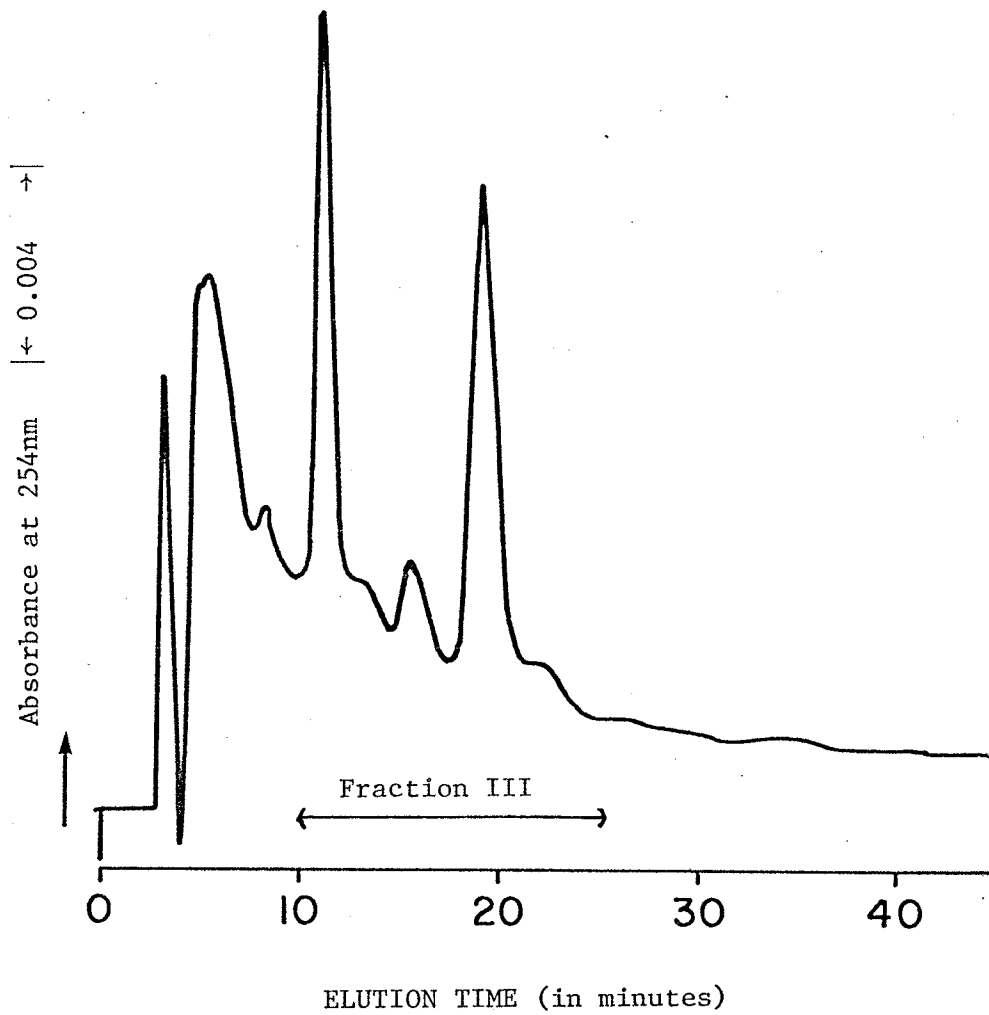


Figure 17: HPLC elution profile of ghost extract. Column: Synchronapak AX-300; Loop: 380 ul; Absorbance range: 0.04; Amount of protein injected: 1.8 mg; Solvent peak: 3 m.

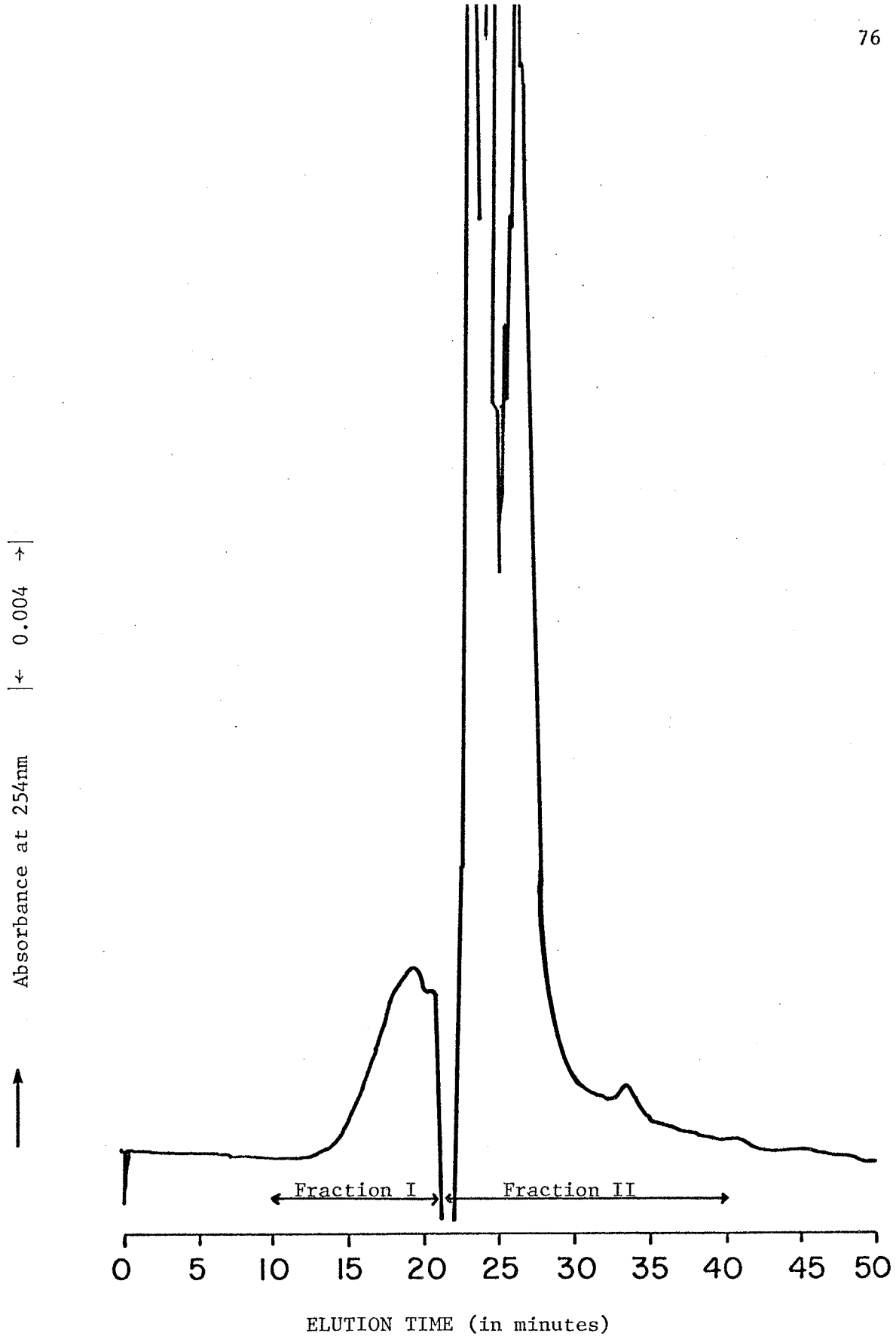


Figure 18: HPLC elution profile of material previously eluted between 4 and 10 m on the Synchronapak AX-300 column (Fig. 17). Column: Micropak TSK G2000; Loop: 380 μ l; Absorbance range: 0.04; Solvent peak: 21-23 m.

The results of the PAGE scans are given in Fig. 19 and show that the SOD activity eluted in fraction I, that is, in the same time frame within which the reference SOD eluted (Fig. 8). This result established that the serial HPLC method separated the membrane-associated SOD from fractions II and III. The tailing in the PAGE activity band toward lower mobility suggests that the protein may still be aggregated with other material. Therefore, it was considered of interest to estimate at this stage the degree of purification of the enzyme attained by serial HPLC.

Purification of the active membrane-associated SOD was followed by calculating A:P ratios, defined as the ratio of Active SOD (as measured by PAGE) to total Protein (as measured by Lowry), with both numerator and denominator values based on weight per unit volume (Fig. 20). The A:P ratio for reference Cu/Zn cytoplasmic SOD was (50.0 ug/ml / 67.4 ug/ml =) 0.74. The values of this ratio for the NP-40 extracts from G14 and G15 ghost preparations are given in Table 6 and were 2.0×10^{-5} and 3.6×10^{-5} , respectively. These values apply to the G14 and G15 materials prior to any purification by HPLC and therefore represent a purification factor of unity in each case. Assuming the membrane-associated SOD has the same specific activity as the reference SOD, purification factors of $(0.74 / 2.0 \times 10^{-5} =)$ 37,000 and $(0.74 / 3.6 \times 10^{-5} =)$ 21,000, respectively, for G14 and G15 were required. After serial HPLC, the A:P ratios for G14 and G15 were 0.0034 and 0.014, respectively. Relative to the starting material of the two ghost extracts, these values represent purification factors of $(0.0034 / 2.0 \times 10^{-5} =)$ 170 and $(0.014 / 3.6 \times 10^{-5} =)$ 390 for G14 and G15, respectively. Thus, to attain the same purity as the reference

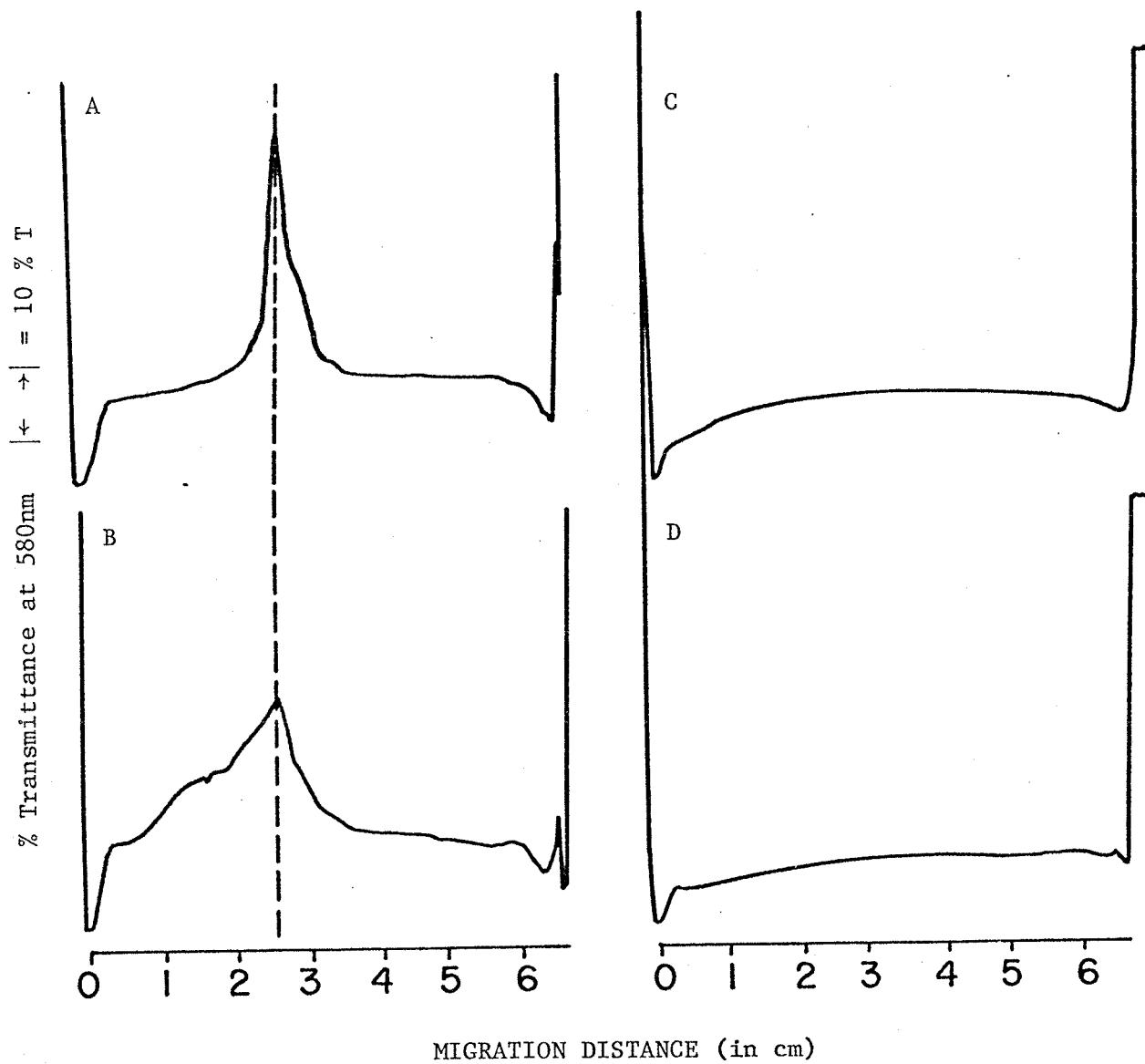
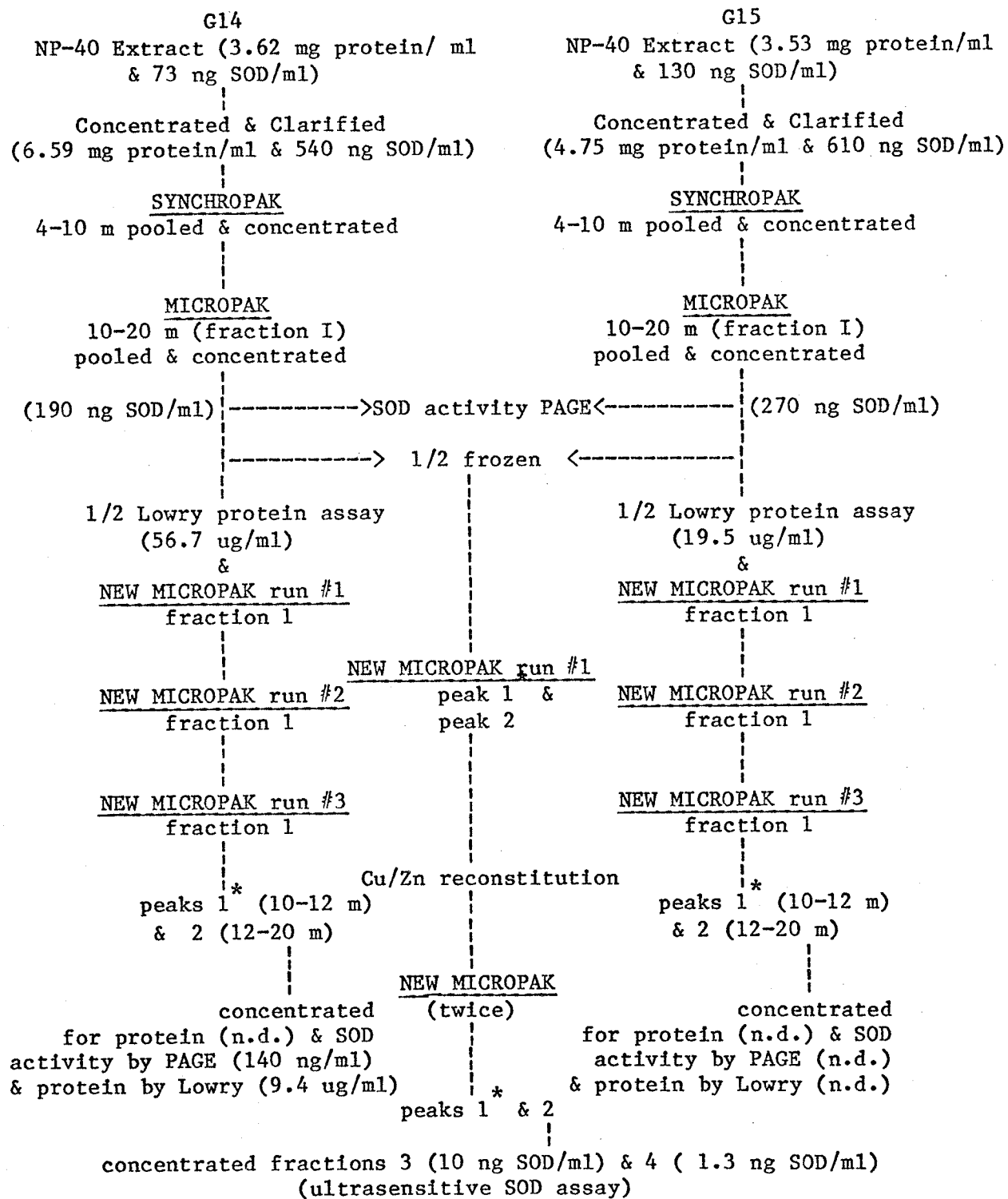


Figure 19: Densitometry tracings of PAGE bands showing SOD activity in HPLC fractions: A, 100 ng reference SOD; B, 300 ul fraction I (Fig. 18) after concentration; C, 300 ul fraction II (Fig. 18) after concentration; D, 300 ul fraction III (Fig. 17) after concentration. See text for details.



* All peak 1's were pooled, concentrated and run on the new Micropak.
 n.d. = not detectable.

Figure 20: Flow diagram of the HPLC sequence of SOD purification from two ghost preparations (G14 and G15) showing the amount of SOD activity as determined by PAGE or by the ultrasensitive assay and the amount of protein by PAGE and by the Lowry method at various stages.

Table 6: Summary of the Purification of Active SOD from Human RBC Ghosts by Serial HPLC for Two Ghost Preparations (G14 and G15)

GHOST	PURIFICATION STAGE		
	PREPARATION	1- Start (ghost extract)	2- After preparation for HPLC
G14:			
Volume	135 ml	380 ul	1.0 ml
[Protein]	3.62 mg/ml	6.59 mg/ml	56.7 ug/ml
Amount of protein	489 mg	2.50 mg	56.7 ug
SOD activity	73 ng/ml	540 ng/ml	190 ng/ml
A:P ratio ¹	2.0×10^{-5}	8.2×10^{-5}	0.0034
A ²	1	4.1	170
B ²	1	---	290
G15:			
Volume	130 ml	380 ul x 3	1.0 ml
[Protein]	3.53 mg/ml	4.75 mg/ml	19.5 ug/ml
Amount of protein	459 mg	5.42 mg	19.5 ug
SOD activity	130 ng/ml	610 ng/ml	270 ng/ml
A:P ratio ¹	3.6×10^{-5}	1.3×10^{-4}	0.014
A ²	1	3.6	390
B ²	1	---	320

¹ The A:P ratio is the ratio of active SOD (as determined by PAGE) to total protein (as determined by Lowry). The values of active SOD and total protein appear in Fig. 24. The A:P ratio for reference SOD is 0.74.

² Values of A and B relate to fraction I (Fig. 18) and are relative purification factors where SOD activity was determined by PAGE and divided by total protein as determined by A, Lowry (i.e.: A:P ratio) or B, semi-quantitatively by extrapolation of the integrated area of the HPLC peak identified in Fig. 18 as fraction I (i.e.: material that eluted between 10 and 20 m from the Micropak TSK G2000 column) assuming all of it was protein.

SOD of cytoplasmic origin, the membrane-associated SOD from the two ghost preparations, G14 and G15, would have to be further purified by factors of $(0.74/0.0034 =)$ 220 and $(0.74/0.014 =)$ 53 times, respectively, assuming similar specific activities.

A possible explanation for the difference in purification factors for G14 and G15 lies in the different centrifugations that were used to clarify the two samples prior to serial HPLC. The longer centrifugation at higher speed of G15 sedimented more material, probably lipid aggregates, with which SOD might have been associated. In comparison with G14, only about a third as much protein was recovered from G15 after serial HPLC. However, this loss of material did not prevent the attainment of a higher purification factor. Nevertheless, appreciable losses of protein and SOD activity was apparent at various stages of the HPLC purification procedure (Table 6).

Alternative purification factors of 290 and 320 for G14 and G15, respectively, were determined by method B (Table 6). Here, total protein was semi-quantitatively determined by extrapolation of the integrated area of the HPLC peak, identified as fraction I in Fig. 18 and assumed to be all protein. Since concentrating the buffer contributed to material eluting between 15 and 20 m (Fig. 21), method B may have overestimated the amount of protein. Thus, the better estimate of the purification factors for G14 and G15, after serial HPLC, is given by method A where total protein was determined by the Lowry technique.

Fraction I was rechromatographed 3 times on a new Micropak TSK G2000 column. The broad peak at 17 m appeared as before (Fig. 22, peak

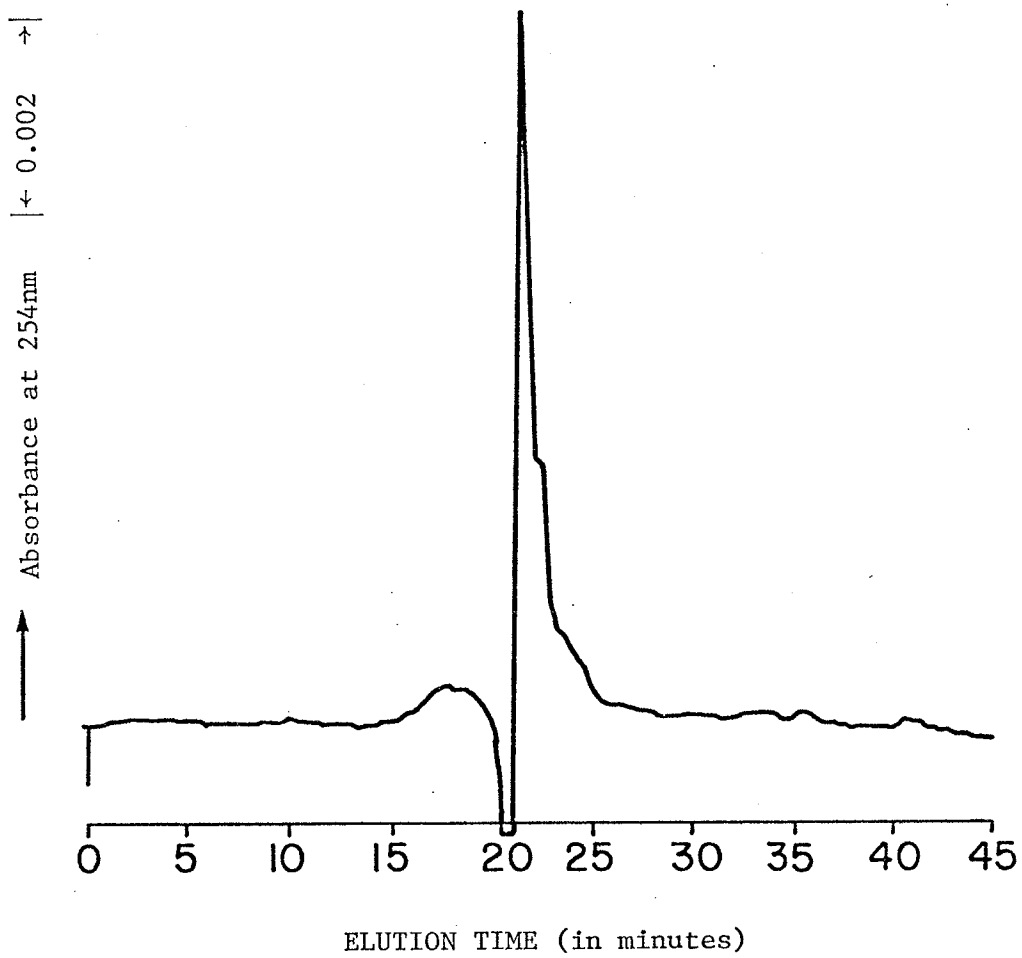


Figure 21: HPLC elution profile of elution buffer concentrated 4.4 times by a filtered stream of argon gas. Column: New Micropak TSK G2000; Loop: 380 ul; Absorbance range: 0.02.

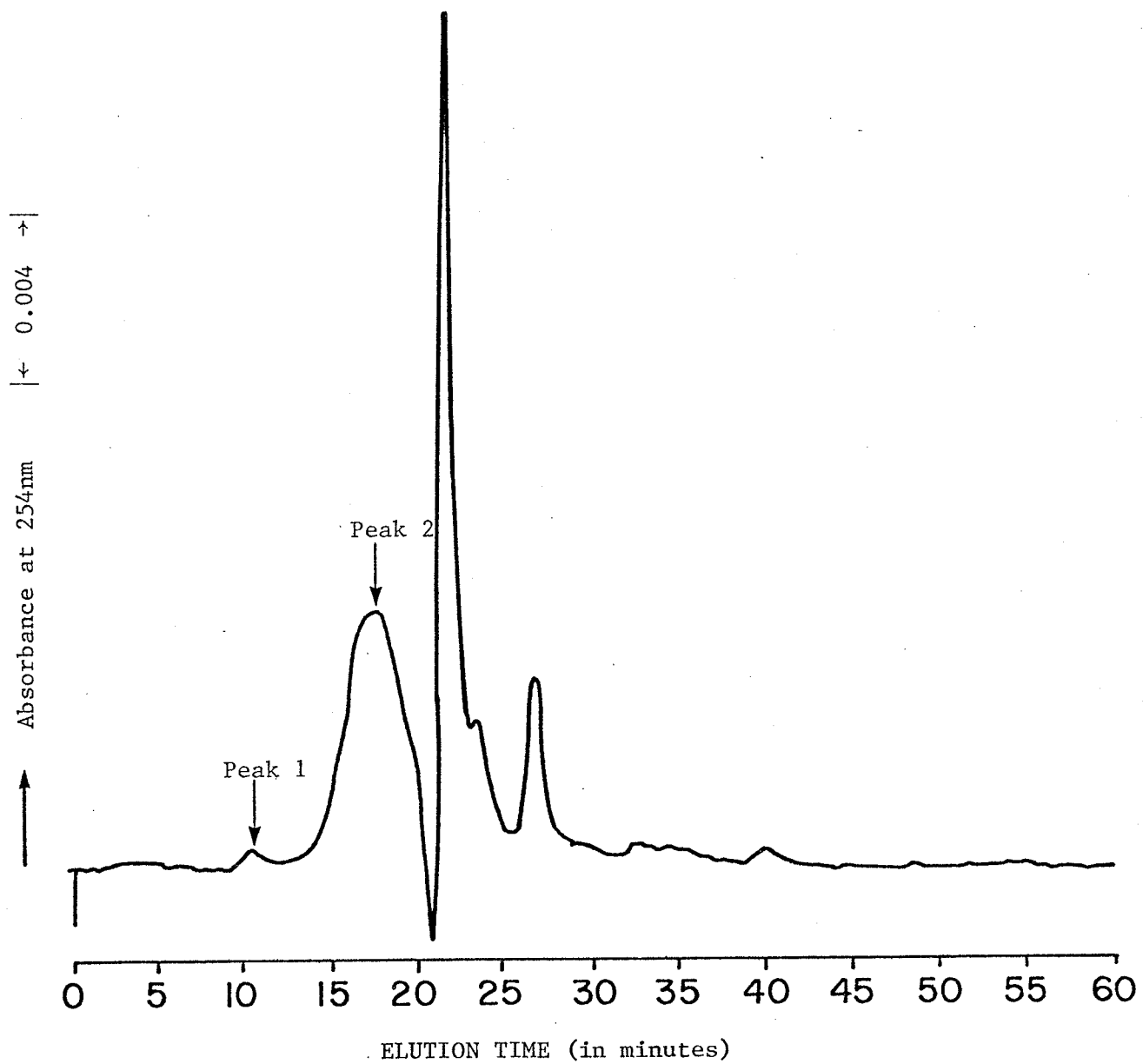


Figure 22: HPLC elution profile of fraction I (Fig. 18) from serial HPLC (ie.: Synchropak AX-300 / Micropak TSK G2000). Column: New Micropak TSK G2000; Loop: 380 ul; Absorbance range: 0.04; Amount injected: 7.4 ug protein.

2) and could be indicative of protein aggregation common to chromatography by size exclusion (129). The aggregation might be due to a natural tendency for the proteins to aggregate or undergo some undefined interaction with the column. In the hope of preventing this possible aggregation, 0.1 % NP-40 was added to the HPLC buffer but was found to absorb excessively at 254nm, making its use inappropriate.

A new peak at 11 m (Fig. 22, peak 1) was evident as early as the first run on the new column. The elution time of 11 m suggested the possible presence of an inactive form of the membrane-associated SOD that might be similar to radiation-inactivated SOD (Fig. 11). Though NP-40 eluted at 11 m (Fig. 13), peak 1 is not due to the detergent as it was removed from the ghost extract by exhaustive dialysis against H₂O.

All material eluting as peak 1 on the Micropak TSK G2000 column was pooled and concentrated under an argon stream at 0°C and reapplied to the Micropak TSK G2000 column, giving the elution profile shown in Fig. 23. It appeared that more material eluted than was previously collected under peak 1 (Fig. 22). This implied that material had been added to the sample during concentration. It may be noted that HPLC of the concentrated buffer on the Micropak TSK G2000 column also gave a broad elution peak at 15 to 20 m (Fig. 21) similar to, but reduced from, peak 2 of Fig. 22. Therefore, it was deduced that concentrating the buffer contributed to the material eluting between 15 and 20 m on the Micropak TSK G2000 column.

To further investigate the above, the material eluting in the 10 to 20 m time interval (Fig. 23) was pooled and dialyzed for 3 days against double distilled H₂O at 5°C and then concentrated to 1 ml by

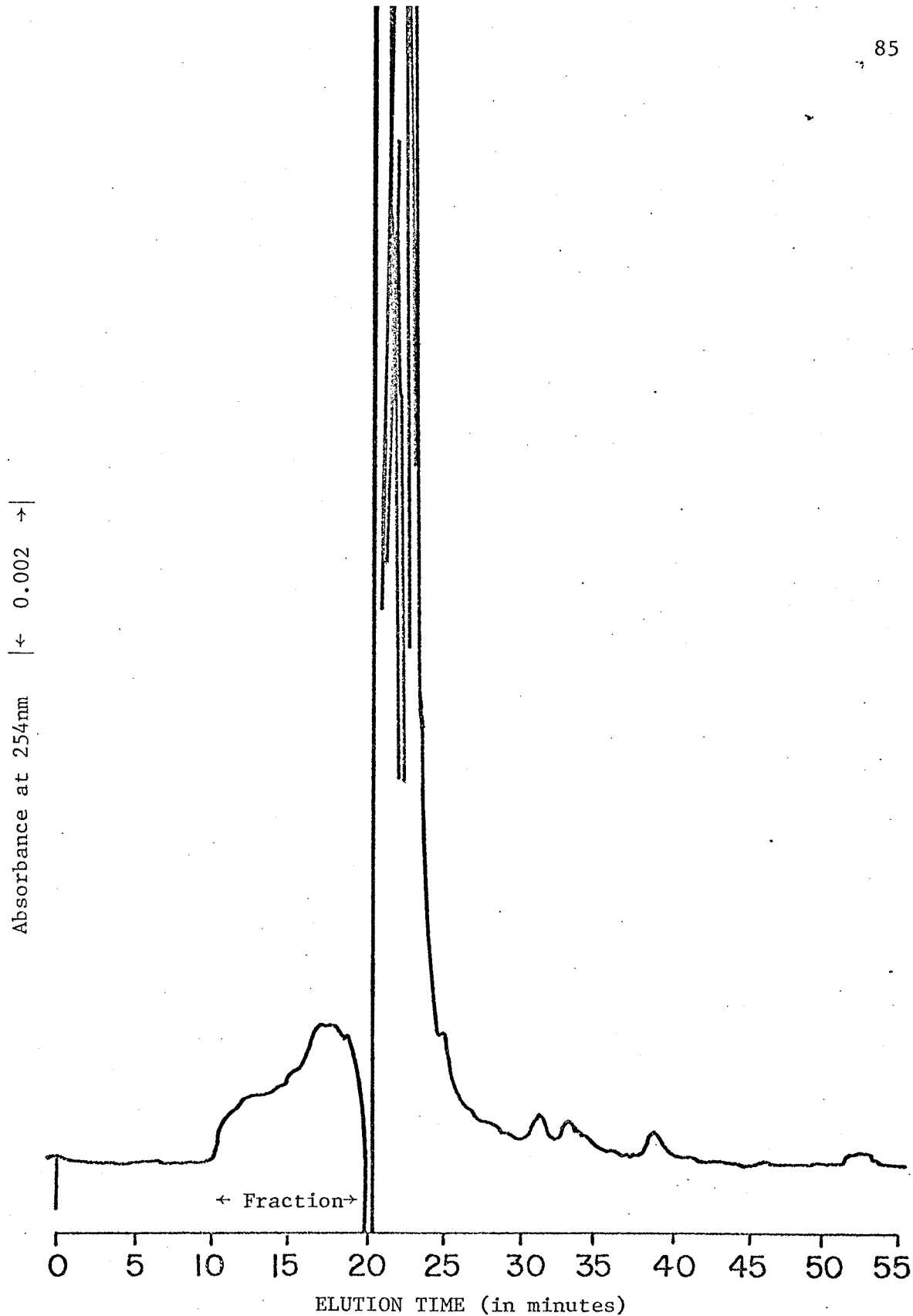


Figure 23: HPLC elution profile of pooled peak 1 material (Fig. 22) from fraction I (pooled and concentrated after serial HPLC and 2 or 3 passes through the new Micropak TSK G2000 column). Column: New Micropak TSK G2000; Loop: 380 ul; Absorbance range: 0.02.

Amicon ultrafiltration using a membrane of 5000 M.W. cutoff. HPLC of the concentrated material on the new Micropak TSK G2000 gave the elution profile shown in Fig. 24. HPLC of H₂O and buffer, concentrated by Amicon ultrafiltration, gave similar elution profiles although with reduced amplitude. This suggested that material was also being introduced during Amicon ultrafiltration. In fact, fine white particles were found suspended in each ultrafiltration chamber, possibly originating from the filtration membranes. Centrifugation of these samples for clarification prior to HPLC did not eliminate the problem.

After the final HPLC run on the Micropak TSK G2000 column (Fig. 20), all fractions eluting as peak 1 (Fig. 22) were pooled and the UV absorption spectrum taken and compared with those of holo- and apo-SOD, thermally-denatured and irradiated-SOD (Fig. 25). Table 7 summarizes and compares the major features of the spectra in Fig. 25. The UV cutoff (ie.: the wavelength below which the absorbance is maximal and nonspecific) of the HPLC fractions suggests the presence of additional material as there is increased absorbance beyond 255nm (the UV cutoff for 1 mg/ml of holo-SOD). However, the UV spectra of the HPLC fractions share similarities with the SOD spectra (eg.: similar λ_{max} and single shoulder). From a comparison of these spectra, the amount of protein in pooled peak 1 was estimated at 0.07 mg/ml, sufficient for doing a protein analysis by Lowry (111) and by PAGE.

The pooled peak 1 material appeared to contain 0.7 ug/ml of protein as determined by the Lowry method. However, the Lowry method is not well suited to measure such low protein concentrations and the

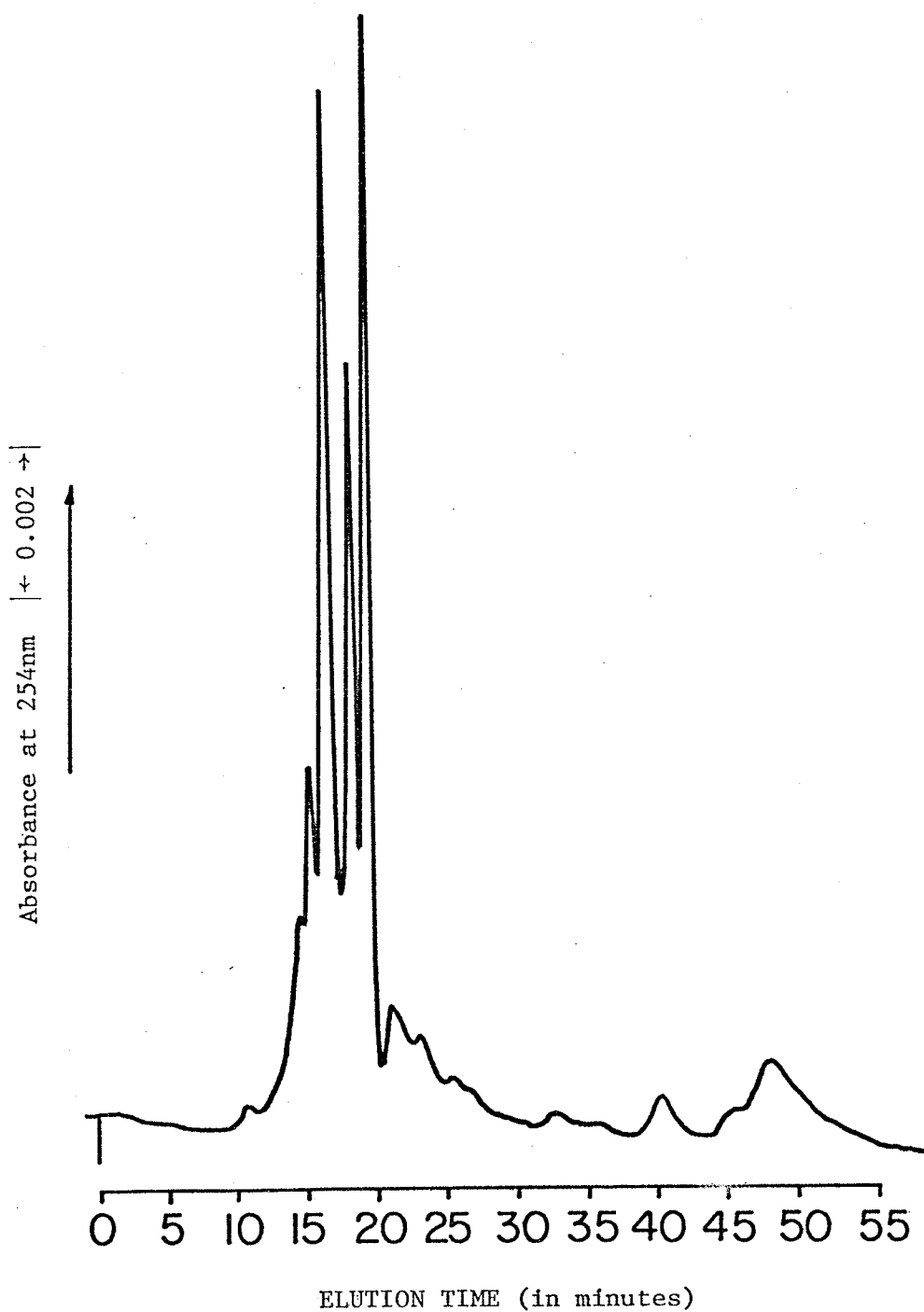


Figure 24: HPLC elution of profile of a fraction (10-20 m, Fig. 23) after exhaustive dialysis against H_2O and concentrating it to 1.2 ml by Amicon ultrafiltration. Column: New Micropak TSK G2000; Loop: 380 μ l; Absorbance range: 0.02.

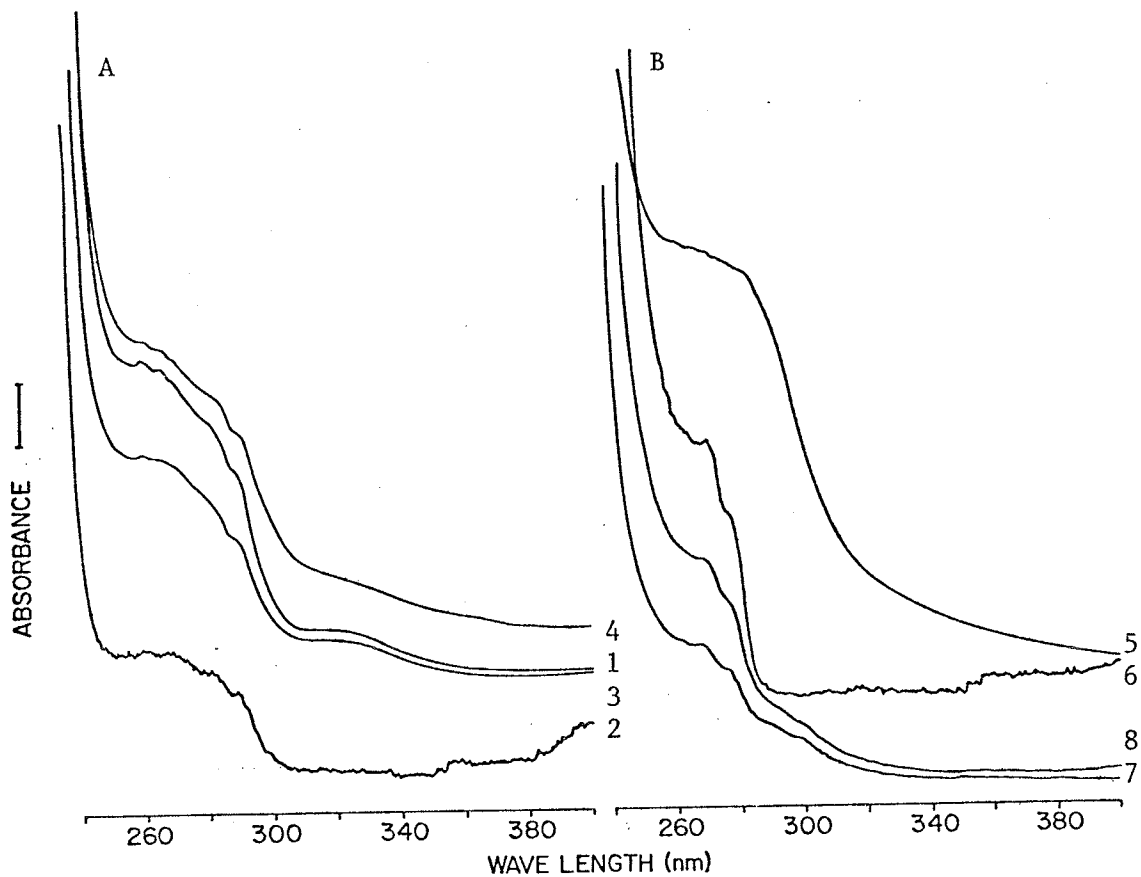


Figure 25: UV absorption spectra of SOD and HPLC fractions. Panel A: 1, holo-SOD, 1.0 mg/ml (bar = 0.1 absorbance units); 2, holo-SOD, 0.053 mg/ml (bar = 0.01 absorbance units); 3, apo-SOD, 0.80 mg/ml (bar = 0.1 absorbance units); 4, thermally denatured SOD, 2.00 mg/ml (bar = 0.1 absorbance units). Panel B: 5, irradiated holo-SOD, 1.0 mg/ml (bar = 0.2 absorbance units); 6, pooled peak 1 from HPLC purification, Fig. 21, 0.73 μ g protein/ml as determined by Lowry (bar = 0.01 absorbance units); 7, fraction 3 from HPLC purification (bar = 0.05 absorbance units); 8, fraction 4 from HPLC purification (bar = 0.05 absorbance units).

Table 7: Comparison of Features of the UV Absorption Spectra of SOD
from Figure 25.

TYPE of SOD	PROTEIN CONCENTRATION (mg/ml)	λ_{\max} (nm)	320 nm CHROMO- PHORE ?	SHOULDERS (nm)	UV CUTOFF (nm)
1- Holo-SOD	1.00	258	yes	288,280,265	254
2- Holo-SOD (HPLC stock SOD)	0.053	250-270	n.d. ¹	288,280	250
3- Apo-SOD	0.80	258	yes	288,265	255
4- Thermally Denatured	2.00	258	yes reduced	288,280,265	255
5- Irradiated Holo-SOD	1.00	258	no	280	255
6- Pooled Peak 1 from HPLC Purification (Fig. 21)	0.07 ²	269	n.d. ¹	277	264
7- Fraction 3 from HPLC Purification	0.73 ²	266	no	300,276	264
8- Fraction 4 from HPLC Purification	0.77 ²	267	no	300,276	265

¹ Not detectable due to insufficient concentration. Samples did not show any absorbance above 290-300 nm.

² As determined by comparison of its absorbance at 265 nm with that of holo-SOD at known concentration (Fig. 25).

value of 0.7 ug/ml is probably unreliable. Further, it is noted that in the Lowry assay, the reaction of proteins with the phenol reagent is largely due to tyrosine groups (130). This amino acid is lacking in human RBC Cu/Zn SOD (89). Thus, the Lowry assay may have underestimated the amount of human SOD protein in the sample. Nonetheless, when this material was applied to PAGE gels in sufficient amounts (up to 1.8 ug protein, based on the Lowry assay) to give a significant area by planimetry (30 arbitrary units of area, Fig. 7 A), no bands were observed when the gels were stained for protein, even though the minimum amount of protein detectable by staining of PAGE gels (0.2 ug) was exceeded. Irradiated SOD (3.2 ug) also failed to show protein bands by the PAGE technique. The latter observation may be explained as follows. Coomassie Brilliant Blue is electrostatically attracted to the NH_3^+ groups of proteins (ie.: to histidine, arginine and lysine) in slightly acidic media (131). Gamma-radiation damages these specific amino acid residues in SOD (132-134) and, therefore, the dye would be less likely to stain the band(s) of irradiated SOD on PAGE gels. Inasmuch as the protein in peak 1, which on the Micropak TSK G2000 column eluted at the same time (11 m) as irradiated SOD, was also not stained by the dye, similarities between the two proteins are suggested. On the basis of the same elution time and non-staining on PAGE gels, peak 1 is expected to contain inactive SOD with damaged amino acids. In contrast, both apo-SOD and thermally-denatured SOD showed the protein bands of SOD but at a lower intensity than holo-SOD. Thermally-denatured SOD could give PAGE bands of reduced intensity due to the inability of some of the denatured aggregates to permeate the gel bed. The reduced protein band intensity of apo-SOD

may be due to conformational changes, which result in decreased optical absorbance (70).

Material eluting as peak 2 (12 to 20 m, Fig. 22) from the new Micropak TSK G2000 column was concentrated under argon and assayed for SOD activity and for protein by both PAGE and Lowry. Table 8 summarizes the results which indicate that active SOD was detected only in G14. The A:P ratio of peak 2 for G14 after this additional HPLC was $(0.14 \text{ ug/ml} / 9.4 \text{ ug/ml}) = 0.015$ (Table 8). This represents a further purification of $(0.015/0.0034) = 4.4$ times, relative to what it was after serial HPLC (Table 6), for an overall purification factor of $(0.015 / 2.0 \times 10^{-5}) = 750$ times from the starting material. To attain the same purity as the reference SOD of cytoplasmic origin and assuming similar specific activities, this G14 material would have to be further purified by a factor of $(0.74/0.015) = 49$ times. The latter value is remarkably close to the value (53 times) calculated for G15 after serial HPLC (Table 6, *vide supra*). Thus, the extra HPLC runs on the G14 material and the longer centrifugation at higher speed of G15 appeared to have achieved the same purpose. These analyses exhausted the materials from the first half portions of the G14 and G15 ghost extracts. Only the frozen portions remained at this stage.

Although peak 2 of G14 was purified further with the additional runs on the new Micropak TSK G2000 column, resolution of active SOD was not possible for the following reasons. The small amount of protein available to work with (ug quantities after serial HPLC, Table 6) was below the detection limit of 0.13 ug/ul of the HPLC detector with a 8 ul optical cell at an absorbance range of 0.04. Concentrating the sample (by argon stream or by Amicon ultrafiltration) between HPLC

Table 8: Analysis of Peak #2 (Figure 22) of G14 and G15 after the Third HPLC on the New Micropak TSK G2000 Column.

Analysis	G14	G15
SOD Activity by PAGE	140 ng/ml	n.d. ¹
SOD-Like Protein by PAGE	n.d.	n.d.
Protein by Lowry	9.4 ug/ml	n.d.
A:P ratio ²	0.015	-
Purification factor ³ based on A:P ratio	750	-

¹ n.d. = not detectable at a sensitivity of 53 ng active SOD/ml (or 16 ng total) by PAGE or 170 ng SOD-like protein/ml (or 50 ng total) by PAGE or 2.5 ug/ml (or 2.5 ug total) by Lowry.

² A:P ratio (or ratio of Active SOD by PAGE to total Protein by Lowry) = 0.14 ug/ml / 9.4 ug/ml = 0.015.

³ Purification factor = Final A:P ratio (0.015) divided by initial A:P ratio (2.0×10^{-5}) equals 750.

runs introduced material from the buffer or from the Amicon filter, as already noted. This interfered with the spectrophotometric detection of protein. Also, detection at 254nm was not optimal since λ_{\max} was found to be 269nm (Fig. 25 and Table 7). However, detection at 254nm was useful in relating the results to the reference SOD.

The remaining ghost material (frozen reserves of G14 and G15 processed through serial HPLC; see Fig. 3) was not assayed for protein or activity after the serial HPLC in order to conserve material. These G14 and G15 portions were run once through the new Micropak TSK G2000 column in order to separate the material eluting as peak 2 (Fig. 22). The material eluting as peak 2, in each case, was subjected to Cu/Zn reconstitution to enhance the SOD activity as much as possible by this technique (117). The reconstituted material was then assayed for SOD activity by PAGE. Only the reconstituted extract from G14 showed activity. After another run of the peak 2 material (12 to 20 m) on the Micropak TSK G2000 column, two fractions were collected:

- a) fraction 3, eluting between 12 to 16 m, in which the active SOD was expected, and,
- b) fraction 4, eluting between 16 to 20 m, in which the presence of active SOD was less likely.

The two fractions were separately concentrated to 1.0 ml by Amicon ultrafiltration. Protein determinations by Lowry and by PAGE were not done in order to conserve material. Assay for SOD activity by PAGE failed to show activity in either fraction. Consequently, a more sensitive assay was attempted (detection limit: 300 pg/ml in a cell of 1 cm path length). Upon assaying for SOD by the ultrasensitive spectrophotometric technique (116), fraction 3 was found to contain 10

ng SOD/ml while fraction 4 contained only 1.3 ng SOD/ml. This confirmed the expectation that the active SOD of the ghost extracts eluted in the same time period (12-16 m) from the Micropak TSK G2000 column as the reference holo-SOD, which eluted at 12.5 m. UV spectra of the two fractions (Fig. 25 and Table 7) were not solely due to concentrating the water or buffer and were very similar to each other. However, on further comparison, the UV spectra (Fig. 25 B) indicate that fraction 4 (0.77 mg/ml; Table 7) contained more material than fraction 3 (0.73 mg/ml; Table 7). The UV spectra of both fractions have features similar to that of reference SOD, particularly in respect to λ_{max} and the shoulder region. However, the UV cutoffs for fractions 3 and 4 begin at a longer wavelength (Table 7). Since the major amount of active SOD was in fraction 3 (10 ng/ml), rather than with fraction 4 (1.3 ng/ml), while the UV spectra indicate an approximate 47:53 split of the optically active material, these results indicate that rerunning the peak 2 material on the Micropak TSK G2000 column and collecting the 12-16 m fraction separately, further purified the active SOD by at least a factor of 2. Thus, the active enzyme in fraction 3, at 10 ng/ml, was enriched at least ($750 \times 2 =$) 1500 times over the starting material, in which the active SOD represented only 0.004 ± 0.002 % of the total ghost protein (Table 2). The yield of partially-purified active SOD in fraction 3 was an estimated 0.04 %.

The inability to recover more active SOD may due to a number of causes other than inactivation by freezing. These include:

a) Sample loss during each HPLC run. For each injection onto the HPLC column, up to 10 % of the sample was irretrievably lost during loading

of the sample loop.

b) Losses during concentrating of samples may have arisen from protein adsorption onto plastic vessels due to changes in solubility. Protein solubility is dependent on pH, ionic strength and type of solvent (ie.: its dielectric constant) and temperature (135). These factors varied during the HPLC purification process and the effects may have been magnified by the repeated HPLC and sample concentration. In general:

- protein solubility increases with increasing temperature (in the range of 0° to 40°C). Temperature of HPLC fractions ranged from 0°C at which samples were concentrated to room temperature at which samples were chromatographed.
- protein solubility decreases with increasing ionic strength, which removes H₂O of hydration from the protein. Hence, sample concentration would cause some proteins to become adsorbed to the sides of the container.
- proteins are least soluble at their isoelectric pH at which the molecules have no net electric charge and, hence, tend to aggregate and precipitate. Concentration would alter the pH of the samples while the buffering capabilities of proteins would minimize such an effect.
- protein solubility decreases with a decrease in the dielectric constant (or polarizability) of the solvent, whereby protein ionization also decreases and proteins tend to aggregate and precipitate. Concentration decreases the dielectric constant.

Note, however, that SOD protein may not have been affected by the higher amounts of salt present during sample concentration since SOD

is not precipitated by high salt (136), while other proteins generally are and could have interfered in the purification of SOD. Nevertheless, the increased salt concentrations may have affected SOD activity.

c) The biological lifetime of the membrane-associated SOD is finite (15) resulting in loss of activity over time. The duration of the experimental period for processing G14 and G15 (including the frozen reserves) was three and two months, respectively.

K) SOD Modification

The effect of certain treatments on reference SOD was important to establish in order to interpret results of similar treatments on ghost extracts. Exposure of our reference SOD to NP-40 and dialysis did not appear to affect the staining intensity of SOD after electrophoresis but slightly increased its electrophoretic mobility, as demonstrated on PAGE gels stained for activity (Fig. 26) or protein (Fig. 27). HPLC of the same samples gave a major peak with the same elution times and heights as the control (Fig. 28 and 29). HPLC of both the NP-40 treated and lipid SOD samples after dialysis on the Micropak TSK G2000 column also demonstrated a small second peak at 23 m (Fig. 28 B and C). In the former case this small peak is not NP-40 because, firstly, the elution time of NP-40 on the Micropak TSK G2000 is 11 m (Fig. 13) and, secondly, dialysis against H₂O would have removed it.

The effect of lipid interacting with the reference SOD was also

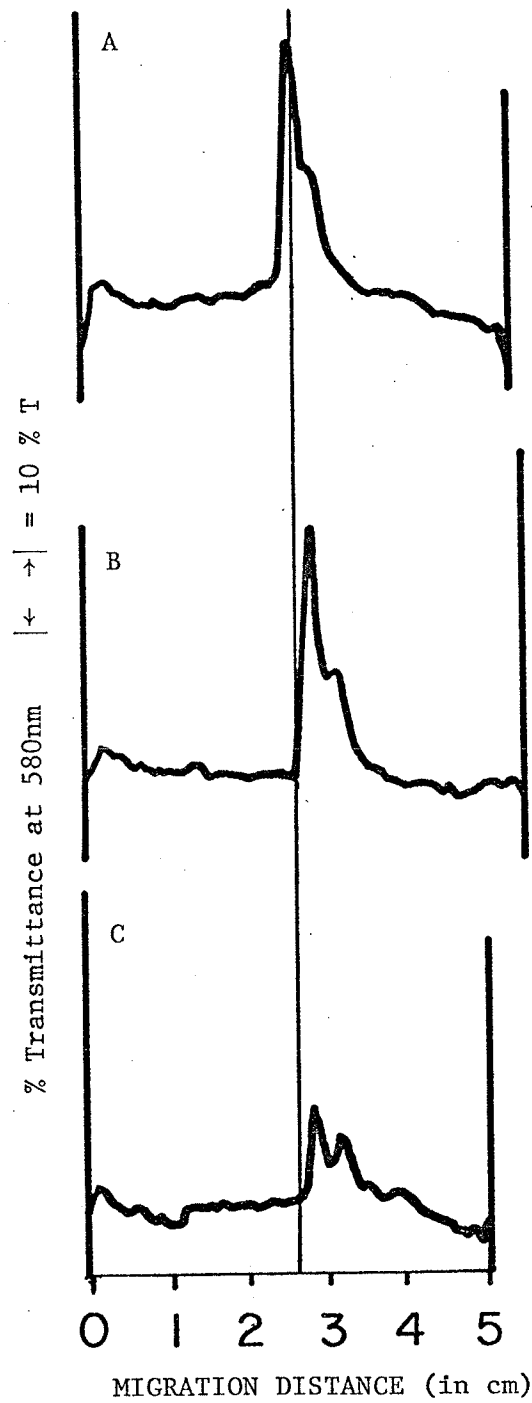


Figure 26: PAGE scans of samples of modified reference SOD stained for activity. A, Control (untreated), 500 ng; B, NP-40 treated and dialyzed, 500 ng; C, Lipid treated and dialyzed, 500 ng.

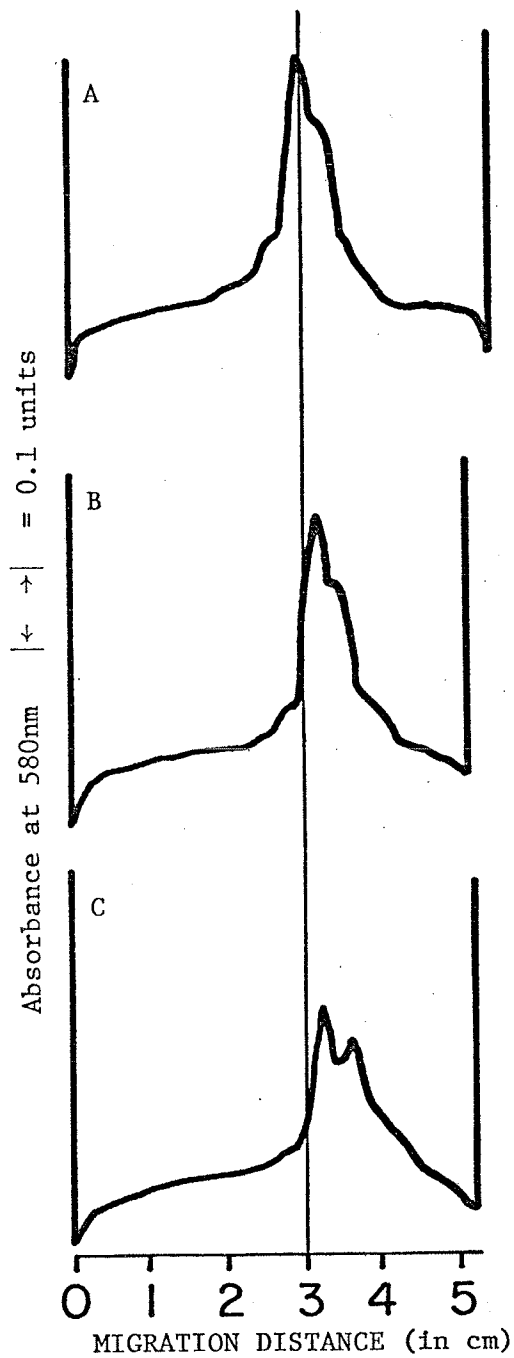


Figure 27: PAGE scans of samples of modified reference SOD stained for protein. A, Control (untreated), 1000 ng; B, NP-40 treated and dialyzed, 1000 ng; C, Lipid treated and dialyzed, 1000 ng.

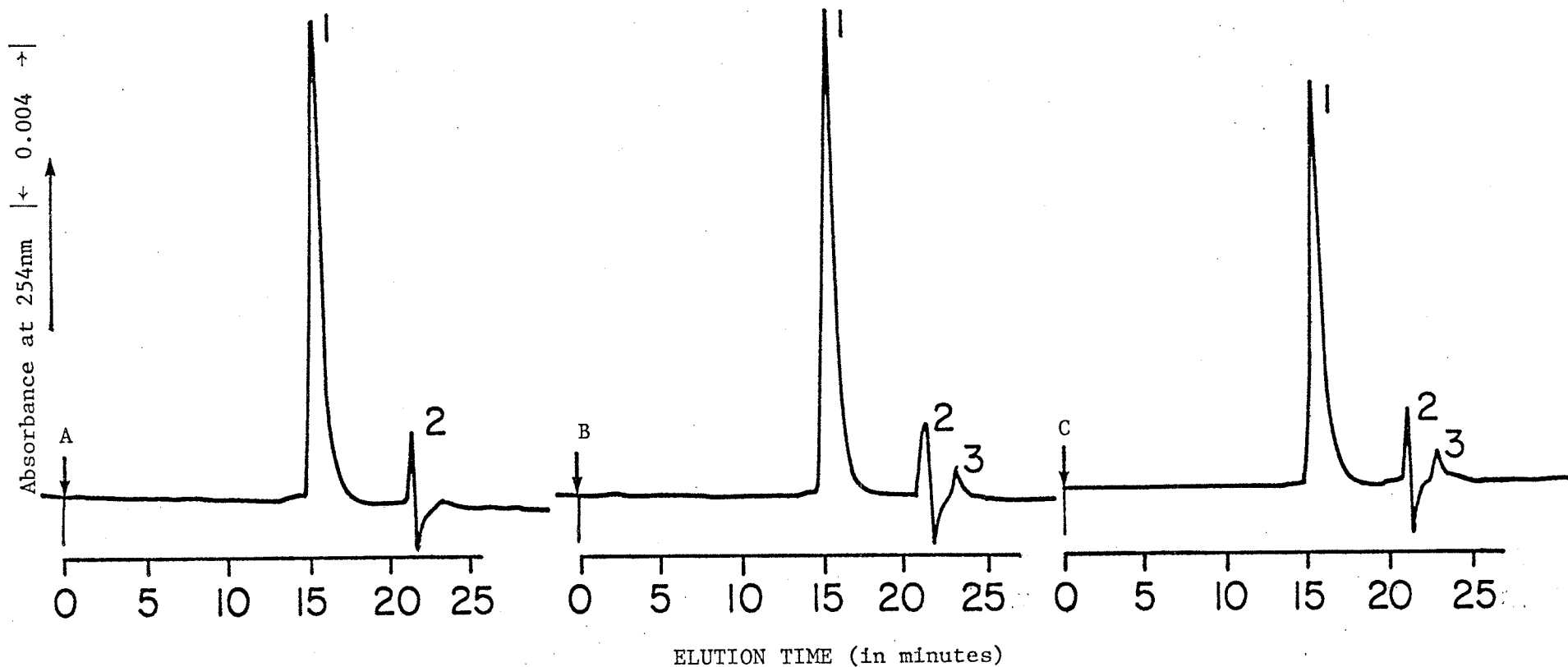


Figure 28: HPLC elution profiles of samples of modified reference SOD. A, Control, 10 ug; B, NP-40 treated and dialyzed, 10 ug; C, Lipid treated and dialyzed, 10 ug. Column: Micropak TSK G2000; Loop: 20 ul; Absorbance range: 0.04; Peaks: SOD (1), sample solvent, H₂O (2), artefact or impurity (3).

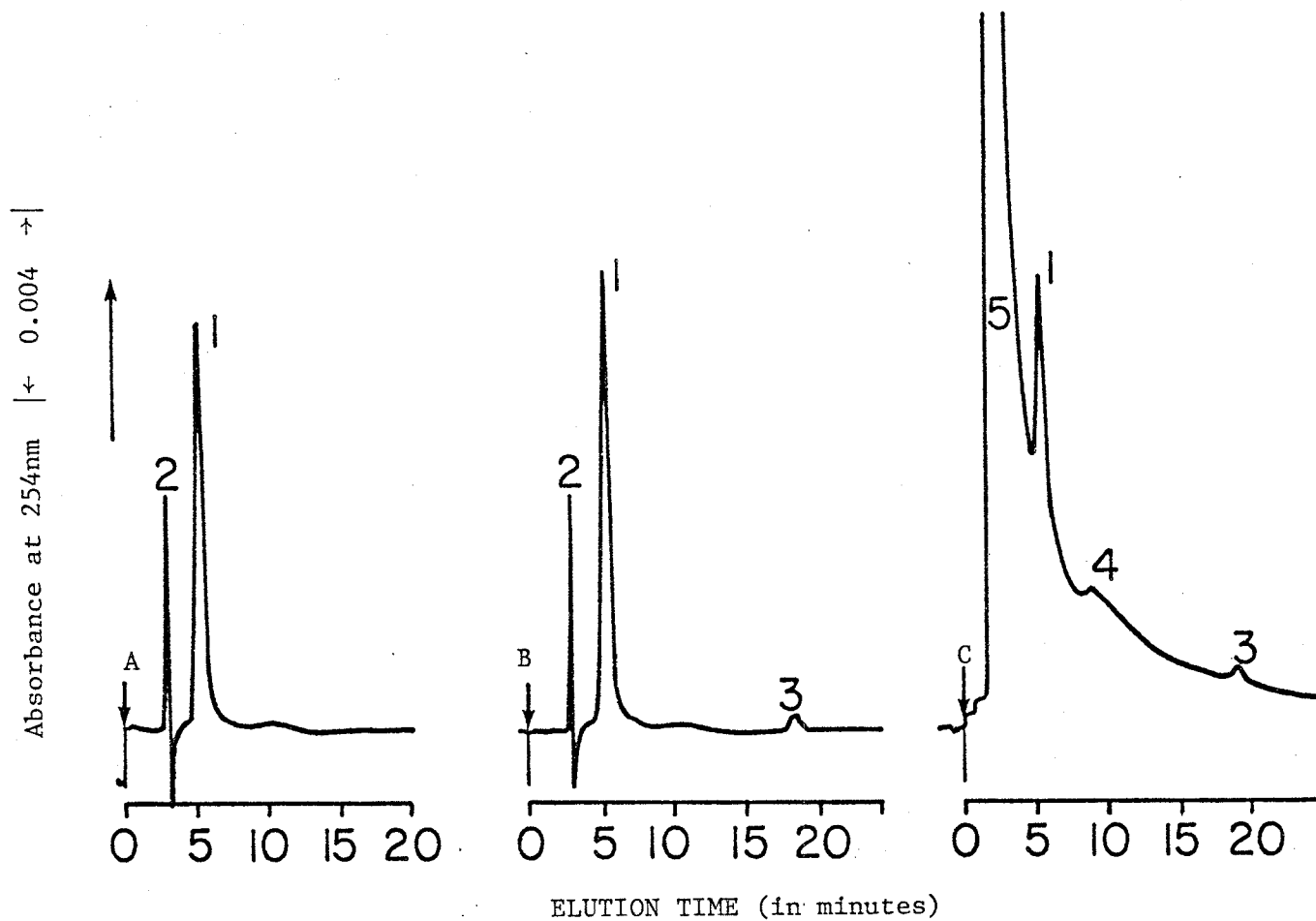


Figure 29: HPLC elution profiles of samples of modified reference SOD. A, Control, 10 ug; B, NP-40 treated and dialyzed, 10 ug; C, Lipid treated and dialyzed, 10 ug. Column: Synchropak AX-300; Loop: 20 ul; Absorbance range: 0.04; Peaks: SOD (1), sample solvent, H₂O (2), impurity (3, 4), possibly lipid (5).

examined. On PAGE, the lipid-treated SOD showed reduced activity and increased mobility (Fig. 26 C, Fig. 27 C). On the Micropak TSK G2000 column, its elution peak was slightly reduced (Fig. 28 C). Taken together, these data indicate that the association of lipid with the reference SOD, of cytoplasmic origin, reduced its activity, increased its electrophoretic mobility and only marginally affected its behaviour on HPLC by gel filtration.

HPLC of the lipid-treated SOD on the Synchronapak AX-300 column resulted in an enlarged peak in the area of the solvent peak (peak 5 of Fig. 29 C) that could include the lipid. The SOD peak at 5 m was not reduced in height and its elution time was the same as that of the untreated SOD. However, on the ion exchange column, the lipid-treated SOD was not separated to baseline resolution.

It is noted that the time of elution of the reference SOD on the Micropak TSK G2000 column in Fig. 28 is 3 m later than normal. This was taken to mean that the column required regeneration in order to renew its efficiency. After regeneration, the reference SOD eluted at its normal time of 12.5 m.

L) "Burton" Ghosts

The Burton method (107) of ghost preparation was found to be a harsher technique than the Hoogeveen method for the following reasons: a) Phase contrast microscopy showed that RBC membranes prepared by the Burton method formed into microvesicles. Hence, no ghosts were obtained. The loss of ghost morphology was considered as the critical factor, mitigating against the use of the Burton method for the

purpose of identifying SOD in the membranes of human RBCs.

b) The total protein recovered from 240 ml of blood was 49.4 mg or 49 % of the amount extracted from the same volume of blood processed by the Hoogveen method.

c) Hemoglobin content and ACHE activity could not be calculated for this ghost preparation because a cellular basis was lacking.

d) The total amount of active SOD extracted from the Burton membranes, as determined by PAGE, was 50 % of the amount determined for ghosts prepared by the Hoogveen method.

CHAPTER 5: Discussion

A) Ghost Quality and Analyses

The ghosts prepared by the method of Hoogeveen, using serial hypotonic hemolysis (19), have been shown to be of a quality suitable for the isolation of membrane-associated enzymes. Phase contrast microscopy found the ghosts morphologically intact in the final hemolysis buffer. Ghost protein ($(0.7 \pm 0.1) \times 10^{-12}$ g/ghost) was comparatively low, as was ghost hemoglobin (0.10 ± 0.01 % of MCH), which argues against artefactual association of cytoplasmic components with the membrane. Within the limit of sensitivity of the colorimetric assay used to measure 5'-AMP-nucleotidase activity, the enzyme was not present in the RBC ghosts. Therefore, it could not be used as a membrane-marker enzyme in this study. The activity of the membrane marker enzyme, ACHE, in the ghosts was the same as reported in the literature (1.7 ± 0.3 umole/m/mg ghost protein), indicating optimal enzyme activity per mg ghost protein and little or no extraneously adsorbed proteins.

Active SOD was found associated with these high quality RBC ghosts. This activity was electrophoretically similar to cytoplasmic Cu/Zn SOD. Although the amount of active SOD was measured to be $(3 \pm 1) \times 10^{-8}$ ng/ghost (or 0.4 ± 0.2 % of the total cellular SOD), the inactive portion of this membrane-associated enzyme was apparently present in greater amounts. By PAGE analysis, the SOD-like protein was

77 times greater than the amount of active SOD. These results compare favorably with the bovine work (15) in which the bulk of the membrane-associated SOD was found to be inactive and unreactive with anti-SOD antibody.

It is noted that ghosts from outdated blood contained more SOD (1600 ± 1200 molecules/ghost) than ghosts from fresh blood (540 ± 240 molecules/ghost). If distributed uniformly throughout the ghost membrane (about 9 nm thickness), the latter value is equivalent to about 0.6 μ M. In contrast, the amount of active SOD in the cytoplasm is estimated at 1.9 μ M. Therefore, the concentration gradient of active SOD in human RBCs is directed radially outwards and the endo-surface of the plasma membrane would be the initial point of contact for cytoplasmic SOD. Physicochemical experiments have shown that the cytoplasmic Cu/Zn SOD interacts with both the surface and the hydrocarbon region of lipid bilayers and that the latter interaction is facilitated by lipid peroxidation (94, 95). These features of the interaction between active Cu/Zn SOD and lipid membranes could account for the fact that ghosts from outdated blood contained a larger number of molecules of active SOD than ghosts from fresh blood. The former ghosts would be expected to have undergone depletion of energy and reductions in activity of metabolic defense mechanisms against lipid peroxidation and in anti-oxidants such as Vit.E. Thus, the larger number of active SOD molecules per ghost from outdated blood is consistent with the free radical theory of cellular aging via the oxidation of cellular constituents (25).

B) HPLC Purification

The HPLC results indicate that the inactive portion of membrane-associated SOD was at least partially separated from the active enzyme. In some respects, the inactive material behaved similarly to radiation-inactivated Cu/Zn SOD of cytoplasmic origin. Their UV spectral characteristics were similar. Also, the inactive protein and the radiation-inactivated SOD eluted at 11 m from the Micropak TSK G2000 column, implying a similarity in molecular size. Lacking enzyme activity, they both did not show PAGE bands after staining for SOD activity or protein. The failure to take up the Coomassie Brilliant Blue dye suggested similar chemical damage, particularly to arginine, histidine and lysine residues. Exposure of reference SOD to lipid was also found to decrease the activity of SOD in vitro. The in vivo effect of lipid association with human Cu/Zn SOD is unknown at this time.

Partial purification by HPLC of active SOD, extracted with NP-40 from human RBC ghosts, has been demonstrated. Serial HPLC of the ghost extract increased the purity of the membrane-associated SOD up to 170 to 390 times, depending on the starting material. Three additional runs of the active fraction (fraction I) on the new Micropak TSK G2000 column increased the purification from 170 to 750 times. The latter value was increased to about 1500 times when the fraction, eluting at 12-16 m on the Micropak TSK G2000 column, was collected separately rather than together with the material eluting at 16-20 m. On the basis of the elution behavior of the reference SOD (elution peak at 12.5 m), the 12-16 m period could be narrowed, possibly resulting in

further improvement in the HPLC purification procedure. Nonetheless, HPLC as employed in this study, involving first the sequential use of ion exchange and size exclusion columns, followed by repeated passage of the active SOD fraction through the size exclusion column and collecting the active fraction over a progressively narrower range in elution times, has succeeded in isolating ng quantities of active SOD which is about 1500 times higher in specific activity than the starting material. Throughout the purification procedure, the active SOD derived from RBC ghost membranes behaved like Cu/Zn SOD of cytoplasmic origin. The overall yield of the partially purified active SOD was an estimated 0.04 % of the amount initially present in the ghosts. This estimate of the yield is based on activity, rather than protein, since the latter could not be specifically measured in the final stages of the purification procedure. As already noted, the absence of tyrosine in human Cu/Zn SOD means that the Lowry technique for estimating the enzyme is not particularly sensitive.

Spectrophotometric resolution of the active SOD, eluting off the Micropak TSK G2000 HPLC column, was not possible. The combined effects of little material, instrument sensitivity and interference introduced by concentrating the sample contributed to the difficulty. More material would be required to overcome these problems. If the inactive portion of the enzyme eluting at 11 m was all SOD protein and if it was 77 times greater than the amount of active SOD, as determined in this study, then to detect active SOD spectrophotometrically and possibly resolve it by HPLC, the amount of active enzyme injected onto the column would have to be at least 77 times greater than it was. To achieve this, a total of 77 units (or about 38 l) of blood would have

to be processed. This scale up in starting material would lessen the need to concentrate samples, thereby reducing the gross nature of peak 2 (Fig. 22). It would also give a better chance of resolving the peak of active membrane-associated SOD, by going to a lower sensitivity of detection. Also, detection at 267nm should be more sensitive than 254nm, as the absorbance maximum of peak 2, in which the SOD activity was found, is at 267nm.

HPLC appears to have separated an inactive SOD-like protein from human RBC ghosts. This protein appears similar to human RBC Cu/Zn SOD of cytoplasmic origin, after inactivation by gamma radiation. The two proteins share the following features:

- 11 m elution times from the size exclusion (Micropak TSK G2000 HPLC) column.
- lack of protein and enzyme activity bands on PAGE.
- UV absorption spectra that show single shoulders at about 278nm and maxima at about 264nm.

Serial HPLC has also partially separated (but not resolved) the active portion of the membrane-associated SOD into a broad peak eluting between 12 and 20 m from the Micropak TSK G2000 column. After serial HPLC, the A:P ratio for SOD in G14 was 0.003 mg SOD/mg protein and in G15 it was 0.014 mg SOD/mg protein. Overall, a purification factor of about 1500 in activity was realized, leaving a further factor of 23 if a purity similar to that of the reference SOD is to be attained. The SOD from the ghost membranes showed the same electrophoretic mobility on PAGE as the reference SOD. Since both the active and inactive SOD were extracted from ghosts of acceptable quality, insofar as assays for membrane-marker enzymes are concerned, it is concluded that they

were membrane-associated.

As the purification procedure must further increase the purity of membrane-associated SOD by 23 times to attain a purity similar to that of the reference SOD, the following recommendations are made in the hope of achieving this end:

- 1) An increase in the amount of starting ghost material to increase the yield and improve resolution. This would require a small change in the ghost preparation method in order to accommodate larger volumes of blood. A preliminary pass of the extract through a liquid chromatography column (eg.: ion exchange with DEAE-cellulose or gel filtration with Ultrogel AcA 54) would remove the bulk of extraneous material which the HPLC columns could not tolerate.
- 2) Development of an HPLC buffer containing an appropriate detergent, which does not affect sensitivity of the method and at the same time prevents possible protein aggregation during HPLC.
- 3) Determination of whether lipids have been totally dissociated from the membrane proteins, including SOD.
- 4) Development of gradient HPLC on the Synchronapak AX-300 ion exchange column and on the Micropak SP C18 reverse phase column. In the latter column, the stationary phase is nonpolar or hydrophobic with elution of proteins being achieved by reducing eluent polarity; eg. addition of methanol. This might complete the HPLC developmental work.

C) SOD Association with the RBC Membrane

The disruptive properties of the non-ionic detergent, NP-40, were required to extract SOD from ghost membranes. In addition, SOD was

still found in the ghost extracts after the use of low ionic strength buffers during hemolysis, which may have removed many weakly bonded extrinsic proteins. Taken together, these data suggest that SOD may be intrinsically membrane-associated.

The active and inactive SOD in ghosts appear to be inherent to them, as opposed to cytoplasmic SOD adsorbed to the endo-face of the plasma membrane during ghost preparation. Several features argue against the latter possibility:

- The Hoogveen method is known to give a high selection factor of 1500:1 for inner surface membrane proteins over hemoglobin (19). Hence, the chance of hemoglobin and other cytoplasmic components being adsorbed to the membranes is small.

- The lower amount of ghost protein in our preparations, $(0.7 \pm 0.1) \times 10^{-12}$ g/ghost, compared to Hoogveen's, 0.91×10^{-12} g/ghost, (19). The lower value obtained in the present work is likely due to the extra third hemolysis in 20 mosM buffer, incorporated into our study, and supports Hoogveen's finding that prolonged exposure of ghosts to the same salt concentrations as used in lysing, actually dissolves inner surface membrane proteins (19).

- Membrane desorption of SOD of the rat liver mitochondrial matrix by low (0.04 M) salt concentrations (137). Thus, another group has specifically shown a desorbing effect of SOD from membranes. The desorbing effect may be more pronounced in the Hoogveen method since it employs even lower concentrations of hemolysis buffers (as low as 0.01 M) (19). In the face of possible desorption of SOD from ghosts during hemolysis, the presence of active SOD in the membranes of such ghosts appears significant as an indicator of the relationship between

SOD and the RBC membrane *in vivo*.

The nature of the association of SOD with the human ghost membrane is unknown. Nevertheless, parallels can be drawn from studies on bovine ghosts discussed in Chapter 2. Just as the SOD, associated with bovine RBC membranes, was found at the cytoplasmic face (endo-face) of the membrane (75), so it is possible that the human RBC membrane-associated SOD is situated at the endo-face as well. SOD intrinsic to the RBC membrane would have lipids or other proteins associated with it, which could facilitate its conversion to the inactive state, the bulk of which appears to have been isolated by HPLC. As discussed in Chapter 2, Cu/Zn SOD possesses the amphipathic character required of intrinsic membrane proteins. An extrinsic SOD would be associated with other proteins or the hydrophilic heads of lipids and be lost during hypotonic hemolysis. For example, it may be bound to the anion pore protein of the RBC membrane with which various other proteins are associated (18).

Other studies have investigated the nature of the interaction of SOD with lipid bilayers in some detail. In particular, physicochemical data demonstrated the affinity of apo- and holo-SOD for lipid membranes (94, 95). Spin-label measurements indicated that the enzyme associates with the liposomal surface and also with the fatty acids (94). In doing so, the surface viscosity is increased and the order of the lipid packing perturbed. Differential scanning calorimetry confirmed this effect (95). Freeze-fracture and etch electron microscopy of liposomes (before and after treatment with SOD) showed that the enzyme induced changes in the texture of the liposomal surface and penetrated the multi-lamellar structure, thereby affecting

their organization (94). Uptake of ^{125}I -labeled SOD by phospholipid bilayers increased with the concentration of the enzyme (holo- or apo-), while treatment with trypsin removed only a fraction of each type of SOD, indicative of a surface interaction (95). Hence, SOD is able to associate with both the surfaces and hydrocarbon region of lipid membranes.

D) The Relevance of Membrane-Associated SOD

This study has shown that both active and inactive SOD are associated with human RBC ghosts. The higher concentration of Cu/Zn SOD in the RBC cytoplasm suggests that the enzyme could diffuse down its concentration gradient and become incorporated into the membrane. So, the membrane is able to take up SOD albeit to a small extent (94). It has also been suggested that the membrane may act as a sink for inactive SOD of cytoplasmic origin (95), just as it does for denatured hemoglobin or 'Heinz bodies', for example (10). A defensive role for active SOD in the membrane is suggested by virtue of its ability to scavenge superoxide. In such a role, even inactive SOD could scavenge hydroxyl radicals (138) and singlet oxygen on a non-specific, non-catalytic basis (139, 140). In view of its antioxidant properties, SOD would probably be most effective at the endo-face or in the hydrocarbon region since superoxide is generated especially in the cytoplasm of RBCs during their life (7). SOD at the ecto-face of the membrane would be less effective in reacting with the free radicals from within the cell. Hence, SOD bound to the anion pore protein at the endo-face of the membrane, for example, might prevent potential

damage by inactivating active oxygen species before they permeate the membrane via this channel. On the other hand, SOD located within the hydrocarbon region of the lipid bilayer would be at the immediate site of free radical production by lipid peroxidation (20, 40).

References

- 1 Steck, T.L. (1978) The Organization of Proteins in the Human Erythrocyte Membrane. *Membr. Transp. Processes* 2, 39-51.
- 2 Schrier, S.L. (1977) Human Erythrocyte Membrane Enzymes: Current Status and Clinical Correlates. *Blood* 50, 227-237.
- 3 Hanahan, D.J. (1973) The Erythrocyte Membrane: Variability and Membrane Enzyme Activity. *Biochim. Biophys. Acta* 300, 319-340.
- 4 Schwoch, G. and Passow, H. (1973) Preparation and Properties of Human Erythrocyte Ghosts. *Molec. Cell. Biochem.* 2, 197-218.
- 5 Gratzer, W.B. (1981) The Red Cell Membrane and its Cytoskeleton. *Biochem. J.* 198, 1-8.
- 6 Shoet, S.B. and Ness, P.M. (1976) Hemolytic Anemias: Failure of the Red Cell Membrane. *Med. Clin. N. Am.* 60, 913-932.
- 7 Carrell, R.W., Winterbourn, C.C. and Rachmilewitz, E.A. (1975) Activated Oxygen and Hemolysis. *British J. Haematol.* 30, 259-264.
- 8 Gray, G.R., Klebanoff, S.J., Stamatoyannopoulos, G., Austin, T., Naiman, S.C., Yoshida, A., Kliman, M.R. and Robinson, G.C.F. (1973) Neutrophil Dysfunction, Chronic Granulomatous Disease, and Non-spherocytic Hemolytic Anemia Caused by Complete Deficiency of Glucose-6-Phosphate Dehydrogenase. *The Lancet*, Sept. 8, 530-534.
- 9 Das, S.K. and Nair, R.C. (1980) Superoxide Dismutase, Glutathione Peroxidase, Catalase and Lipid Peroxidation of Normal and Sickled Erythrocytes. *Br. J. Haematol.* 44: 87-92.
- 10 Gordon-Smith, E.C. and White, J.M. (1974) Oxidative Hemolysis and Heinz Body Hemolytic Anemia. *Br. J. Haematol.* 26, 513-517.
- 11 Fridovich, I. (1978) The Biology of Oxygen Radicals. *Science*, 201, 875-880.
- 12 Lynch, R.E. and Fridovich, I. (1978) Effects of Superoxide on the Erythrocyte Membrane. *J. Biol. Chem.* 253, 1838-1845.
- 13 Lynch, R.E. and Fridovich, I. (1978) Permeation of the Erythrocyte Stroma by Superoxide Radical. *J. Biol. Chem.* 253, 4679-4699.

- 14 Pederson, T.C. and Aust, S.D. (1972) NADPH-Dependent Lipid Peroxidation Catalyzed by Purified NADPH-Cytochrome c Reductase from Rat Liver Microsomes. *Biochem. Biophys. Res. Comm.* 48, 789-795.
- 15 Petkau, A., Copps, T.P. and Kelly, K. (1981) Superoxide Dismutase Within the Bovine Erythrocyte Membrane. *Biochim. Biophys. Acta* 645, 71-80.
- 16 Singer, S.J. and Nicolson, G.L. (1972) The Fluid Mosaic Model of the Structure of Cell Membranes. *Science* 175, 720-731.
- 17 Wilson, J.E. (1978) Ambiquitous Enzymes: Variation in Intracellular Distribution as a Regulatory Mechanism. *Trends Biochem. Sci.* 7, 124-125.
- 18 Gillies, R.J. (1982) The Binding Site for Aldolase and G3PDH in Erythrocyte Membranes. *Trends Biochem. Sci.* 7, 41-42.
- 19 Hoogeveen, J.Th., Juliano, R., Coleman, J. and Rothstein, A. (1970) Water-soluble Proteins of the Human Red Cell Membrane. *J. Membr. Biol.* 3, 156-172.
- 20 Tappel, A.L. (1975) Lipid Peroxidation and Fluorescent Molecular Damage to Membranes in Pathobiology of Cell Membranes, Vol. 1 (Trump, B.F. and Arstila, A.V., eds.) Academic Press, New York, pp. 145-172.
- 21 Dormandy, T.L. (1969) Biological Rancidification. *The Lancet.* 2, 684-688.
- 22 George, P. (1965) in *Oxidases and Related Redox Systems* (King, T.E., Mason, H.S. and Morrison, M., eds.) Wiley & Sons, New York.
- 23 Singh, A. (1982) Chemical and Biochemical Aspects of Superoxide Radicals and Related Species of Activated Oxygen. *Can. J. Physiol. Pharmacol.* 60, 1330-1345.
- 24 Borg, D.C., Schaich, K.M., Elmore, Jr., J.J. and Bell, J.A. (1978) Cytotoxic Reactions of Free Radical Species of Oxygen. *Photochem. Photobiol.* 28, 887-907.
- 25 Pryor, W.A. (1978) The Formation of Free Radicals and the Consequences of their Reactions In Vivo. *Photochem. Photobiol.* 28, 787-801.
- 26 Misra, H.P. and Fridovich, I. (1972) The Generation of Superoxide Radical during the Autoxidation of Hemoglobin. *J. Biol. Chem.* 247, 6960-6962.

- 27 Carrell, R.W., Krishnamoorthy, R. and Winterbourn, C.C. (1978) Hemoglobin Autoxidation: The Risk to the Red Cell and the Contribution of Copper in The Red Cell, Alan R. Liss, Inc., New York, pp. 669-681 .
- 28 Wever, R., Oudega, B. and Van Gelder, B.F. (1973) Generation of Superoxide Radicals During the Autoxidation of Mammalian Oxyhemoglobin. *Biochim. Biophys. Acta* 302, 475-478.
- 29 Halliwell, B. (1982) Superoxide-dependent Formation of Hydroxyl Radicals in the Presence of Iron Salts is a Feasible Source of Hydroxyl Radicals In Vivo. *Biochem. J.* 205, 461-462.
- 30 Hochstein, P., Kumar, K.S. and Forman, S.J. (1978) Mechanisms of Copper Toxicity in Red Cells in The Red Cell, Alan R. Liss, Inc., New York, pp. 687-695.
- 31 Purohit, S.C., Bisby, R.H. and Cundall, R.B. (1980) Chemical Damage in Gamma-irradiated Human Erythrocyte Membranes. *Int. J. Radiat Biol.* 38, 159-166.
- 32 Inouye, B., Aono, K., Iida, S. and Utsumi, K. (1979) Influence of Superoxide Generating System, Vitamin E, and Superoxide Dismutase on Radiation Consequences. *Physiol. Chem. Phys.* 11, 151-160.
- 33 Singh, A. (1978) Introduction: Interconversion of Singlet Oxygen and Related Species. *Photochem. Photobiol.* 28, 429-433.
- 34 Bielski, B.H.J. and Richter, H.W. (1977) A Study of the Superoxide Radical Chemistry by Stopped-flow Radiolysis and Radiation Induced Oxygen Consumption. *J. Am. Chem. Soc.* 99, 3019-3023.
- 35 Tyler, D.D. (1975) Role of Superoxide Radicals in the Lipid Peroxidation of Intracellular Membranes. *FEBS LETT.* 51, 180-183.
- 36 Petkau, A. and Chelack, W.S. (1974) Protection of Acholeplasma Laidlawii B by Superoxide Dismutase. *Int. J. Radiat. Biol.* 26, 421-426.
- 37 Bielski, B.H.J. and Chan, P.C. (1973) Enzyme-catalyzed Free Radical Reactions with Nicotinamide-adenine Nucleotides: I. Lactate Dehydrogenase-catalyzed Chain Oxidation of Bound NADH by Superoxide Radicals. *Arch. Biochem. Biophys.* 159, 873-879.
- 38 McCay, P.B., Fong, K.L., Lai, E.K. and King, M.M. (1978) Possible Role of Vitamin E as a Free Radical Scavenger and Singlet Oxygen Quencher in Biological Systems which Initiate Radical-mediated Reactions in Tocopherol, Oxygen, and

- Biomembranes; symp. 1977 (DeDuve, C. and Hayaishi, O., eds.) Elsevier North Holland Biomedical Press, New York, pp. 41-57.
- 39 Fee, J.A. and Teitelbaum, H.D. (1972) Evidence that Superoxide Dismutase Plays a Role in Protecting Red Blood Cells Against Peroxidative Hemolysis. *Biochem. Biophys. Res. Comm.* 49, 150-158.
- 40 Svingen, B.A., O'Neal, F.O. and Aust, S.D. (1978) The Role of Superoxide and Singlet Oxygen in Lipid Peroxidation. *Photochem. Photobiol.* 28, 803-809.
- 41 Cohen, G. (1978) The Generation of Hydroxyl Radicals in Biologic Systems: Toxicological Aspects. *Photochem. Photobiol.* 28, 669-675.
- 42 Kobayashi, Y., Okahata, S. and Usui, T. (1979) Hemolysis of Human Erythrocytes by Paraquat in Relation to Superoxide Dismutase Activity. *Biochem. J. Biophys. Res. Comm.* 91, 1288-1294.
- 43 Kellogg III, E.W. and Fridovich, I. (1975) Superoxide, Hydrogen Peroxide, and Singlet Oxygen in Lipid Peroxidation by a Xanthine Oxidase System. *J. Biol. Chem.* 250, 8812-8817.
- 44 Kirschner, R.J. and Goldberg, A.I. (1982) Exposure of Erythrocytes to Peroxide or Superoxide Stimulates the Degradation of Cellular Proteins. *Fed. Proc.* 41, 865.
- 45 Agro, F., De Sole, P., Rotilio, G. and Mondovi, B. (1973) Influence of Catalase and Superoxide Dismutase on Side Oxidations Involving Singlet Oxygen. *Ital. J. Biochem.* 22, 217-231.
- 46 McMahon, S.E. and Stern, A. (1978) Reactive Oxygen Metabolites and Hemolysis. *FEBS: Molecular Diseases* 56, 41-46.
- 47 Anonymous (1978) The Function of Vitamin E as an Antioxidant, as Revealed by a New Method for Measuring Lipid Peroxidation. *Nutrition Reviews* 36, 84-86.
- 48 Arkhipenko, Y.V., Lobrina, S.K., Kagan, V.E., Kozlov, Y.P., Nadirov, N.K., Pisarev, V.A., Ritov, V.B., and Khafizov, R.Kh. (1977) Stabilizing Action of Vitamin-E on Biological Membranes in Peroxide Oxidation of Lipids. *Biochem. USSR* 42, 1194-1198.
- 49 Bland, J., Canfield, W., Kennedy, T., Vincent, J. and Wells, R. (1978) Effect of Tocopherol on Photooxidation Rate of Human Erythrocyte Membrane In Vitro. *Physiol. Chem. Phys.* 10, 145-152.

- 50 Yagi, K., Yamada, H. and Nishikimi, M. (1978) Oxidation of Alfa-Tocopherol with O_2 in Tocopherol, Oxygen and Biomembranes; symp. 1977 (DeDuve, C. and Hayaishi, O., eds.) Elsevier North Holland Biomedical Press, New York, pp. 1-11.
- 51 Molenaar, I., Vos, J. and Hommes, F.A. (1972) Effect of Vitamin E Deficiency on Cellular Membranes. *Vit. Horm.* 30, 45-82.
- 52 Nair, P.P., Patnaik, R.N. and Hauswirth, J.W. (1978) Cellular Transport and Binding of d-Alfa-Tocopherol in Tocopherol, Oxygen, and Biomembranes; symp. 1977 (DeDuve, C. and Hayaishi, O. eds.) Elsevier North Holland Biomedical Press, New York, pp. 121-142.
- 53 Diplock, A.T. (1974) Vitamin E, Selenium, and the Membrane-Associated Drug-Metabolizing Enzyme System of Rat Liver. *Vit. Horm.* 32, 445-461.
- 54 Brownlee, N.R., Huttner, J.J., Panganamala, R.V. and Cornwell, D.G. (1977) Role of Vitamin E in Glutathione-Induced Oxidant Stress: Methemoglobin, Lipid Peroxidation, and Hemolysis. *J. Lipid Res.* 18, 365-644.
- 55 Foldes-Papp, Z. and Maretzki, D. (1982) Glutathione Peroxidase Activity of Human Erythrocyte Membranes. *Acta Biol. Med. Germ. Band* 41, 1003-1008.
- 56 Yang, N.Y.J. and Desai, I.D. (1978) Glutathione Peroxidase and Vitamin E Interrelationship in Tocopherol, Oxygen, and Biomembranes; symp. 1977 (DeDuve, C. and Hayaishi, O., eds.) Elsevier North Holland Biomedical Press, New York, pp. 233-245.
- 57 Lucy, J.A. (1978) Structural Interactions Between Vitamin E and Polyunsaturated Phospholipids in Tocopherol, Oxygen and Biomembranes (deDuve, C. and Hayaishi, O., eds.) Elsevier/North Holland Biomedical Press, New York, pp. 109-120.
- 58 Brunori, M., Falcioni, G., Fioretti, E., Giardina, B. and Rotilio, G. (1975) Formation of Superoxide in the Autoxidation of the Isolated Alfa and Beta Chains of Hemoglobin and its Involvement in Hemichrome Precipitation. *Eur. J. Biochem.* 53, 99-104.
- 59 Winterbourn, C.C., McGrath, B.M. and Carrell, R.W. (1976) Reactions Involving Superoxide and Normal and Unstable Hemoglobins. *Biochem. J.* 155, 493-502.
- 60 Carrell, R.W. and Winterbourn, C.C. (1978) Hemoglobin Precipitation and Red Cell Hemolysis. *FEBS: Molecular Diseases* 56, 57-65.

- 61 Rachmilewitz, E.A., Knyszynski, A. and Skutelsky, E. (1978) Red Blood Cell Membrane Defects in Beta-Thalassemia and the Therapeutic Role of Alpha-Tocopherol (Vitamin E). *FEBS: Molecular Diseases* 56, 47-56.
- 62 Rachmilewitz, E.A., Lubin, B.H. and Shohet, S.B. (1976) Lipid Membrane Peroxidation in Beta-Thalassemia Major. *Blood* 47, 495-505.
- 63 Arena, V. (1971) Action of Ionizing Radiation on Molecules in Ionizing Radiation and Life. The C.V. Mosby Co., Saint Louis, pp. 298-326.
- 64 Nerurkar, L.S., Zeligs, B.J. and Bellanti, J.A. (1978) Changes in Superoxide Dismutase, Catalase and Glucose-6-Phosphate Dehydrogenase Activities of Rabbit Alveolar Macrophages: Induced by Postnatal Maturation and/or In Vitro Hyperoxia. *Photochem. Photobiol.* 28, 781-786.
- 65 Autor, A.P. and Stevens, J.B. (1978) Mechanism of Oxygen Detoxification in Neonatal Rat Lung Tissue. *Photochem. Photobiol.* 28, 775-780.
- 66 Mann, T. and Keilin, D. (1939) *Proc. Roy. Soc., Ser. B. Biol. Sci.*, 126, 303.
- 67 McCord, J.M. and Fridovich, I. (1969) Superoxide Dismutase: An Enzymic Function for Erythrocuprein (Hemocuprein) *J. Biol. Chem.* 244: 6049-6055.
- 68 Fridovich, I. (1974) Superoxide Dismutases in *Advances in Enzymology and Related Areas of Molecular Biology*, Vol. 41 (Meister, A., ed.) J. Wiley & Sons, New York, pp. 35-97.
- 69 Fridovich, I. (1979) Superoxide and Superoxide Dismutase in *Advances in Inorganic Biochemistry* (Eichhorn, G.L. and Marzilli, L.G., eds.) Elsevier/North Holland, New York, pp. 67-90.
- 70 Fee, J.A. (1973) Studies on the Reconstitution of Bovine Erythrocyte Superoxide Dismutase: 1. The Presence of Four Divalent Metal-binding Sites on the Apo-protein which are Different from the Native Sites. *Biochim. Biophys. Acta* 295, 87-95.
- 71 Ahuja, B.S. and Nath, R. (1973) A Kinetic Study of Superoxide Dismutase in Normal Human Erythrocytes and its Possible Role in Anemia and Radiation Damage. *Proc. Symp. Contr. Mech. Cell. Proc. (Bombay)* 531-544.
- 72 Bannister, W.H., Anastasi, A. and Bannister, J.V. (1977) Human Erythrocyte Superoxide Dismutase (Erythrocuprein) in Superoxide, Superoxide Dismutases (*Proc. Embo. Workshop*), 1976 (Michelson, A.M., McCord, J.M. and Fridovich, I., eds.) Academic Press, New York, pp. 107-128.

- 73 Lippard, S.J., Burger, A.R., Ugurbil, K., Valentine, J.S. and Pantoliano, M.W. (1977) Physical and Chemical Studies of Bovine Erythrocyte Superoxide Dismutase. *Adv. Chem. Ser.* 162, 251-262.
- 74 Kobayashi, Y., Ishigame, K., Ishigame, Y. and Usui, T. (1977) Superoxide Dismutase Activity of Human Blood Cells in Biochemical and Medical Aspects of Active Oxygen (Symp. 1976) (Hayaishi, O. and Asada, K., eds.) University Park Press, Baltimore, pp. 261-274.
- 75 Petkau, A., Copps, T.P. and Kelly, K. (1979) Distribution of Superoxide Dismutase in the Erythrocyte Membrane. *Biophys. J.* 25, 190a.
- 76 Hartz, J.W. and Deutsch, H.F. (1969) Preparation and Physicochemical Properties of Human Erythrocyte Superoxide Dismutase. *J. Biol. Chem.* 244, 4565-4572.
- 77 Zepp, R.A., Chelack, W.S. and Petkau, A. (1980) Bovine Superoxide Dismutase Preparation: A Comparison of their Biochemical and Biological Characteristics in Chemical and Biochemical Aspects of Superoxide and Superoxide Dismutase, Vol. 11A (Bannister, J.V. and Hill, H.A.O., eds.) Elsevier, New York, pp. 201-211.
- 78 Marklund, S. (1980) Distribution of CuZn Superoxide Dismutase and Mn Superoxide Dismutase in Human Tissues and Extracellular Fluids. *Acta Physiol. Scand. Suppl.* 492, 19-23.
- 79 Michelson, A.M. and Puget, K. (1980) Cell Penetration by Exogenous Superoxide Dismutase. *Acta Physiol. Scand. Suppl.* 492, 67-80.
- 80 Gerli, G.C., Beretta, L., Bianchi, M., Pellegatta, A. and Agostoni, A. (1980) Erythrocyte Superoxide Dismutase, Catalase and Glutathione Peroxidase Activities in Beta-Thalassaemia (Major and Minor). *Scand. J. Hematol.* 25, 87-92.
- 81 Hill, H.A.O., Lee, W.K., Bannister, J.V. and Bannister, W.H. (1980) Investigation of Human Erythrocyte Superoxide Dismutase by ^1H Nuclear-Magnetic-Resonance Spectroscopy. *Biochem. J.* 185, 245-252.
- 82 Michelson, A.M., Puget, K., Durosay, P. and Rousselet, A. (1980) Penetration of Erythrocytes by Superoxide Dismutase. *Devel. in Biochemistry* 11B, 348-366.
- 83 Martel, P., Powell, B.M., Johnston, R.A.Z. and Petkau, A. (1983) Small Angle Neutron Scattering from Native and Irradiated Superoxide Dismutase in Aqueous Solution. *Biophys. J.* 41, 237a.

- 84 Kelly, K., Boux, H., Petkau, A. and Sehon, A. (1982) On the Safety of Treatment with Bovine Superoxide Dismutase: Production of a Humoral Antibody Response in Rabbits with Repeated Treatment. *Can. J. Physiol. Pharmacol.* 60, 1374-1381.
- 85 Petkau, A., Chelack, W.S., Kelly, K. and Friesen, H.G. (1982) Superoxide Dismutase and Radiosensitivity: Implications for Human Mammary Carcinomas in Pathology of Oxygen (Autor, A.P., ed.) Academic Press, New York, pp. 223-243.
- 86 Petkau, A. (1982) Concluding Remarks: a Prospective View of Active Oxygen in Medicine. *Can. J. Physiol. Pharmacol.* 60, 1425-1429.
- 87 Fried, R. (1977) Biochemical Functions of Superoxide Dismutase. *Acta Univ. Lodz.*, Ser. 2, 11, 273-295.
- 88 Abernethy, J.L., Steinman, H.M. and Hill, R.L. (1974) Bovine Erythrocyte Superoxide Dismutase: Subunit Structure and Sequence Location of the Intrasubunit Disulfide Bond. *J. Biol. Chem.* 249, 7339-7347.
- 89 Barra, D., Martini, F., Bannister, J.V., Schinina, M.E., Rotilio, G., Bannister, W.H. and Bossa, F. (1980) The Complete Amino Acid Sequence of Human Cu/Zn Superoxide Dismutase. *FEBS Letters* 120, 53-56.
- 90 Henry, L.E.A., Palmer, J.M. and Hall, D.O. (1978) The Induction of Histochemically-detectable Superoxide Dismutase (Cu/Zn Type) Bands on Acrylamide Gels. *FEBS LETT.* 93, 327-330.
- 91 Lumsden, J. and Hall, D.O. (1974) Soluble and Membrane-bound Superoxide Dismutases in a Blue-green Alga (*Spirulina*) and Spinach. *Biochem. Biophys. Res. Comm.* 58, 35-41.
- 92 Elstner, E.F. and Heupel, A. (1975) Lamellar Superoxide Dismutase of Isolated Chloroplasts. *Planta (Berl.)* 123, 145-154.
- 93 Michelson, A.M. and Durosay, P. (1977) Hemolysis of Human Erythrocytes by Activated Oxygen Species. *Photochem. Photobiol.* 25, 55-63.
- 94 Petkau, A., Kelly, K. and Lepock, J.R. (1980) Interaction of Superoxide Dismutase with Membranes in Biological and Clinical Aspects of Superoxide Anion and Superoxide Dismutase (Bannister, W.H. and Bannister, J.V., eds.) Elsevier, New York, pp. 335-347.
- 95 Lepock, J.R., Arnold, L.D., Petkau, A. and Kelly, K. (1981) Interaction of Superoxide Dismutase with Phospholipid Liposomes: an Uptake, Spin Label and Calorimetric Study. *Biochim. Biophys. Acta* 649, 45-57.

- 96 Hirai, K.-I., Ueno, S. and Ogawa, K. (1980) Plasma Membrane-associated NAD(P)H Oxidase and Superoxide Dismutase in Pulmonary Macrophages. *Acta Histochem. Cytochem.* 13, 113-126.
- 97 Miura, T. and Ogiso, T. (1982) Lipid Peroxidation of Erythrocyte Membrane Induced by Xanthine Oxidase System: Modification of Superoxide Dismutase Effect by Hemoglobin. *Chem. Pharm. Bull.* 30, 3662-6668.
- 98 MacKellar, W.C. and Crane, F.L. (1982) Iron and Copper in Plasma Membranes. *J. Bioenerg. Biomembr.* 14, 241-247.
- 99 Richards, D.E. and Eisner, D.A. (1982) Preparation and Use of Resealed Red Cell Ghosts in Red Cell Membranes: A Methodological Approach (Ellory, C.J. and Young, J.D., eds.) Academic Press, London, pp. 165-177.
- 100 Dodge, J.T., Mitchell, C. and Hanahan, D.J. (1963) The Preparation and Chemical Characteristics of Hemoglobin-Free Ghosts of Human Erythrocytes. *Arch. Biochem. Biophys.* 100, 119-130.
- 101 Bartosz, G., Soszynski, M. and Wasilewski, A. (1982) Aging of the Erythrocyte: XII Protein Composition of the Membrane. *Mech. Ageing Devel.* 19, 45-52.
- 102 Bartosz, G., Tannert, C., Fried, R. and Leyko, W. (1978) Superoxide Dismutase Activity Decreases during Erythrocyte Aging. *Experientia* 34, 1464.
- 103 Maddy, A.H. and Dunn, M.J. (1976) The Solubilization of Membranes in Biochemical Analysis of Membranes (Maddy, A.H., ed.) Chapman and Hall (London), pp. 177-196.
- 104 Maddy, A.H. (1982) The Solubilization of Erythrocyte Membrane Proteins in Red Cell Membranes: A Methodological Approach (Ellory, C.J. and Young, J.D., eds.) Academic Press, London, pp. 43-66.
- 105 Bellhorn, M.S.B. (1971) Acetylcholinesterase of the Human Erythrocyte Membrane: Study of an Enzyme within a Membrane Matrix. *Diss. Abst. Int. B*, 550-551.
- 106 Sihotang, K. (1974) A Simple Method for Purification of Acetylcholinesterase from Human Erythrocyte Membranes. *Biochim. Biophys. Acta* 370, 468-476.
- 107 Burton, G.W., Ingold, K.U. and Thompson, K.E. (1981) An Improved Procedure for the Isolation of Ghost Membranes from Human Red Blood Cells. *Lipids* 16, 946.

- 108 Anderson, T.F. (1951) Techniques for the Preservation of Three Dimensional Structures in Preparing Specimens for the Electron Microscope. Acad. Sci., New York, 13, 130-133.
- 109 Louis, J., Best, R. and Limarzi, L.R. (1961) Hematology in Clinical Laboratory Diagnosis, 6th ed. (Levison, S.A. and MacFate, R.P., eds.) Lea & Febiger, Philadelphia, pp. 697-899.
- 110 Fee, J.A. (1973) Studies on the Reconstitution of Bovine Erythrocyte Superoxide Dismutase: 4. Preparation and Some Properties of the Enzyme in which Co(II) is Substituted for Zn(II) J. Biol. Chem. 248, 4229-4234.
- 111 Lowry, O.H., Rosebrough, N.J., Farr, A.L. and Randall, R.J. (1951) Protein Measurement with the Folin Phenol Reagent. Biol. Chem. 193, 265-275.
- 112 Ellman, G.L., Courtney, K.D., Andres, Jr., V. and Featherstone, R.M. (1961) A New and Rapid Colorimetric Determination of Acetylcholinesterase Activity. Biochem. Pharm. 7, 88-95.
- 113 Touster, O., Aronson, Jr., N.N., Dulaney, J.T. and Hendrickson, H. (1970) Isolation of Rat Liver Plasma Membranes: Use of Nucleotide Pyrophosphatase and Phosphodiesterase I as Marker Enzymes. J. Cell Biol. 47, 604-618.
- 114 Chen, P.S., Toribara, T.Y. and Warner, H. (1956) Microdetermination of Phosphorus. Anal. Chem. 28, 1756-1758.
- 115 Beauchamp, C. and Fridovich, I. (1971) Superoxide Dismutase: Improved Assays and an Assay Applicable to Acrylamide Gels. Anal. Biochem. 44, 276-287.
- 116 Kirby, T.W. and Fridovich, I. (1982) A Picomolar Spectrophotometric Assay for Superoxide Dismutase. Anal. Biochem. 127, 435-440.
- 117 Jewett, S.L., Latrenta, G.S. and Beck, C.M. (1982) Metal-Deficient Copper-Zinc Superoxide Dismutases. Arch. Biochem. Biophys. 215, 116-128.
- 118 Steck, T.L., Weinstein, R.S., Straus, J.H. and Wallach, D.F. (1970) Inside-out Red Cell Membrane Vesicles: Preparation and Purification. Science 183, 255-257.
- 119 Steck, T.L. and Kant, J.A. (1974) Preparation of Impermeable Ghosts and Inside-out Vesicles from Human Erythrocyte Membranes in Methods in Enzymology, Vol. 32 B (Fleischer, S. and Packer, L., eds.) Academic Press, New York, pp. 172-180.

- 120 Delaunay, J., Fischer, S., Tortolero, M. Piau, J.-P. and Schapira, G. (1978) Absence of any Detectable Activity of the Membrane Marker Enzyme 5'-Nucleotidase in Human Red Blood Cells. *Biomedicine* 29, 173-175.
- 121 Parker, J.C. (1970) Metabolism of External Adenine Nucleotides by Human Red Blood Cells. *Am. J. Physiol.* 218, 1568-1573.
- 122 Sloan, E.P., Crawford, D.R. and Schneider, D.L. (1981) Isolation of Plasma Membrane from Human Neutrophils and Determination of Cytochrome B and Quinone Content. *J. Exp. Med.* 153, 1316-1328.
- 123 Van den Hoek, A.K. and Zail, S.S. (1977) Polyacrylamide Gel Electrophoresis of Human Erythrocyte Membrane Enzymes Solubilized with Triton X-100. *Clin. Chim. Acta* 79, 7-14.
- 124 Petkau, A. and Chelack, W.S. (1972) Permeability of Phospholipid Membranes to Inorganic Phosphate. *Can. J. Biochem.* 50, 1030-1033.
- 125 Valentine, W.N., Fink, K., Paglia, D.E., Harris, S.R., and Adams, W.S. (1974) Hereditary Hemolytic Anemia with Human Erythrocyte Pyrimidine 5'-Nucleotidase Deficiency. *J. Clin. Invest.* 54, 866-879.
- 126 Widnell, C.C. (1974) Purification of Rat Liver 5'-Nucleotidase as a Complex with Sphingomyelin in *Methods in Enzymology*, Vol. 32 B (Fleischer, S. and Packer, L., eds.) Academic Press, New York, pp. 368-374.
- 127 Zachowski, A., Simonin, G., Aubry, J. and Pommier, P. (1981) Plasma Membrane Enzymes in Balb/c Lymphomas with either T or B Cell Properties: 1. 5'-Nucleotidase. *J. Receptor Res.* 2, 97-118.
- 128 Glastris, B. and Pfeiffer, S.E. (1974) Mammalian Membrane Marker Enzymes in *Methods in Enzymology*, Vol. 32 B (Fleischer, S. and Packer, L., eds.) Academic Press, New York, pp. 124-131.
- 129 Dunn, M.J. and Maddy, A.H. (1976) Techniques for the Analysis of Membrane Proteins in *Biochemical Analysis of Membranes* (Maddy, A.H., ed.) Chapman and Hall, London, pp. 197-251.
- 130 Wu, H. (1922) A New Colorimetric Method for the Determination of Plasma Proteins. *J. Biol. Chem.* 51, 33-39.
- 131 Fazekas, S., Webster, R.G. and Datyner, A. (1963) Two New Staining Procedures for Quantitative Estimation of Proteins on Electrophoretic Strips. *Biochim. Biophys. Acta* 71, 377-391.

- 132 Roberts, P.B., Fielden, E.M., Rotilio, G., Calabrese, L. Bannister, J.V. and Bannister, W.H. (1974) Superoxide Dismutase Inactivation by Radiation-Induced Radicals: Evidence for Histidine Residues in the Active Site. *Radiation Res.* 60, 441-452.
- 133 Barra, D., Bossa, F., Calabrese, L., Rotilio, G., Roberts, P.B. and Fielden, E.M. (1975) Selective Destruction of Amino Acid Residues in Irradiated Solutions of Superoxide Dismutase. *Biochem. Biophys. Res. Comm.* 64, 1303-1309.
- 134 Malinowski, D.P. and Fridovich, I. (1979) Chemical Modification of Arginine at the Active Site of the Bovine Erythrocyte Superoxide Dismutase. *Biochem.* 18, 5909-5917.
- 135 Green, A.A. and Hughes, W.L. (1955) Protein Fractionation on the Basis of Solubility in Aqueous Solutions of Salts and Organic Solvents in *Methods in Enzymology*, Vol. 1 (Colowick, S.P. and Kaplan, N.O., eds.) Academic Press, New York, pp. 67-90.
- 136 Markowitz, H., Cartwright, G.E. and Wintrobe, M.M. (1959) Studies on Copper Metabolism. XXVII. The Isolation and Properties of an Erythrocyte Cuproprotein (Erythrocuprein). *J. Biol. Chem.* 234, 40-45.
- 137 Peeters-Joris, C., Vandevoorde, A.-M. and Baudhuin, P. (1975) Subcellular Localization of Superoxide Dismutase in Rat Liver. *Biochem. J.* 150, 31-39.
- 138 Chuaqui, C.A. and Petkau, A. (1982) Radiation-Induced Inactivation of Superoxide Dismutase in Nitrous Oxide Saturated Solutions. *Biochim. Biophys. Acta* 702, 112-116.
- 139 Paschen, W. and Weser, U. (1973) Singlet Oxygen Decontaminating Activity of Erythrocuprein (Superoxide Dismutase) *Biochim. Biophys. Acta* 327, 217-222.
- 140 Matheson, I.B.C., Etheridge, R.D., Kratowich, N.R. and Lee, J. (1975) The Quenching of Singlet Oxygen by Amino Acids and Proteins. *Photochem. Photobiol.* 21, 165-171.